

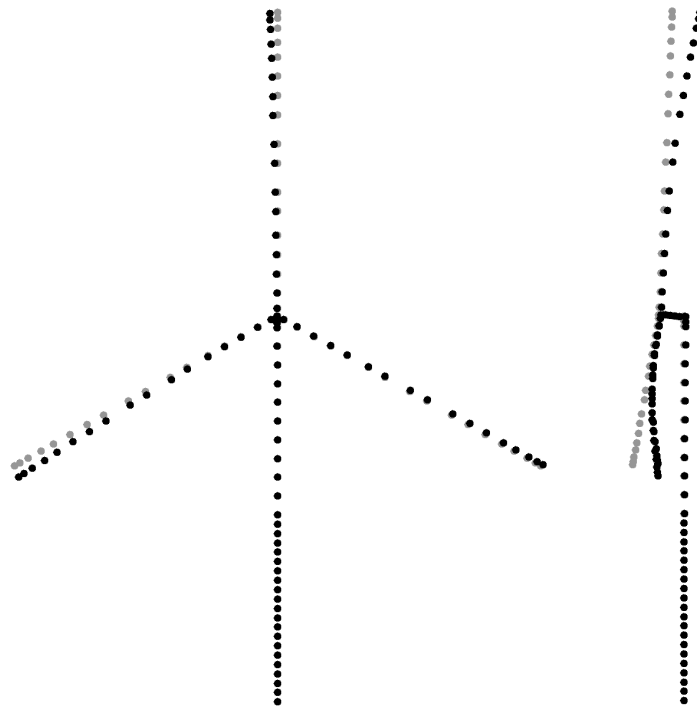
2018:00834 - Unrestricted

Report

STAS Aeroelastic 1.0 – Theory Manual

Author(s)

Karl Merz



SINTEF Energi AS
SINTEF Energy Research AS

Address:
Postboks 4761 Torgarden
7465 Trondheim
NORWAY

www.sintef.no

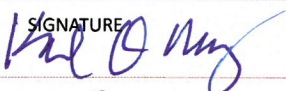
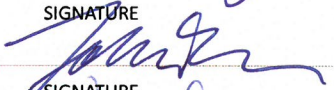

Enterprise Number: NO 939 350 675 MVA

Report

STAS Aeroelastic 1.0 – Theory Manual

KEYWORDS:

Wind energy
Dynamics
Optimization
Control
State space

VERSION 1.0	DATE August 24, 2018
AUTHOR(S) Karl Merz	
CLIENT(S) OPWIND	CLIENT'S REFERENCE Part of D1.1.2
PROJECT 502001647	NUMBER OF PAGES AND ATTACHMENTS 50
ABSTRACT A version 1.0 of the STAS Aeroelastic module has been released as open source on GitHub. This consists of Matlab scripts implementing nonlinear/linear pairs of dynamic equations. The linear equations match the dynamics of the nonlinear equations, at a given operating point, to within the square root of machine precision. In addition, the code is written to support complex-step gradients for other input parameters. The high-precision tangent-dynamic model makes possible Newton-Raphson solutions for operating points; gradients of a dynamic cost function by direct and adjoint methods; velocity-based linearization for gain-scheduled control design; eigenmode decomposition; and model reduction using linear basis functions.	
PREPARED BY Karl Merz	SIGNATURE 
CHECKED BY John Olav Tande	SIGNATURE 
APPROVED BY Knut Samdal	SIGNATURE 
REPORT NUMBER 2018:00834	ISBN 978-82-14-06938-9
CLASSIFICATION Unrestricted	CLASSIFICATION THIS PAGE Unrestricted

Document History

VERSION	DATE	VERSION DESCRIPTION
1.0	23.08.2018	Original document

Contents

1	Background	4
2	Nonlinear structural dynamics	4
2.1	Notation and coordinate systems	4
2.2	Blade section properties	7
2.3	A geometrically nonlinear finite element model	10
2.4	Lagrange equations	14
2.5	Constraints	19
2.6	Nonlinear state space	23
3	Linear structural dynamics	23
3.1	Expressions for partial derivatives	24
3.2	Linear constraints	28
3.3	Modal reduction and damping	30
4	Aerodynamics	31
4.1	Blade profile input	31
4.2	Nonlinear blade element momentum model	32
4.3	Linearized aerodynamic equations	36
4.3.1	Structural velocity in global and airfoil coordinates	36
4.3.2	Local flow velocity	36
4.3.3	Quasi-steady angle-of-attack	37
4.3.4	Dynamic angle-of-attack	37
4.3.5	Airfoil coefficients	37
4.3.6	Airfoil forces	37
4.3.7	Forces in pitch (blade body reference) coordinates	37
4.3.8	Local flow velocity at the rotor plane	38
4.3.9	Projected blade element on the rotor plane	38
4.3.10	Prandtl factor	39
4.3.11	Rotorplane flow velocity	39
4.3.12	Projected forces on the rotor plane	39
4.3.13	Quasi-steady induced velocity	40
4.3.14	Dynamic induced velocity	41
4.4	Unified aeroelastic equations	42
5	Verification of the equations	42
5.1	Static structural deformation	42
5.2	Natural frequencies and stress stiffening	43
5.3	A rotating cantilever beam	44
5.4	A parked wind turbine	45
5.5	Newton's method solution of an operating wind turbine	46
5.6	Equilibrium aerodynamics	47
6	Summary and conclusions	47

1 Background

STAS WPP is a MATLAB/Octave program for the system dynamics, control, and optimization of wind power plants. At the highest level, STAS is implemented as a series of modules. The STAS Aeroelastic module, for which this theory manual is written, contains the wind turbine structures and aerodynamics.

Tangent dynamics is the central theme to the STAS approach. Tangent dynamics involves the generation and manipulation of linear state-space models, obtained along a nonlinear dynamic trajectory. A linear state-space model is usually defined about an equilibrium point – but it does not need to be. Namely, a linear model can be derived about any initial condition. It then represents the tangent dynamics of the nonlinear system. This representation is useful for studying the stability and stochastic response of the system during off-design and transient operating conditions. It is also useful for the design of gain-scheduled controllers, and for developing reduced-order parameter-varying models with linear systems theory.

Each equation set in STAS is provided in nonlinear and linearized variants. At the operating point at which they are generated, the linear equations match the nonlinear equations to within at least $\sqrt{\varepsilon}$, ε being the machine precision of the computer.¹ STAS also supports *complex step* gradients on all input parameters. Though it is possible to run time-domain simulations using the nonlinear equations, STAS is not optimized for this purpose, and users will obtain faster results with a commercial aeroelastic package. Rather, the strength of STAS lies in applications where a high-precision linearization is important: for instance, adjoint computations of gradients for brief time-domain load cases, Newton-Raphson solution for steady-state operating points, and various applications of linear systems theory, such as control system design and stochastic analysis of fatigue.

The present memo supercedes previous documentation (Merz 2015) describing the equations of motion in STAS Aeroelastic. The updated equations include large structural deformations; yaw offsets and the possibility for dynamic yaw control; the ability to link the turbine to a floating platform; aerodynamics that follow blade deflections; and a dynamic wake model suitable for operation in yawed flow.

Though not based directly on the same sets of equations, the present work has taken inspiration from the precedence set by Hansen (2004) and van Engelen and Braam (2004).

2 Nonlinear structural dynamics

The structural model in STAS Aeroelastic is a multibody, corotational finite-element beam representation of the wind turbine. The turbine consists of a number of bodies: foundation, tower, nacelle, driveshaft, and blades. Each body can move rigidly in space, and deform elastically. The position and orientation of each finite element is also decomposed into rigid-body and elastic displacements. This enables the model to account for large deflections, which are of especial importance for the blades, as well as large joint rotations.

2.1 Notation and coordinate systems

Vectors and matrices are denoted with a bold font, for instance the state vector \mathbf{x} and matrix \mathbf{A} . When a vector or matrix has a certain coordinate system as a basis, then this is indicated by the use of a superscript. It may be important to keep track of two coordinate systems, one the basis in which the components of a vector are expressed, and another relative to which the vector is measured. In this case the basis is indicated by a superscript, and the relative is indicated by a slash in the subscript. Thus the position of a node \mathbf{r} – that is, the vector from the origin to the node – might be measured

¹On the system used to generate the results in this report, $\varepsilon = 2.2 \times 10^{-16}$.

relative to the global coordinate system, but the components expressed in a local body coordinate system; this would be written as $\mathbf{r}_{/g}^B$.

Subscripts are frequently used in other contexts as well. When a spatial vector has a subscript, for instance the induced velocity \mathbf{V}_i , then one of the spatial components is indicated by an additional subscript outside a parentheses; so the Z^r component of the induced velocity, a scalar, would be written $(\mathbf{V}_i)_z$. Where there is no need to be so explicit, the shorthand convention $\mathbf{v} = [v_x, v_y, v_z]$ is also used. Subscripts never denote derivatives.

The structural and aerodynamic analyses employ a variety of coordinate systems. Most of these are sketched in Fig. 1. For clarity, the following description is given as if the structure were rigid. The formulation of structural displacements in Section 2.3 allows for elastic rotations which may misalign the various coordinate systems.

The foundation coordinate system is located at the bottom node of the foundation. The X^F axis is parallel with the undisturbed ocean surface and indicates the direction of zero yaw angle; at zero yaw, the X^F axis points downwind. The Z^F axis is normal to the undisturbed ocean surface and typically passes through the center of the undeformed tower.

The tower coordinate system is located at the base of the tower, or equivalently, for offshore turbines, the top of the transition piece. In the undeformed state it is aligned with the foundation coordinate system.

The yaw coordinate system indicates the position of the yaw bearing. At zero yaw and no deformation, the yaw coordinate system is aligned with the tower and foundation coordinate systems. A positive yaw angle χ involves a rotation about the $Z^y = Z^T$ axis.

The nacelle coordinate system is aligned with the axis of rotation of the driveshaft. The Z^n axis points in the direction of the X^y axis, except that it is rotated about the Y^y axis by the driveshaft tilt angle δ : positive tilt angle raises the rotor hub. Note that the yaw coordinate system is the reference coordinate system for the nacelle structure. The “nacelle” coordinate system serves as an intermediate frame against which driveshaft rotation is measured.

Thus, the driveshaft coordinate system is rotated, with respect to the nacelle coordinate system, by the azimuth angle Ψ about the $Z^d = Z^n$ axis.

The rotorplane coordinate system is used in the aerodynamic analysis. It is aligned with the nacelle coordinate system, but has its origin at the center of the rotor hub. Quantities expressed in rotorplane coordinates have in general an “axial” component, in the Z^r direction, and a “tangential” component, which is tangent to a particular radius, for instance

$$(\mathbf{V}_i)_t := (\mathbf{V}_i)_x \sin \Psi_b + (\mathbf{V}_i)_y \cos \Psi_b. \quad (1)$$

This decomposition of the coordinates is convenient, because the spanwise component of relative velocity is neglected when computing aerodynamic forces.

The remaining coordinate systems occur in triplets, one associated with each blade. The hub coordinate system is not shown in Fig. 1. Its origin is the same as the rotorplane coordinate system, at the center of the rotor hub, and the X^h axis points from the axis of rotation to the pitch bearing. The hub coordinate system is aligned with the driveshaft coordinate system for Blade 1, and is rotated about the $Z^h = Z^d$ axis by the blade offset angle of $2\pi/3$ for Blade 2 and $4\pi/3$ for Blade 3.

The blade coordinate system is located at the pitch bearing. It is rotated, with respect to the hub coordinate system, about the $Y^h = Y^b$ axis by the blade cone angle ϕ . (The blade cone angle is not shown in Fig. 1.)

The blade pitch coordinate system is offset from the hub coordinates system by rotation about the $X^b = X^p$ axis by the *negative* of the pitch angle. The negative sign is required such that, by convention, positive pitch rotates the leading edge of the blades into the wind.

There are additional coordinate systems associated with each blade element in the aerodynamic analysis. These are shown in Fig. 2. The section coordinate system is offset from the pitch coordinate system by rotation about the $X^p = X^s$ axis by the *negative* of the blade aerodynamic twist angle.

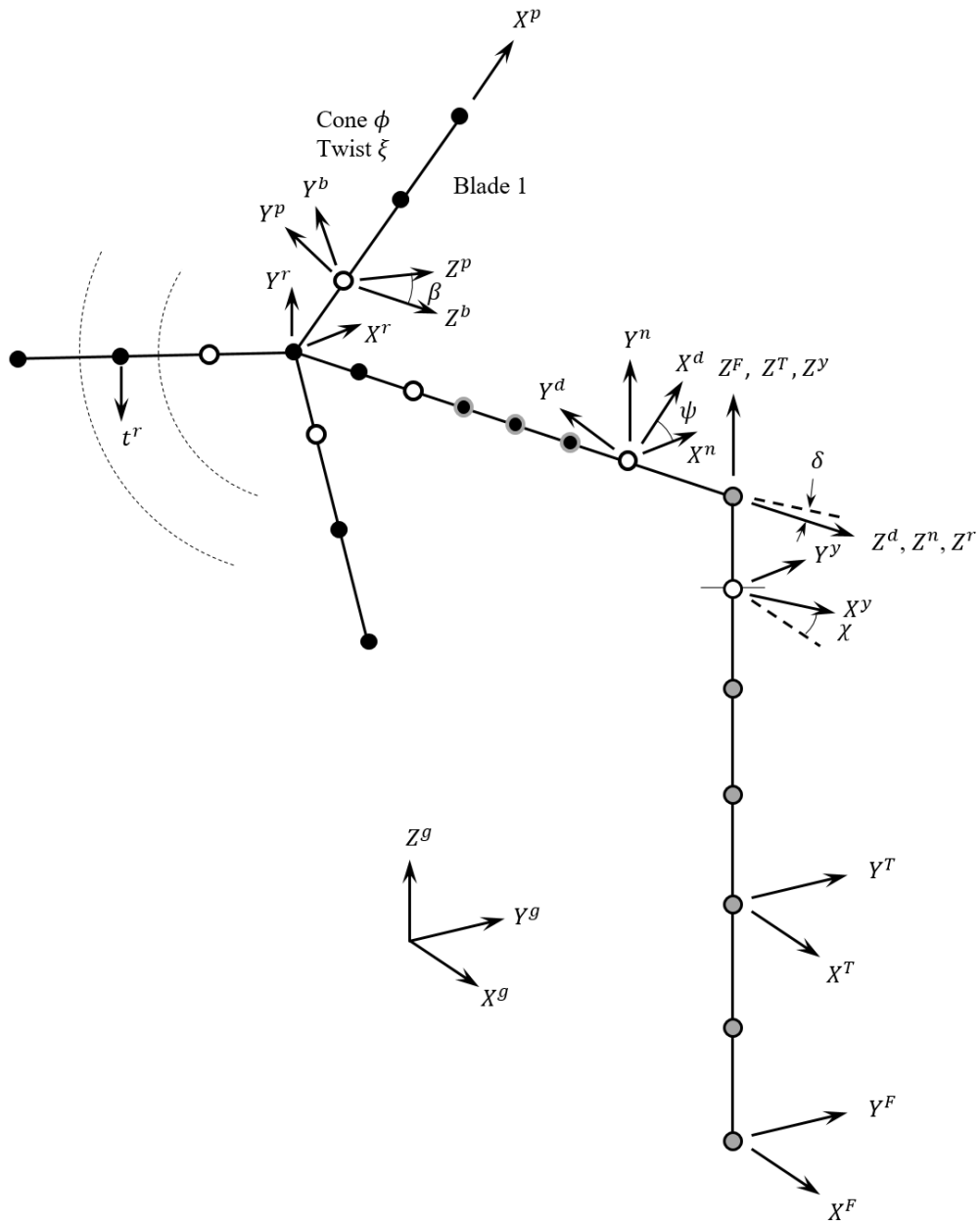


Figure 1: Important coordinate systems and angles used in the wind turbine model. The wind turbine structures are represented by finite beam elements. Rotating nodes are shown by black dots, and fixed nodes by gray dots. White dots show joints. All joints restrain 5 degrees-of-freedom, allowing one rotational degree-of-freedom, with the exception of the front driveshaft bearing, which restrains only X^n and Y^n displacements.

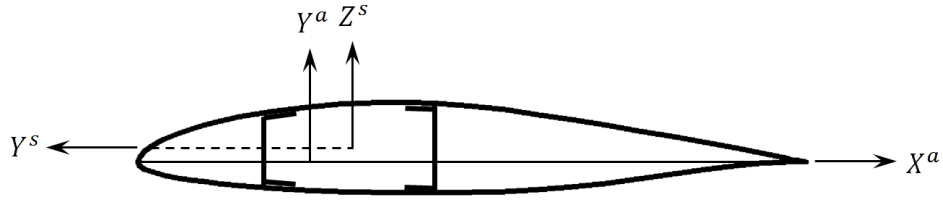


Figure 2: The airfoil and blade section coordinate systems.

The airfoil coordinate system is the traditional one used to represent lift and drag, or normal and chordwise, forces. The origin is one quarter-chord aft from the leading edge, and the X^a axis lies along the chordline.

Structural finite elements also have associated nodal and section coordinate systems. These are described in Section 2.3.

2.2 Blade section properties

Wind turbine blades have irregular cross-sections made of composite materials. They may therefore exhibit couplings which are not present in the basic finite beam elements addressed by, for instance, Cook *et al.* (1989). The coupling between degrees-of-freedom, in particular flapwise bending and twisting, is a first-order effect that should be included in a linear dynamic model.

A beam element is associated with twelve nodal degrees-of-freedom \mathbf{w} , consisting of three displacements and three rotations at each of the nodes.² The element mass and stiffness matrices \mathbf{m}_e and \mathbf{k}_e are thus 12-by-12. They can be found by manipulating the expressions for kinetic and potential energy, respectively, into the forms

$$E_K = \frac{1}{2} \frac{d\mathbf{w}^T}{dt} \mathbf{m}_e \frac{d\mathbf{w}}{dt} \quad (2)$$

and

$$E_P = \frac{1}{2} \mathbf{w}^T \mathbf{k}_e \mathbf{w}. \quad (3)$$

The kinetic energy can be obtained by integrating the density and particle velocity over the body, as

$$E_K = \frac{1}{2} \int_B \rho \frac{d\mathbf{r}^T}{dt} \frac{d\mathbf{r}}{dt} dB, \quad (4)$$

where the vector $\mathbf{r} := [r_x \ r_y \ r_z]^T$ points from the origin of the element section (reference) coordinate system to a point of mass. Making simplified assumptions about the beam deformation, especially that plane sections remain plane, and that deformations are small, the movement of the points on the section can be related to that of the reference line which defines the beam element:

$$\frac{dr_x}{dt} = \frac{dW_x}{dt} + r_z \frac{d\Theta_y}{dt} - r_y \frac{d\Theta_z}{dt}, \quad (5)$$

$$\frac{dr_y}{dt} = \frac{dW_y}{dt} - r_z \frac{d\Theta_x}{dt}, \quad (6)$$

and

$$\frac{dr_z}{dt} = \frac{dW_z}{dt} + r_y \frac{d\Theta_x}{dt}. \quad (7)$$

²For the present purpose of describing the section properties, we start with a simple representation of the elastic deformations. A more elaborate corotational formulation is presented in Section 2.3. We then have to worry about rigid translations and rotations, in addition to elastic deformation, and so a different and more elaborate convention is adopted to describe the degrees-of-freedom. Please do not be confused by the differences in terminology.

For uniform beam elements,

$$\frac{d\mathbf{r}}{dt}(x, y, z, t) = \mathbf{R}(y, z) \frac{d\mathbf{W}}{dt}(x, z). \quad (8)$$

The reference line displacement is W , and its rotation is Θ . The finite element method involves assuming that W and Θ are related to nodal displacements \mathbf{w} by prescribed functions of the x coordinate, along the reference line. For standard beam elements,

$$W_x = \left(1 - \frac{x}{L}\right) w_{1x} + \frac{x}{L} w_{2x} \quad (9)$$

$$W_y = \left(1 - \frac{3x^2}{L^2} + \frac{2x^3}{L^3}\right) w_{1y} + \left(x - \frac{2x^2}{L} + \frac{x^3}{L^2}\right) \theta_{1z} + \left(\frac{3x^2}{L^2} - \frac{2x^3}{L^3}\right) w_{2y} + \left(-\frac{x^2}{L} + \frac{x^3}{L^2}\right) \theta_{2z} \quad (10)$$

$$W_z = \left(1 - \frac{3x^2}{L^2} + \frac{2x^3}{L^3}\right) w_{1z} + \left(-x + \frac{2x^2}{L} - \frac{x^3}{L^2}\right) \theta_{1y} + \left(\frac{3x^2}{L^2} - \frac{2x^3}{L^3}\right) w_{2z} + \left(\frac{x^2}{L} - \frac{x^3}{L^2}\right) \theta_{2y} \quad (11)$$

$$\Theta_x = \left(1 - \frac{x}{L}\right) \theta_{1x} + \frac{x}{L} \theta_{2x} \quad (12)$$

$$\begin{aligned} \Theta_y &= -\frac{\partial W_z}{\partial x} \\ &= \left(\frac{6x}{L^2} - \frac{6x^2}{L^3}\right) w_{1z} + \left(1 - \frac{4x}{L} + \frac{3x^2}{L^2}\right) \theta_{1y} + \left(-\frac{6x}{L^2} + \frac{6x^2}{L^3}\right) w_{2z} + \left(-\frac{2x}{L} + \frac{3x^2}{L^2}\right) \theta_{2y} \end{aligned} \quad (13)$$

and

$$\begin{aligned} \Theta_z &= \frac{\partial W_y}{\partial x} \\ &= \left(-\frac{6x}{L^2} + \frac{6x^2}{L^3}\right) w_{1y} + \left(1 - \frac{4x}{L} + \frac{3x^2}{L^2}\right) \theta_{1z} + \left(\frac{6x}{L^2} - \frac{6x^2}{L^3}\right) w_{2y} + \left(-\frac{2x}{L} + \frac{3x^2}{L^2}\right) \theta_{2z} \end{aligned} \quad (14)$$

These shape functions can be written in matrix form as

$$\mathbf{W}(x, t) = \mathbf{S}(x) \mathbf{w}(t). \quad (15)$$

The kinetic energy is thus

$$E_K = \frac{1}{2} \frac{d\mathbf{w}^T}{dt} \int_L \mathbf{S}^T \left(\int_A \rho \mathbf{R}^T \mathbf{R} dA \right) \mathbf{S} dx \frac{d\mathbf{w}}{dt}, \quad (16)$$

and

$$\mathbf{m}_e = \int_L \mathbf{S}^T \left(\int_A \rho \mathbf{R}^T \mathbf{R} dA \right) \mathbf{S} dx. \quad (17)$$

The integral in parentheses is a 6-by-6 matrix describing the inertia properties of the beam element cross-section; specifically,

$$\int_A \rho \begin{bmatrix} 1 & 0 & 0 & 0 & r_z & -r_y \\ 0 & 1 & 0 & -r_z & 0 & 0 \\ 0 & 0 & 1 & r_y & 0 & 0 \\ 0 & -r_z & r_y & r_y^2 + r_z^2 & 0 & 0 \\ r_z & 0 & 0 & 0 & r_z^2 & -r_y r_z \\ -r_y & 0 & 0 & 0 & -r_y r_z & r_y^2 \end{bmatrix} dA \quad (18)$$

Some of these inertia properties are typically given as part of the description of a wind turbine blade. In particular, the mass-per-unit-length

$$\int_A \rho dA$$

and torsional inertia

$$\int_A \rho(r_y^2 + r_z^2) dA$$

are usually available. For a balanced section, with the center-of-mass aligned with the reference line, all the off-diagonal terms are zero. The terms r_y^2 and r_z^2 – that is, the rotational inertia of the section in bending – are frequently neglected.

The outer integral in (17) acts only on the two matrices \mathbf{S} , as the section properties are, for uniform elements, not a function of x . \mathbf{S} is a 6-by-12 matrix, such that the total size of \mathbf{m}_e is 12-by-12.

The potential energy stored in the straining of a body is

$$E_P = \iint_B \boldsymbol{\sigma}^T d\boldsymbol{\varepsilon} dB, \quad (19)$$

where $\boldsymbol{\sigma}$ is a vector of stress components and $\boldsymbol{\varepsilon}$ is a vector of strains. For an elastic material,

$$\boldsymbol{\sigma} = \mathbf{E} \boldsymbol{\varepsilon}, \quad (20)$$

with \mathbf{E} a symmetric matrix. Then,

$$E_P = \iint_B \boldsymbol{\varepsilon}^T \mathbf{E}^T d\boldsymbol{\varepsilon} dB = \frac{1}{2} \int_B \boldsymbol{\varepsilon}^T \mathbf{E} d\boldsymbol{\varepsilon} dB. \quad (21)$$

For elastic displacements u_x , u_y , and u_z of a point of material, the relationships between strain and displacement are

$$\varepsilon_x = \frac{\partial u_x}{\partial x}, \quad \varepsilon_y = \frac{\partial u_y}{\partial y}, \quad \varepsilon_z = \frac{\partial u_z}{\partial z}, \quad \gamma_{xy} = \frac{\partial u_x}{\partial y} + \frac{\partial u_y}{\partial x}, \quad \gamma_{xz} = \frac{\partial u_x}{\partial z} + \frac{\partial u_z}{\partial x}, \quad \gamma_{yz} = \frac{\partial u_y}{\partial z} + \frac{\partial u_z}{\partial y}. \quad (22)$$

Material displacements are related to the beam reference line displacement in the same manner as (8) for the velocities,

$$\mathbf{u}(x, y, z, t) = \mathbf{R}(y, z) \mathbf{W}(x, t). \quad (23)$$

This gives

$$\varepsilon_x = \frac{\partial W_x}{\partial x} + r_z \frac{\partial \Theta_y}{\partial x} - r_y \frac{\partial \Theta_z}{\partial x}, \quad (24)$$

$$\varepsilon_y = 0, \quad \varepsilon_z = 0, \quad (25)$$

$$\gamma_{xy} = -\Theta_z + \frac{\partial W_y}{\partial x} - r_z \frac{\partial \Theta_x}{\partial x} = -\frac{\partial W_y}{\partial x} + \frac{\partial W_y}{\partial x} - r_z \frac{\partial \Theta_x}{\partial x} = -r_z \frac{\partial \Theta_x}{\partial x}, \quad (26)$$

$$\gamma_{xz} = \Theta_y + \frac{\partial W_z}{\partial x} + r_y \frac{\partial \Theta_x}{\partial x} = -\frac{\partial W_z}{\partial x} + \frac{\partial W_z}{\partial x} + r_y \frac{\partial \Theta_x}{\partial x} = r_y \frac{\partial \Theta_x}{\partial x}, \quad (27)$$

and

$$\gamma_{yz} = -\Theta_x + \Theta_x = 0. \quad (28)$$

These relationships can be written as

$$\boldsymbol{\varepsilon}(x, y, z, t) = \begin{bmatrix} \varepsilon_x \\ \gamma_{xy} \\ \gamma_{xz} \end{bmatrix} = \mathbf{D}(y, z) \frac{\partial \mathbf{W}}{\partial x}(x, t) = \mathbf{D}(y, z) \frac{\partial \mathbf{S}}{\partial x} \mathbf{w}(t). \quad (29)$$

The elasticity matrix \mathbf{E} is thus 3-by-3.

The potential energy is then

$$E_P = \frac{1}{2} \mathbf{w}^T \int_L \frac{\partial \mathbf{S}^T}{\partial x} \left(\int_A \mathbf{D}^T \mathbf{E} \mathbf{D} dA \right) \frac{\partial \mathbf{S}}{\partial x} dx \mathbf{w} \quad (30)$$

such that

$$\mathbf{k}_e = \int_L \frac{\partial \mathbf{S}^T}{dx} \left(\int_A \mathbf{D}^T \mathbf{E} \mathbf{D} dA \right) \frac{\partial \mathbf{S}}{\partial x} dx. \quad (31)$$

Multiplying out the terms within the inner integral gives

$$\int_A \begin{bmatrix} E_{11} & 0 & 0 & -r_z E_{12} + r_y E_{13} & r_z E_{11} & -r_y E_{11} \\ 0 & 0 & 0 & 0 & 0 & 0 \\ 0 & 0 & 0 & 0 & 0 & 0 \\ -r_z E_{12} + r_y E_{13} & 0 & 0 & r_z^2 E_{22} - 2r_y r_z E_{23} + r_y^2 E_{33} & -r_z^2 E_{12} + r_y r_z E_{13} & r_y r_z E_{12} - r_y^2 E_{13} \\ r_z E_{11} & 0 & 0 & -r_z^2 E_{12} + r_y r_z E_{13} & r_z^2 E_{11} & -r_y r_z E_{11} \\ -r_y E_{11} & 0 & 0 & r_y r_z E_{12} - r_y^2 E_{13} & -r_y r_z E_{11} & r_y^2 E_{11} \end{bmatrix} dA. \quad (32)$$

A description of a wind turbine blade would typically provide the axial stiffness

$$\int_A E_{11} dA,$$

bending stiffnesses

$$\int_A r_y^2 E_{11} dA \quad \text{and} \quad \int_A r_z^2 E_{11} dA,$$

and torsional stiffness

$$\int_A (r_z^2 E_{22} - 2r_y r_z E_{23} + r_y^2 E_{33}) dA.$$

Other terms are zero for symmetrical, isotropic sections. If the material couples axial and shear deformation, then terms with E_{12} and E_{13} become active.

For sections composed of thin composite plates or shells, the material properties are transformed into beam section coordinates before implementing them in the above equations.

2.3 A geometrically nonlinear finite element model

A corotational finite element formulation (Felippa and Haugen 2005) is employed to update the matrices to the deformed position and orientation, “pose” for short. The nice thing about the corotational formulation is that only three rotational parameters describe the orientation of a node. The elastic and rigid-body portions are stored together, and then extracted, during formation of the stiffness and inertia matrices, based on some criteria. Here we assume that the nodal positions define the rigid-body motion of an element, and rotations relative to the lines connecting the nodes are elastic deformations.

Consider a finite beam element, as sketched in Fig. 3. The orientation and deformed state of the element can be described by the nodal positions and rotations, six degrees-of-freedom per node. We adopt an axis-angle (exponential map) convention to define the orientation of the nodes relative to the body coordinate system, as well as the body coordinate system relative to some master coordinate system. As implemented here, the exponential map uses three rotation variables θ_x^a , θ_y^a , and θ_z^a to code for a 3-by-3 transform matrix \mathbf{T}_b^a . The variables represent an axis of rotation, in the “a” frame, and their norm $[(\theta_x^a)^2 + (\theta_y^a)^2 + (\theta_z^a)^2]^{1/2}$ an angle of rotation. A rotation about the axis by the angle gives the orientation of the “b” frame in the coordinates of the “a” frame.

Let the undeformed structure be defined by

$$\mathbf{P}_k := \begin{bmatrix} \mathbf{p}_{k0} \\ \boldsymbol{\xi}_{s0}^{B0} \end{bmatrix}, \quad (33)$$

where \mathbf{p}_k is a vector of nodal positions relative to the body origin, and $\boldsymbol{\xi}_{s0}^{B0}$ specifies, via \mathbf{T}_{s0}^{B0} , the orientation of the beam sections at each node. \mathbf{P}_k is a constant whose time derivative is zero. At time t , the state of the structure is defined by its deformed position and velocity. The pose of a node can

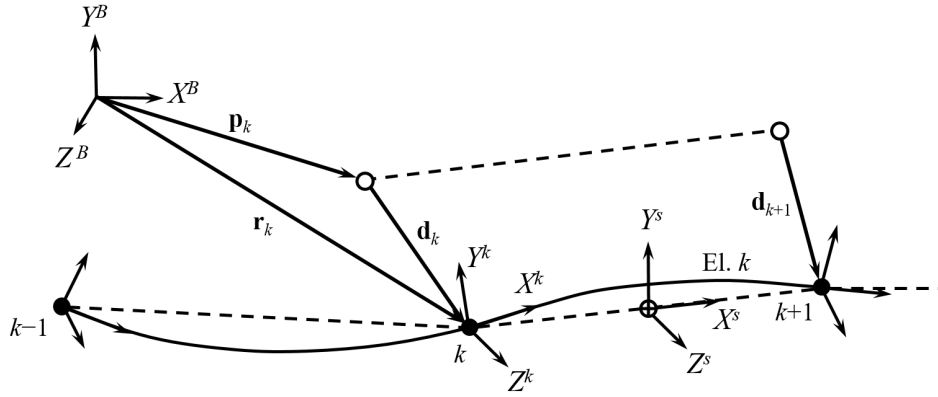


Figure 3: A sketch of a deformed finite beam element, relative to the undeformed location (dashed line with white nodes).

be expressed in terms of a set of displacements $\mathbf{d}_{k/k0}$, relative to \mathbf{p}_k ; and the rotations $\boldsymbol{\theta}_k^{k0}$ that code for \mathbf{T}_k^{k0} , the transform from the deformed to undeformed orientation of the node:

$$\mathbf{q}_k := \begin{bmatrix} \mathbf{d}_{k/k0} \\ \boldsymbol{\theta}_k^{k0} \end{bmatrix}. \quad (34)$$

The \mathbf{q}_k are the degrees-of-freedom for the nodes.

One node on each body, typically the node at the joint closest to the ground, is the reference node. This node has coordinates

$$\mathbf{P}_B := \begin{bmatrix} \mathbf{O}_{B0/g} \\ \boldsymbol{\Phi}_{B0}^g \end{bmatrix}, \quad \mathbf{q}_B := \begin{bmatrix} \mathbf{O}_{B/B0} \\ \boldsymbol{\Phi}_B^{B0} \end{bmatrix} \quad (35)$$

which together specify the origin and orientation of the body with respect to the global coordinate system. That is,

$$\mathbf{T}_B^g = \mathbf{T}_{B0}^g \mathbf{T}_B^{B0}, \quad (36)$$

where \mathbf{T}_{B0}^g is constant.

In addition to the nodal and body reference degrees-of-freedom, in the assembled structure there is an angle associated with each joint: nacelle yaw, driveshaft azimuth, and the pitch of each blade. These angles are adopted as redundant degrees-of-freedom. While it is possible to express the rotation at the joint in terms of the nodal degrees-of-freedom alone, it is more convenient to use the rotation angle. The redundancy is eliminated by the constraint equations, Section 2.5.

The relationship between the exponential map parameters $\boldsymbol{\theta}_b^a$ and transform matrix \mathbf{T}_b^a is

$$\mathbf{T}_b^a = \exp \boldsymbol{\Theta}_b^a; \quad \boldsymbol{\Theta}_b^a = \ln \mathbf{T}_b^a = \begin{bmatrix} 0 & -(\boldsymbol{\theta}_b^a)_z & (\boldsymbol{\theta}_b^a)_y \\ (\boldsymbol{\theta}_b^a)_z & 0 & -(\boldsymbol{\theta}_b^a)_x \\ -(\boldsymbol{\theta}_b^a)_y & (\boldsymbol{\theta}_b^a)_x & 0 \end{bmatrix}. \quad (37)$$

By expanding the infinite series, an exact representation is³

$$\exp \boldsymbol{\Theta}_b^a = \mathbf{I} + \frac{\sin \theta}{\theta} \boldsymbol{\Theta}_b^a + \frac{1 - \cos \theta}{\theta^2} (\boldsymbol{\Theta}_b^a)^2, \quad \theta := \sqrt{(\boldsymbol{\theta}_b^a)_x^2 + (\boldsymbol{\theta}_b^a)_y^2 + (\boldsymbol{\theta}_b^a)_z^2}, \quad (38)$$

³Felippa and Haugen (2005)

from which the partial derivatives $\partial^n \mathbf{T}_b^a / \partial \boldsymbol{\theta}^n$ can be computed, the first being⁴

$$\frac{\partial \mathbf{T}_b^a}{\partial \theta_i} = \frac{\theta_i \boldsymbol{\Theta} + \text{spin}(\boldsymbol{\Theta}(\mathbf{I} - \mathbf{T}_b^a \mathbf{e}_i))}{\boldsymbol{\theta}^T \boldsymbol{\theta}} \mathbf{T}_b^a. \quad (39)$$

Write this as

$$\frac{\partial \mathbf{T}_b^a}{\partial \theta_i} = \mathbf{R}_i(\boldsymbol{\theta}) \mathbf{T}_b^a. \quad (40)$$

Then higher order derivatives are

$$\frac{\partial^2 \mathbf{T}_b^a}{\partial \theta_i \partial \theta_j} = \frac{\partial \mathbf{R}_i}{\partial \theta_j} \mathbf{T}_b^a + \mathbf{R}_i \frac{\partial \mathbf{T}_b^a}{\partial \theta_j} \quad (41)$$

and

$$\frac{\partial^3 \mathbf{T}_b^a}{\partial \theta_i \partial \theta_j \partial \theta_k} = \frac{\partial^2 \mathbf{R}_i}{\partial \theta_j \partial \theta_k} \mathbf{T}_b^a + \frac{\partial \mathbf{R}_i}{\partial \theta_j} \frac{\partial \mathbf{T}_b^a}{\partial \theta_k} + \frac{\partial \mathbf{R}_i}{\partial \theta_k} \frac{\partial \mathbf{T}_b^a}{\partial \theta_j} + \mathbf{R}_i \frac{\partial^2 \mathbf{T}_b^a}{\partial \theta_j \partial \theta_k}. \quad (42)$$

The partial derivatives of \mathbf{R}_i are

$$\frac{\partial \mathbf{R}_i}{\partial \theta_j} = \frac{1}{\boldsymbol{\theta}^T \boldsymbol{\theta}} \left[\delta_j \boldsymbol{\Theta} + \theta_i \frac{\partial \boldsymbol{\Theta}}{\partial \theta_j} + \text{spin} \left(\frac{\partial \boldsymbol{\Theta}}{\partial \theta_j} (\mathbf{I} - \mathbf{T}_b^a) \mathbf{e}_i - \boldsymbol{\Theta} \frac{\partial \mathbf{T}_b^a}{\partial \theta_j} \mathbf{e}_i \right) \right] - 2 \frac{\theta_j}{\boldsymbol{\theta}^T \boldsymbol{\theta}} \mathbf{R}_i \quad (43)$$

and

$$\begin{aligned} \frac{\partial^2 \mathbf{R}_i}{\partial \theta_j \partial \theta_k} = & -2 \frac{\delta_{jk}}{\boldsymbol{\theta}^T \boldsymbol{\theta}} \mathbf{R}_i - 2 \frac{\theta_k}{\boldsymbol{\theta}^T \boldsymbol{\theta}} \frac{\partial \mathbf{R}_i}{\partial \theta_j} - 2 \frac{\theta_j}{\boldsymbol{\theta}^T \boldsymbol{\theta}} \frac{\partial \mathbf{R}_i}{\partial \theta_k} \\ & + \frac{1}{\boldsymbol{\theta}^T \boldsymbol{\theta}} \left[\delta_{ij} \frac{\partial \boldsymbol{\Theta}}{\partial \theta_k} + \delta_{ik} \frac{\partial \boldsymbol{\Theta}}{\partial \theta_j} + \text{spin} \left(-\frac{\partial \boldsymbol{\Theta}}{\partial \theta_j} \frac{\partial \mathbf{T}_b^a}{\partial \theta_k} \mathbf{e}_i - \frac{\partial \boldsymbol{\Theta}}{\partial \theta_k} \frac{\partial \mathbf{T}_b^a}{\partial \theta_j} \mathbf{e}_i - \boldsymbol{\Theta} \frac{\partial^2 \mathbf{T}_b^a}{\partial \theta_j \partial \theta_k} \mathbf{e}_i \right) \right]. \end{aligned} \quad (44)$$

The above equations do not work when θ approaches zero. In the present implementation, when the magnitude of θ is less than $\varepsilon^{1/4}$, ε being the machine precision, alternative equations are employed. These are based on a series expansion of (37) about $\theta = 0$,

$$\mathbf{T}_b^a \approx \mathbf{I} + \left(1 - \frac{\theta^2}{6} + \frac{\theta^4}{120}\right) \boldsymbol{\Theta} + \left(\frac{1}{2} - \frac{\theta^2}{24} + \frac{\theta^4}{720}\right) \boldsymbol{\Theta}^2. \quad (45)$$

Derivatives are then, to second order in θ ,

$$\frac{\partial \mathbf{T}_b^a}{\partial \theta_i} \approx \frac{1}{3} \theta_i \boldsymbol{\Theta} + \left(1 - \frac{\theta^2}{6}\right) \boldsymbol{\Sigma}_i + \frac{1}{2} (\boldsymbol{\Sigma}_i \boldsymbol{\Theta} + \boldsymbol{\Theta} \boldsymbol{\Sigma}_i), \quad (46)$$

$$\begin{aligned} \frac{\partial \mathbf{T}_b^a}{\partial \theta_i \partial \theta_j} \approx & -\frac{1}{3} \delta_{ij} \boldsymbol{\Theta} - \frac{1}{3} \theta_i \boldsymbol{\Sigma}_j - \frac{1}{3} \theta_j \boldsymbol{\Sigma}_i \\ & - \frac{1}{12} \delta_{ij} \boldsymbol{\Theta}^2 - \frac{1}{12} \theta_i (\boldsymbol{\Sigma}_j \boldsymbol{\Theta} + \boldsymbol{\Theta} \boldsymbol{\Sigma}_j) - \frac{1}{12} \theta_j (\boldsymbol{\Sigma}_i \boldsymbol{\Theta} + \boldsymbol{\Theta} \boldsymbol{\Sigma}_i) \\ & + \left(\frac{1}{2} - \frac{\theta^2}{24}\right) (\boldsymbol{\Sigma}_j \boldsymbol{\Sigma}_i + \boldsymbol{\Sigma}_i \boldsymbol{\Sigma}_j) \end{aligned} \quad (47)$$

⁴Grassia (1998) provides a method for computing these derivatives via quaternions, while Gallego (2015) provides a simplified formula in terms of the exponential map parameters.

$$\begin{aligned}
\frac{\partial^3 \mathbf{T}_b^a}{\partial \theta_i \partial \theta_j \partial \theta_k} &\approx \frac{1}{15} \delta_{ij} \theta_k \boldsymbol{\Theta} + \frac{1}{15} \delta_{ik} \theta_j \boldsymbol{\Theta} + \frac{1}{15} \delta_{jk} \theta_i \boldsymbol{\Theta} \\
&+ \frac{1}{15} \theta_j \theta_k \boldsymbol{\Sigma}_i + \frac{1}{15} \theta_i \theta_j \boldsymbol{\Sigma}_k + \frac{1}{15} \theta_i \theta_k \boldsymbol{\Sigma}_j \\
&+ \left(-\frac{1}{3} + \frac{\theta^2}{30} \right) \delta_{jk} \boldsymbol{\Sigma}_i + \left(-\frac{1}{3} + \frac{\theta^2}{30} \right) \delta_{ij} \boldsymbol{\Sigma}_k + \left(-\frac{1}{3} + \frac{\theta^2}{30} \right) \delta_{ik} \boldsymbol{\Sigma}_j \\
&- \frac{1}{12} \delta_{jk} (\boldsymbol{\Sigma}_i \boldsymbol{\Theta} + \boldsymbol{\Theta} \boldsymbol{\Sigma}_i) - \frac{1}{12} \delta_{ij} (\boldsymbol{\Sigma}_k \boldsymbol{\Theta} + \boldsymbol{\Theta} \boldsymbol{\Sigma}_k) - \frac{1}{12} \delta_{ik} (\boldsymbol{\Sigma}_j \boldsymbol{\Theta} + \boldsymbol{\Theta} \boldsymbol{\Sigma}_j) \\
&- \frac{1}{12} \theta_j (\boldsymbol{\Sigma}_k \boldsymbol{\Sigma}_i + \boldsymbol{\Sigma}_i \boldsymbol{\Sigma}_k) - \frac{1}{12} \theta_j (\boldsymbol{\Sigma}_j \boldsymbol{\Sigma}_i + \boldsymbol{\Sigma}_i \boldsymbol{\Sigma}_j) - \frac{1}{12} \theta_j (\boldsymbol{\Sigma}_k \boldsymbol{\Sigma}_j + \boldsymbol{\Sigma}_j \boldsymbol{\Sigma}_k).
\end{aligned} \tag{48}$$

The orientation of the element section coordinate system – which determines the rigid-body motion of the element – is determined by the following rules. Its origin, sketched in Fig. 3, lies at the midpoint between the nodes. The X^s axis is aligned with the line connecting the nodes. Then, the orientation of the Y^s and Z^s axes – that is, the twist about the X^s axis – is determined as a best fit to the orientation of the Y^n and Z^n axes at the adjacent nodes. On the blades, this position and orientation differs from the aerodynamic section coordinate system only by a single rotation, about the X^s axis by the structural twist angle.

We are given \mathbf{r}_{k+1} and \mathbf{r}_k , and rotations $\boldsymbol{\theta}_{k+1}$ and $\boldsymbol{\theta}_k$, with corresponding transforms $\mathbf{T}_{n,k+1}^{n0}$ and $\mathbf{T}_{n,k}^{n0}$. The definition of the nodal coordinate system is arbitrary; but the transforms $\mathbf{T}_{n0,k}^{s0,k}$ and $\mathbf{T}_{n0,k+1}^{s0,k}$ between the undeformed nodal and element section coordinate systems are needed. Here a convention is chosen whereby the undeformed nodal coordinate system of node $k+1$ is aligned with the undeformed section coordinate system of element k . This gives

$$\mathbf{T}_{n0,k+1}^{s0,k} = \mathbf{I} \quad \text{and} \quad \mathbf{T}_{n0,k}^{s0,k} = \mathbf{T}_{s0,k-1}^{s0,k} = \mathbf{T}_B^{s0,k} \mathbf{T}_{s0,k-1}^B. \tag{49}$$

When the structure deforms, the element origin is located at $(\mathbf{r}_{k+1} + \mathbf{r}_k)/2$. The X^s axis is aligned with $\mathbf{r}_{k+1} - \mathbf{r}_k$, and so

$$\mathbf{x}_s^B = (\mathbf{T}_s^B)_{k1} = \frac{\mathbf{r}_{k+1}^B - \mathbf{r}_k^B}{|\mathbf{r}_{k+1} - \mathbf{r}_k|}. \tag{50}$$

The reference twist of the element section coordinate system is important, as it has a significant influence on the aerodynamic loads, via the angle-of-attack. It must be an accurate average, in some sense, of the deformed orientations of the adjacent nodes. To this end, let us define two “element” coordinate systems, one associated with each node, initially aligned with the undeformed element section coordinate system. Let these element coordinates deform independently, following the deformation of each node. In the deformed pose, we can then write

$$\mathbf{T}_{e,k}^{s0,k} = \mathbf{T}_{n0,k}^{s0,k} \mathbf{T}_{n,k}^{n0}(\boldsymbol{\theta}_k) \mathbf{T}_{s0,k}^{n0,k} \quad \text{and} \quad \mathbf{T}_{e,k+1}^{s0,k} = \mathbf{T}_{n,k+1}^{n0}(\boldsymbol{\theta}_{k+1}) \tag{51}$$

for nodes k and $k+1$, respectively. Now, $\mathbf{T}_{e,k}^{s0,k}$ and $\mathbf{T}_{e,k+1}^{s0,k}$ differ only by the small elastic deformations of the element. Let the direction of a $Y^{s'}$ axis be defined by a vector $\mathbf{y}_{s'}^B$, according to

$$\mathbf{y}_{s'}^B = \frac{1}{2} \mathbf{T}_{s0,k}^B [(\mathbf{T}_{e,k}^{s0,k})_2 + (\mathbf{T}_{e,k+1}^{s0,k})_2]; \tag{52}$$

that is, the average of the second columns of the transforms, intermediate in direction between the Y^e axes associated with each node. Finally, the Y^s and Z^s axes may be computed as

$$\mathbf{z}_s^B = (\mathbf{T}_s^B)_{k3} = \frac{\mathbf{x}_s^B \times \mathbf{y}_{s'}^B}{|\mathbf{x}_s^B \times \mathbf{y}_{s'}^B|}; \quad \mathbf{y}_s^B = (\mathbf{T}_s^B)_{k2} = \frac{\mathbf{z}_s^B \times \mathbf{x}_s^B}{|\mathbf{z}_s^B \times \mathbf{x}_s^B|}, \tag{53}$$

ensuring unit length and orthogonality with the \mathbf{x}_s^B axis.

The *elastic* rotations at the nodes, associated with the element, can be found by computing

$$\boldsymbol{\zeta}_{n/s}^s = \frac{1}{2} \begin{bmatrix} (\mathbf{T}_e^s)_{32} - (\mathbf{T}_e^s)_{23} \\ (\mathbf{T}_e^s)_{13} - (\mathbf{T}_e^s)_{31} \\ (\mathbf{T}_e^s)_{21} - (\mathbf{T}_e^s)_{12} \end{bmatrix}; \quad \mathbf{T}_e^s = \mathbf{T}_B^s \mathbf{T}_{s0}^B \mathbf{T}_{n0}^{s0} \mathbf{T}_n^{n0} \mathbf{T}_{s0}^{n0}. \quad (54)$$

Due to the definition of the section coordinate system, the elastic displacement is limited to axial stretch,

$$\begin{aligned} \delta_x &= L - L_0 = (\mathbf{r}_{k+1}^s)_x - (\mathbf{r}_k^s)_x - L_0 \\ &= [1 \ 0 \ 0] [\mathbf{T}_B^s (\mathbf{p}_2^B + \mathbf{d}_2^B - \mathbf{p}_1^B - \mathbf{d}_1^B) - \mathbf{T}_B^{s0} (\mathbf{p}_2^B - \mathbf{p}_1^B)]. \end{aligned} \quad (55)$$

The time derivative of the elastic rotations is needed in the equations of motion. This is computed as

$$\frac{d\boldsymbol{\zeta}_{n/s}^s}{dt} = \frac{\partial \boldsymbol{\zeta}_{n/s}^s}{\partial (\mathbf{T}_n^s)_{ij}} \frac{\partial (\mathbf{T}_n^s)_{ij}}{\partial q_k} \frac{dq_k}{dt}, \quad (56)$$

$$\frac{\partial \mathbf{T}_n^s}{\partial q_k} = \frac{\partial \mathbf{T}_B^s}{\partial q_k} \mathbf{T}_{s0}^B \mathbf{T}_{n0}^{s0} \mathbf{T}_n^{n0} \mathbf{T}_{s0}^{n0} + \mathbf{T}_B^s \mathbf{T}_{s0}^B \mathbf{T}_{n0}^{s0} \frac{\partial \mathbf{T}_n^{n0}}{\partial \theta_k} \mathbf{T}_{s0}^{n0}. \quad (57)$$

Derivatives of \mathbf{T}_s^B are thus needed in parts of the calculation. Note that

$$\mathbf{x}_s^B(\mathbf{r}), \quad \mathbf{y}_{s'}^B(\boldsymbol{\theta}), \quad \mathbf{z}_s^B(\mathbf{x}_s^B, \mathbf{y}_{s'}^B), \quad \mathbf{y}_s^B(\mathbf{x}_s^B, \mathbf{z}_s^B).$$

For the terms involving cross products,

$$\frac{\partial}{\partial a_i} \frac{\mathbf{a} \times \mathbf{b}}{|\mathbf{a} \times \mathbf{b}|} = \frac{(\mathbf{e}_i \times \mathbf{b})(\mathbf{a} \times \mathbf{b})^T (\mathbf{a} \times \mathbf{b}) - (\mathbf{a} \times \mathbf{b})(\mathbf{e}_i \times \mathbf{b})^T (\mathbf{a} \times \mathbf{b})}{|\mathbf{a} \times \mathbf{b}| (\mathbf{a} \times \mathbf{b})^T (\mathbf{a} \times \mathbf{b})}. \quad (58)$$

Also,

$$\frac{\partial}{\partial a_i} \frac{\mathbf{a} - \mathbf{b}}{|\mathbf{a} - \mathbf{b}|} = \frac{\mathbf{e}_i (\mathbf{a} - \mathbf{b})^T (\mathbf{a} - \mathbf{b}) - (\mathbf{a} - \mathbf{b}) \mathbf{e}_i^T (\mathbf{a} - \mathbf{b})}{|\mathbf{a} - \mathbf{b}| (\mathbf{a} - \mathbf{b})^T (\mathbf{a} - \mathbf{b})}. \quad (59)$$

Then

$$\frac{\partial \mathbf{T}_s^B}{\partial r_i} = \left[\frac{\partial \mathbf{x}_s^B}{\partial r_i}, \quad \frac{\partial \mathbf{y}_{s'}^B}{\partial \mathbf{x}_s^B} \frac{\partial \mathbf{x}_s^B}{\partial r_i} + \frac{\partial \mathbf{y}_{s'}^B}{\partial \mathbf{z}_s^B} \frac{\partial \mathbf{z}_s^B}{\partial \mathbf{x}_s^B} \frac{\partial \mathbf{x}_s^B}{\partial r_i}, \quad \frac{\partial \mathbf{z}_s^B}{\partial \mathbf{x}_s^B} \frac{\partial \mathbf{x}_s^B}{\partial r_i} \right] \quad (60)$$

and

$$\frac{\partial \mathbf{T}_s^B}{\partial \theta_i} = \left[\mathbf{0}, \quad \frac{\partial \mathbf{y}_{s'}^B}{\partial \mathbf{z}_s^B} \frac{\partial \mathbf{z}_s^B}{\partial \mathbf{y}_{s'}^B} \frac{\partial \mathbf{y}_{s'}^B}{\partial \theta_i}, \quad \frac{\partial \mathbf{z}_s^B}{\partial \mathbf{y}_{s'}^B} \frac{\partial \mathbf{y}_{s'}^B}{\partial \theta_i} \right]. \quad (61)$$

2.4 Lagrange equations

The equations of motion are developed using the Lagrange equations, written as

$$\frac{d}{dt} \frac{\partial E_K}{\partial \dot{\mathbf{q}}} + \frac{1}{2} \frac{\partial \dot{E}_D}{\partial \dot{\mathbf{q}}} + \frac{\partial E_P}{\partial \mathbf{q}} = \frac{\partial E_K}{\partial \mathbf{q}} + \frac{\partial W}{\partial \mathbf{q}}. \quad (62)$$

The term $\partial E_K / \partial \mathbf{q}$ is responsible for centrifugal stiffening of the blade, a coupling between bending and centrifugal forces which tends to stiffen the structure in bending. Centrifugal stiffening appears naturally in $\partial E_K / \partial \mathbf{q}$ when the blade nodes are allowed to displace radially as the blade bends. The most basic formulation of finite beam elements does not provide this coupling between bending and radial displacement. In previous versions of the STAS aeroelastic model, centrifugal stiffening was accounted for by an ad-hoc modification to the structural stiffness matrix.

We revisit the equations of motion from earlier versions of STAS (Merz 2015, 2016) in light of the definitions (33) and (34) for the degrees-of-freedom. In contrast with the previous versions of

STAS, which defined the pose of each body with respect to a reference coordinate system attached to the previous body, now the pose is defined relative to the global coordinate system. The bodies are connected at joints which, with the exception of the rigid foundation-tower connection, allow revolution about an axis. The axis of revolution follows the deformed position of the structure at the joint.

Let us formulate the equations of motion for a single element. These will later be superposed to obtain the equations for the entire structure. The element degrees-of-freedom are

$$\mathbf{q}_e = [\mathbf{d}_{m/m0} \quad \boldsymbol{\theta}_m^{n0} \quad \mathbf{d}_{n/n0} \quad \boldsymbol{\theta}_n^{n0}]^T. \quad (63)$$

That is, for each node, the displacement relative to the undeformed position of the node, and the parameters coding for the transform from the displaced to undeformed orientation of the node. The position of a node, relative to global coordinates, is

$$\mathbf{r}_{n/g}^g = \mathbf{O}_{B0/g}^g + \mathbf{O}_{B/B0}^g + \mathbf{p}_{n0/B}^g + \mathbf{d}_{n/n0}^g. \quad (64)$$

In terms of (33) and (34), this works out to

$$\mathbf{r}_{n/g}^g = \mathbf{O}_{B0/g}^g + \mathbf{O}_{B/B0}^g + \mathbf{T}_B^g (\mathbf{p}_{n0/B}^B + \mathbf{d}_{n/n0}^B). \quad (65)$$

which can also be written

$$\mathbf{r}_{n/g}^g = [\mathbf{I} \quad \mathbf{0} \quad \mathbf{I} \quad \mathbf{0}] \begin{bmatrix} \mathbf{I} & & & \mathbf{0} \\ & \mathbf{I} & & \\ & & \mathbf{T}_B^g & \\ \mathbf{0} & & & \mathbf{I} \end{bmatrix} \left(\begin{bmatrix} \mathbf{O}_{B/B0}^g \\ \boldsymbol{\Phi}_{B0}^g \\ \mathbf{d}_{n/n0}^B \\ \boldsymbol{\theta}_n^{n0} \end{bmatrix} + \begin{bmatrix} \mathbf{O}_{B0/g}^g \\ \boldsymbol{\Phi}_{B0}^g \\ \mathbf{p}_{n0/B}^B \\ \boldsymbol{\xi}_{n0}^B \end{bmatrix} \right) \quad (66)$$

or

$$\mathbf{r}_{n/g}^g = \mathbf{A}_n \tilde{\mathbf{T}}_B^g (\mathbf{q} + \mathbf{P}), \quad \mathbf{q} := \begin{bmatrix} \mathbf{q}_B \\ \mathbf{q}_n \end{bmatrix}, \quad \mathbf{P} := \begin{bmatrix} \mathbf{P}_B \\ \mathbf{P}_n \end{bmatrix}. \quad (67)$$

The transforms that multiply \mathbf{q} and \mathbf{P} have the identity matrix in the part associated with rotations, and as a reminder of this they are marked with tildes. The reason is that the exponential map parameters do not transform as vectors; rather, they code for a particular transformation matrix. The linear velocity is obtained by taking the time derivative of (67), giving

$$\mathbf{v}_{n/g}^g = \frac{d\mathbf{r}_{n/g}^g}{dt} = \mathbf{A}_n \tilde{\mathbf{T}}_B^g \frac{d\mathbf{q}}{dt} + \mathbf{A}_n \frac{d\tilde{\mathbf{T}}_B^g}{dt} (\mathbf{q} + \mathbf{P}). \quad (68)$$

The rotation of a node relative to the body coordinate system is $\mathbf{T}_{n0}^B \mathbf{T}_n^{n0}$; the former is encoded by the constant $\boldsymbol{\xi}_{n0}^B$, the latter by $\boldsymbol{\theta}_n^{n0}$. The rotation of the body relative to the undeformed orientation, \mathbf{T}_B^{B0} , is encoded by $\boldsymbol{\Phi}_{B0}^g$, and the initial orientation relative to global coordinates, \mathbf{T}_{B0}^g , is encoded by $\boldsymbol{\Phi}_{B0}^g$. The angular velocity of a node relative to global coordinates is

$$\mathbf{S}_{n/g}^g = \begin{bmatrix} 0 & -(\boldsymbol{\omega}_{n/g}^g)_z & (\boldsymbol{\omega}_{n/g}^g)_y \\ (\boldsymbol{\omega}_{n/g}^g)_z & 0 & -(\boldsymbol{\omega}_{n/g}^g)_x \\ -(\boldsymbol{\omega}_{n/g}^g)_y & (\boldsymbol{\omega}_{n/g}^g)_x & 0 \end{bmatrix} = \frac{d\mathbf{T}_n^g}{dt} \mathbf{T}_n^g; \quad \mathbf{T}_n^g = \mathbf{T}_{B0}^g \mathbf{T}_B^{B0} \mathbf{T}_{n0}^B \mathbf{T}_n^{n0}. \quad (69)$$

In terms of the rotations,

$$\begin{aligned} \mathbf{S}_{n/g}^g &= \frac{d\mathbf{T}_n^g}{dt} \mathbf{T}_n^g = \mathbf{T}_{B0}^g \frac{\partial \mathbf{T}_B^{B0}}{\partial (\boldsymbol{\Phi}_{B0}^g)_j} \mathbf{T}_{B0}^g \mathbf{T}_g^{B0} \frac{d(\boldsymbol{\Phi}_{B0}^g)_j}{dt} \\ &\quad + \mathbf{T}_{B0}^g \mathbf{T}_B^{B0} \mathbf{T}_{n0}^B \frac{d\mathbf{T}_n^{n0}}{\partial (\boldsymbol{\theta}_n^{n0})_j} \mathbf{T}_{n0}^B \mathbf{T}_{B0}^g \mathbf{T}_g^{B0} \frac{d(\boldsymbol{\theta}_n^{n0})_j}{dt}. \end{aligned} \quad (70)$$

Equation 70 establishes a relationship between the rotation parameters and the angular velocity. If we define

$$\mathbf{F}_j = \mathbf{T}_{B0}^g \frac{\partial \mathbf{T}_B^{B0}}{\partial (\Phi_B^{B0})_j} \mathbf{T}_B^B \mathbf{T}_g^{B0} \quad \text{and} \quad \mathbf{G}_j = \mathbf{T}_{B0}^g \mathbf{T}_B^{B0} \mathbf{T}_B^B \frac{d\mathbf{T}_n^{n0}}{\partial (\theta_n^{n0})_j} \mathbf{T}_n^n \mathbf{T}_B^{n0} \mathbf{T}_B^B \mathbf{T}_g^{B0}, \quad (71)$$

then (70) can be written in a vector form,

$$\begin{aligned} \boldsymbol{\omega}_{n/g}^g &= \begin{bmatrix} -F_{x,23} & -F_{y,23} & -F_{z,23} \\ F_{x,13} & F_{y,13} & F_{z,13} \\ -F_{x,12} & -F_{y,12} & -F_{z,12} \end{bmatrix} \frac{d\Phi_B^{B0}}{dt} + \begin{bmatrix} -G_{x,23} & -G_{y,23} & -G_{z,23} \\ G_{x,13} & G_{y,13} & G_{z,13} \\ -G_{x,12} & -G_{y,12} & -G_{z,12} \end{bmatrix} \frac{\boldsymbol{\theta}_n^{n0}}{dt} \\ &= \tilde{\mathbf{F}} \frac{d\Phi_B^{B0}}{dt} + \tilde{\mathbf{G}} \frac{d\boldsymbol{\theta}_n^{n0}}{dt}. \end{aligned} \quad (72)$$

Combining this with (68), we can write

$$\begin{bmatrix} \mathbf{v}_{n/g}^B \\ \boldsymbol{\omega}_{n/g}^B \end{bmatrix} = \mathbf{T}_{B0}^B \mathbf{T}_g^{B0} \left(\tilde{\mathbf{A}}_n \tilde{\mathbf{T}}_{B0}^g \tilde{\mathbf{T}}_B^{B0} \frac{d\mathbf{q}}{dt} + \mathbf{A}_n \tilde{\mathbf{T}}_{B0}^g \frac{d\tilde{\mathbf{T}}_B^{B0}}{dt} (\mathbf{q} + \mathbf{P}) \right), \quad (73)$$

where $\tilde{\mathbf{A}}_n$ includes the angular velocity,⁵ specifically

$$\tilde{\mathbf{A}}_n = \begin{bmatrix} \mathbf{I} & \mathbf{0} & \mathbf{I} & \mathbf{0} \\ \mathbf{0} & \tilde{\mathbf{F}}(\Phi) & \mathbf{0} & \tilde{\mathbf{G}}(\Phi, \boldsymbol{\theta}) \end{bmatrix} \quad \text{and} \quad \mathbf{A}_n = \begin{bmatrix} \mathbf{I} & \mathbf{0} & \mathbf{I} & \mathbf{0} \\ \mathbf{0} & \mathbf{0} & \mathbf{0} & \mathbf{0} \end{bmatrix} \quad (74)$$

The $\tilde{\mathbf{A}}_n$ matrix differs from that in earlier versions of the STAS documentation. Some caution is required regarding the transforms in (73). Once multiplied by $\tilde{\mathbf{A}}_n$, the resulting rotational quantities become *angular velocities*, and *these transform as vectors*. Thus the transforms in (73) without a tilde transform both the translational and rotational parts.

From (70), the time derivatives of the transform matrices can be expanded as

$$\frac{d\mathbf{T}_B^{B0}}{dt} = \frac{\partial \mathbf{T}_B^{B0}}{\partial (\Phi_B^{B0})_j} \frac{d(\Phi_B^{B0})_j}{dt}. \quad (75)$$

Thus (73) can be written

$$\begin{bmatrix} \mathbf{v}_{n/g}^B \\ \boldsymbol{\omega}_{n/g}^B \end{bmatrix} = \mathbf{T}_{B0}^B \mathbf{T}_g^{B0} \left(\tilde{\mathbf{A}}_n \tilde{\mathbf{T}}_{B0}^g \tilde{\mathbf{T}}_B^{B0} + \mathbf{A}_n \tilde{\mathbf{T}}_{B0}^g \frac{\partial \tilde{\mathbf{T}}_B^{B0}}{\partial \mathbf{q}} (\mathbf{q} + \mathbf{P}) \right) \frac{d\mathbf{q}}{dt} \quad (76)$$

or

$$\begin{bmatrix} \mathbf{v}_{n/g}^B \\ \boldsymbol{\omega}_{n/g}^B \end{bmatrix} = \mathbf{Q}_v(\mathbf{q}) \frac{d\mathbf{q}}{dt}. \quad (77)$$

The first derivative of \mathbf{Q}_v is needed for the equations of motion; in general this is

$$\begin{aligned} \frac{\partial (\mathbf{Q}_v)_i}{\partial q_j} &= \frac{\partial \mathbf{T}_{B0}^B \mathbf{T}_g^{B0}}{\partial q_j} \left((\tilde{\mathbf{A}}_n \tilde{\mathbf{T}}_{B0}^g \tilde{\mathbf{T}}_B^{B0})_i + \mathbf{A}_n \tilde{\mathbf{T}}_{B0}^g \frac{\partial \tilde{\mathbf{T}}_B^{B0}}{\partial q_i} (\mathbf{q} + \mathbf{P}) \right) \\ &+ \mathbf{T}_{B0}^B \mathbf{T}_g^{B0} \left(\frac{\partial \tilde{\mathbf{A}}_n \tilde{\mathbf{T}}_{B0}^g \tilde{\mathbf{T}}_B^{B0}}{\partial q_j} + \tilde{\mathbf{A}}_n \tilde{\mathbf{T}}_{B0}^g \frac{\partial \tilde{\mathbf{T}}_B^{B0}}{\partial q_j} \right)_i \\ &+ \mathbf{T}_{B0}^B \mathbf{T}_g^{B0} \left[\mathbf{A}_n \tilde{\mathbf{T}}_{B0}^g \frac{\partial^2 \tilde{\mathbf{T}}_B^{B0}}{\partial q_i \partial q_j} (\mathbf{q} + \mathbf{P}) + \left(\mathbf{A}_n \tilde{\mathbf{T}}_{B0}^g \frac{\partial \tilde{\mathbf{T}}_B^{B0}}{\partial q_i} \right)_j \right], \end{aligned} \quad (78)$$

⁵In (73), the rotation parameters do not transform as vectors. It is understood that the transforms apply only to the position degrees-of-freedom, and multiply the rotation degrees-of-freedom with the identity.

which evaluates to

$$\frac{\partial(\mathbf{Q}_v)_i}{\partial O_j} = \frac{\partial(\mathbf{Q}_v)_i}{\partial d_j} = \mathbf{T}_{B_0}^B \mathbf{T}_g^{B_0} \left(\mathbf{A}_n \tilde{\mathbf{T}}_{B_0}^g \frac{\partial \tilde{\mathbf{T}}_B^{B_0}}{\partial \Phi_i} \right)_j, \quad (79)$$

$$\begin{aligned} \frac{\partial(\mathbf{Q}_v)_i}{\partial \Phi_j} &= \frac{\partial \mathbf{T}_{B_0}^B}{\partial \Phi_j} \mathbf{T}_g^{B_0} \left((\tilde{\mathbf{A}}_n \tilde{\mathbf{T}}_{B_0}^g \tilde{\mathbf{T}}_B^{B_0})_i + \mathbf{A}_n \tilde{\mathbf{T}}_{B_0}^g \frac{\partial \tilde{\mathbf{T}}_B^{B_0}}{\partial \Phi_i} (\mathbf{q} + \mathbf{P}) \right) \\ &+ \mathbf{T}_{B_0}^B \mathbf{T}_g^{B_0} \left(\frac{\partial \tilde{\mathbf{A}}_n}{\partial \Phi_j} \tilde{\mathbf{T}}_{B_0}^g \tilde{\mathbf{T}}_B^{B_0} + \tilde{\mathbf{A}}_n \tilde{\mathbf{T}}_{B_0}^g \frac{\partial \tilde{\mathbf{T}}_B^{B_0}}{\partial \Phi_j} \right)_i \\ &+ \mathbf{T}_{B_0}^B \mathbf{T}_g^{B_0} \mathbf{A}_n \tilde{\mathbf{T}}_{B_0}^g \frac{\partial^2 \tilde{\mathbf{T}}_B^{B_0}}{\partial \Phi_i \partial \Phi_j} (\mathbf{q} + \mathbf{P}), \end{aligned} \quad (80)$$

and

$$\frac{\partial(\mathbf{Q}_v)_i}{\partial \theta_j} = \mathbf{T}_{B_0}^g \mathbf{T}_g^{B_0} \left(\frac{\partial \tilde{\mathbf{A}}_n}{\partial \theta_j} \tilde{\mathbf{T}}_{B_0}^g \tilde{\mathbf{T}}_B^{B_0} \right)_i \quad (81)$$

with

$$\frac{\partial \tilde{\mathbf{A}}_n}{\partial q_i} = \begin{bmatrix} \mathbf{0} & \mathbf{0} & \mathbf{0} & \mathbf{0} \\ \mathbf{0} & \partial \mathbf{F} / \partial q_i & \mathbf{0} & \partial \mathbf{G} / \partial q_i \end{bmatrix}. \quad (82)$$

Linearization of the equations of motion requires yet a further derivative, but this is left to Section 3.

With $\mathbf{u}_e = [\mathbf{v}_{1/g}^B, \boldsymbol{\omega}_{1/g}^B, \mathbf{v}_{2/g}^B, \boldsymbol{\omega}_{2/g}^B]$ expressed in body coordinates, the kinetic energy associated with the element is

$$E_K = \frac{1}{2} \mathbf{u}_e^T \mathbf{T}_s^B \mathbf{m}_e^s \mathbf{T}_B^s \mathbf{u}_e. \quad (83)$$

Computing the terms in the Lagrange equations,

$$\frac{\partial E_K}{\partial \dot{q}_i} = \frac{\partial \mathbf{u}_e^T}{\partial \dot{q}_i} \mathbf{m}_e^B \mathbf{u}_e, \quad (84)$$

such that

$$\begin{aligned} \frac{d}{dt} \frac{\partial E_K}{\partial \dot{q}_i} &= \left(\frac{\partial \mathbf{u}_e^T}{\partial \dot{q}_i} \mathbf{T}_s^B \mathbf{m}_e^s \mathbf{T}_B^s \frac{\partial \mathbf{u}_e}{\partial \dot{q}_j} \right) \frac{d^2 q_j}{dt^2} + \left[\frac{\partial^2 \mathbf{u}_e^T}{\partial \dot{q}_i \partial \dot{q}_j} \mathbf{T}_s^B \mathbf{m}_e^s \mathbf{T}_B^s \mathbf{u}_e \right. \\ &+ \left. \frac{\partial \mathbf{u}_e^T}{\partial \dot{q}_i} \mathbf{T}_s^B \mathbf{m}_e^s \mathbf{T}_B^s \frac{\partial \mathbf{u}_e}{\partial q_j} + \frac{\partial \mathbf{u}_e^T}{\partial \dot{q}_i} \left(\frac{\partial \mathbf{T}_s^B}{\partial q_j} \mathbf{m}_e^s \mathbf{T}_B^s + \mathbf{T}_s^B \mathbf{m}_e^s \frac{\partial \mathbf{T}_B^s}{\partial q_j} \right) \mathbf{u}_e \right] \frac{dq_j}{dt}. \end{aligned} \quad (85)$$

Here the first term has been simplified by noting that $\partial^2 \mathbf{u}_e^T / \partial \dot{q}_i \partial \dot{q}_j = \mathbf{0}$. Also, for any given node,

$$\frac{\partial \mathbf{u}_e}{\partial \dot{q}_i} = (\mathbf{Q}_v)_i, \quad \frac{\partial^2 \mathbf{u}_e}{\partial \dot{q}_i \partial q_j} = \frac{\partial(\mathbf{Q}_v)_i}{\partial q_j}, \quad \text{and} \quad \frac{\partial \mathbf{u}_e}{\partial q_i} = \frac{\partial \mathbf{Q}_v}{\partial q_i} \frac{d\mathbf{q}}{dt}. \quad (86)$$

The next term is

$$\frac{\partial E_K}{\partial q_i} = \frac{\partial \mathbf{u}_e^T}{\partial q_i} \mathbf{T}_s^B \mathbf{m}_e^s \mathbf{T}_B^s \mathbf{u}_e + \mathbf{u}_e^T \frac{\partial \mathbf{T}_s^B}{\partial q_i} \mathbf{m}_e^s \mathbf{T}_B^s \mathbf{u}_e. \quad (87)$$

This can be expressed in terms of \mathbf{q} and $d\mathbf{q}/dt$ using (77) and (86).

The potential energy can be written

$$E_P = \frac{1}{2} \boldsymbol{\mu}_e^T \mathbf{k}_e^s \boldsymbol{\mu}_e, \quad \boldsymbol{\mu}_e = [\delta_{x,1}^s, 0, 0, \boldsymbol{\zeta}_1^s, \delta_{x,2}^s, 0, 0, \boldsymbol{\zeta}_2^s], \quad (88)$$

where δ_x from (55) is the elastic extension, while $\boldsymbol{\zeta}^s$ is a vector of three small elastic nodal rotations, (54). Note that half the extension δ_x is associated with node 1, and the other half with node 2. The term in the equations of motion is

$$\frac{\partial E_P}{\partial q_i} = \frac{\partial \boldsymbol{\mu}_e^T}{\partial q_i} \mathbf{k}_e^s \boldsymbol{\mu}_e. \quad (89)$$

Structural damping – that which is inherent to the structural deformation, apart from any externally applied forces – can be implemented in one of two ways. The preferred way is to work with equations that have been reduced in terms of natural modes of vibration, and assign each structural mode an empirical damping ratio; a bit under 1% is typical. Modal damping is described in Section 3.3. Alternatively, one can work directly with an element damping matrix \mathbf{c}_e^s . In this case, the term in the Lagrange equations is

$$\frac{\partial \dot{E}_D}{\partial \dot{q}_i} = \left(\frac{\partial \boldsymbol{\mu}_e^T}{\partial q_i} \mathbf{c}_e^s \frac{\partial \boldsymbol{\mu}_e}{\partial q_j} \right) \frac{dq_j}{dt}. \quad (90)$$

The term in parentheses is an element damping matrix, in generalized coordinates. It is common practice, though questionable both theoretically and empirically, to specify \mathbf{c}_e^s as some linear combination of the element mass and stiffness matrices,

$$\mathbf{c}_e^s = \alpha \mathbf{m}_e^s + \beta \mathbf{k}_e^s. \quad (91)$$

The stiffness-proportional term β is more important, as this tends to preferentially damp extraneous high-frequency vibrations. With some trial and error, values of α and β can be found that effectively damp high-frequency noise, while not unduly influencing the important low-frequency response.

The incremental work done during deformation by the applied forces is

$$\delta W = (\delta \mathbf{x}_{/g}^g)^T \mathbf{F}^g, \quad (92)$$

where $\delta \mathbf{x}_{/g}^g$ is an incremental displacement or rotation of the nodes, relative to global coordinates. Then,

$$\frac{\partial W}{\partial q_i} = \frac{\partial W}{\partial \mathbf{x}_{/g}^g} \frac{\partial \mathbf{x}_{/g}^g}{\partial q_i}, \quad (93)$$

leading to

$$\frac{\partial W}{\partial q_i} = \frac{\partial (\mathbf{x}_{/g}^g)^T}{\partial q_i} \mathbf{T}_{B0}^g \mathbf{T}_B^{B0} \mathbf{F}^B. \quad (94)$$

The term

$$\frac{\partial (\mathbf{x}_{/g}^g)^T}{\partial q_i} \mathbf{T}_{B0}^g \mathbf{T}_B^{B0}$$

is essentially the transpose of (76),

$$\frac{\partial (\mathbf{x}_{/g}^g)^T}{\partial q_i} \mathbf{T}_{B0}^g \mathbf{T}_B^{B0} = \left\{ \mathbf{T}_{B0}^B \mathbf{T}_g^{B0} \left(\tilde{\mathbf{A}}_n \tilde{\mathbf{T}}_{B0}^g \tilde{\mathbf{T}}_B^{B0} + \mathbf{A}_n \tilde{\mathbf{T}}_{B0}^g \frac{\partial \tilde{\mathbf{T}}_B^{B0}}{\partial \mathbf{q}} (\mathbf{q} + \mathbf{P}) \right) \right\}^T, \quad (95)$$

where again the tildes on the \mathbf{T} 's serve as a reminder to transform only the translational degrees-of-freedom.

The pieces are now in place to write the nonlinear equations of motion. In shorthand tensor notation,

$$\tilde{M}_{ij} \frac{d^2 q_j}{dt^2} + (\tilde{C}_{ij} + \tilde{G}_{ij}) \frac{dq_j}{dt} - \tilde{H}_i + \tilde{K}_i = \tilde{Q}_{ij} F_j^B, \quad (96)$$

where

$$\begin{aligned} \tilde{M}_{ij} &= \sum \frac{\partial \mathbf{u}_e^T}{\partial \dot{q}_i} \mathbf{T}_s^B \mathbf{m}_e^s \mathbf{T}_B^s \frac{\partial \mathbf{u}_e}{\partial \dot{q}_j} \\ \tilde{G}_{ij} &= \sum \left[\frac{\partial^2 \mathbf{u}_e^T}{\partial \dot{q}_i \partial \dot{q}_j} \mathbf{T}_s^B \mathbf{m}_e^s \mathbf{T}_B^s \mathbf{u}_e + \frac{\partial \mathbf{u}_e^T}{\partial \dot{q}_i} \mathbf{T}_s^B \mathbf{m}_e^s \mathbf{T}_B^s \frac{\partial \mathbf{u}_e}{\partial q_j} + \frac{\partial \mathbf{u}_e^T}{\partial \dot{q}_i} \left(\frac{\partial \mathbf{T}_s^B}{\partial q_j} \mathbf{m}_e^s \mathbf{T}_B^s + \mathbf{T}_s^B \mathbf{m}_e^s \frac{\partial \mathbf{T}_B^s}{\partial q_j} \right) \mathbf{u}_e \right] \\ \tilde{H}_i &= \sum \left(\frac{\partial \mathbf{u}_e^T}{\partial q_i} \mathbf{T}_s^B \mathbf{m}_e^s \mathbf{T}_B^s \mathbf{u}_e + \mathbf{u}_e^T \frac{\partial \mathbf{T}_s^B}{\partial q_i} \mathbf{m}_e^s \mathbf{T}_B^s \mathbf{u}_e \right) \end{aligned} \quad (97)$$

$$\begin{aligned}\tilde{C}_{ij} &= \sum \frac{\partial \boldsymbol{\mu}_e^T}{\partial q_i} \mathbf{c}_e^s \frac{\partial \boldsymbol{\mu}_e}{\partial q_j} \\ \tilde{K}_i &= \sum \frac{\partial \boldsymbol{\mu}_e^T}{\partial q_i} \mathbf{k}_e^s \boldsymbol{\mu}_e \\ \tilde{\mathbf{Q}}_i &= \left[(\tilde{\mathbf{T}}_{B_0}^B \tilde{\mathbf{T}}_g^{B_0} \tilde{\mathbf{A}}^T)_i + (\mathbf{q}^T + (\mathbf{P}^B)^T) \frac{\partial \tilde{\mathbf{T}}_{B_0}^B}{\partial q_i} \tilde{\mathbf{T}}_g^{B_0} \mathbf{A}^T \right].\end{aligned}$$

Sums in (97) indicate a summation over the elements in the wind turbine structure.

2.5 Constraints

The bodies comprising the wind turbine – foundation, tower, nacelle, driveshaft, and blades – are connected to each other at joints, and these connections are expressed in terms of constraint equations. The redefinition of degrees-of-freedom means that we must derive the constraint equations anew; they are not the same as those in Merz (2015).

At each joint, the orientation, relative to the global coordinate frame, of the slave body is aligned with the axis of rotation, defined by a coordinate system attached to the outermost node on the master body. The slave body is rotated with respect to the master body by a joint angle: nacelle yaw, rotor azimuth, or blade pitch. Exceptions are the foundation, which may be connected to the soil by springs, and the tower, which is rigidly linked to the foundation.

The constraint equations are nonlinear functions of the pose of the bodies, and can be written in terms of the structural degrees-of-freedom as

$$\mathbf{C}(\mathbf{q}) = \mathbf{0}, \quad \mathbf{q} = \begin{bmatrix} \hat{\mathbf{q}} \\ \mathbf{q}_s \end{bmatrix}, \quad (98)$$

with \mathbf{q}_s the slave and $\hat{\mathbf{q}}$ the remaining degrees-of-freedom. The constraints are applied to the nonlinear equations of motion by using (98) to solve for \mathbf{q}_s in terms of $\hat{\mathbf{q}}$. In other words, the state vector is based on $\hat{\mathbf{q}}$, and excludes \mathbf{q}_s . It is possible to make direct substitutions for the velocity $d\mathbf{q}/dt$ and acceleration $d^2\mathbf{q}/dt^2$ in terms of $\hat{\mathbf{q}}$ and its time derivatives, as will be shown shortly; but the pose \mathbf{q} , in the nonlinear case, is obtained by a Newton-Raphson numerical solution of (98).

What, then, are the constraint equations (98)? Starting with the foundation-tower connection, the slave node on the tower is aligned with the deformed nodal coordinate system of the master node on the foundation. Therefore, the global positions of these two nodes are equal

$$\mathbf{r}_{m/g}^g = \mathbf{r}_{B/g}^g. \quad (99)$$

By (65), this is

$$\mathbf{O}_{F_0/g}^g + \mathbf{O}_{F/F_0}^g + \mathbf{T}_{F_0}^g \mathbf{T}_F^{F_0} (\mathbf{p}_{m_0/F}^F + \mathbf{d}_{m/m_0}^F) = \mathbf{O}_{T_0/g}^g + \mathbf{O}_{T/T_0}^g. \quad (100)$$

For implementation into the equations of motion, we take the first variation with respect to the deformational degrees-of-freedom, giving

$$\delta \mathbf{O}_{F/F_0}^g + \mathbf{T}_{F_0}^g \mathbf{T}_F^{F_0} \delta \mathbf{d}_{m/m_0}^F + \mathbf{T}_{F_0}^g \frac{\partial \mathbf{T}_F^{F_0}}{\partial \Phi_{F,k}^{F_0}} (\mathbf{p}_{m_0/F}^F + \mathbf{d}_{m/m_0}^F) \delta \Phi_{F,k}^{F_0} = \delta \mathbf{O}_{T/T_0}^g. \quad (101)$$

Here the retained degrees-of-freedom are written on the left-hand side of the equation, while slave degrees-of-freedom are written on the right. The rotations of the slave node are equal to the rotations of the master node, as there is no joint. This is formulated as

$$\mathbf{T}_{T_0}^g \mathbf{T}_T^{T_0} = \mathbf{T}_{F_0}^g \mathbf{T}_F^{F_0} \mathbf{T}_{m_0}^F \mathbf{T}_m^{m_0} \mathbf{T}_T^m, \quad \mathbf{T}_T^m = \begin{bmatrix} 0 & 0 & 1 \\ 1 & 0 & 0 \\ 0 & 1 & 0 \end{bmatrix} \quad (102)$$

Directly taking the first variation of this equality of transform matrices,

$$\mathbf{T}_{F0}^g \frac{\partial \mathbf{T}_F^{F0}}{\partial \Phi_{F,k}^{F0}} \mathbf{T}_{m0}^F \mathbf{T}_m^{m0} \mathbf{T}_T^m \delta \Phi_{F,k}^{F0} + \mathbf{T}_{F0}^g \mathbf{T}_F^{F0} \mathbf{T}_{m0}^F \frac{\partial \mathbf{T}_m^{m0}}{\partial \theta_{m,k}^{m0}} \mathbf{T}_T^m \delta \theta_{m,k}^{m0} = \mathbf{T}_{T0}^g \frac{\partial \mathbf{T}_T^{T0}}{\partial \Phi_{T,k}^{T0}} \delta \Phi_{T,k}^{T0}, \quad (103)$$

does not produce an equation of the appropriate form. However, in a manner similar to (72), a matrix-vector equation can be generated from the transforms by writing

$$\mathbf{T}_T^g(\Phi_F^{F0}, \theta_m^{m0}) \mathbf{T}_g^T(\Phi_T^{T0}) = \mathbf{I}, \quad (104)$$

from which

$$\frac{\partial \mathbf{T}_T^g}{\partial \Phi_{F,k}^{F0}} \mathbf{T}_g^T \delta \Phi_{F,k}^{F0} + \frac{\partial \mathbf{T}_T^g}{\partial \theta_{m,k}^{m0}} \mathbf{T}_g^T \delta \theta_{m,k}^{m0} + \mathbf{T}_T^g \frac{\partial \mathbf{T}_g^T}{\partial \Phi_{T,k}^{T0}} \delta \Phi_{T,k}^{T0} = \mathbf{0} \quad (105)$$

The matrix products

$$\frac{\partial \mathbf{T}}{\partial \theta} \mathbf{T}^T \quad \text{and} \quad \mathbf{T} \frac{\partial \mathbf{T}^T}{\partial \theta}$$

are skew-symmetric. The diagonals are zero, and the three independent off-diagonal elements can be used to write three matrix-vector equations for the rotation parameters, like

$$\mathbf{F} \delta \Phi_F^{F0} + \mathbf{G} \delta \theta_m^{m0} = -\mathbf{H} \delta \Phi_T^{T0}, \quad (106)$$

with \mathbf{F} , \mathbf{G} , and \mathbf{H} being 3-by-3 matrices.

The tower-nacelle joint is offset by the yaw angle. The position constraints are the same as (99), the variation giving

$$\mathbf{T}_{T0}^g \mathbf{T}_T^{T0} \delta \mathbf{d}_{m/m0}^T = -\delta \mathbf{O}_{T/T0}^g - \mathbf{T}_{T0}^g \frac{\partial \mathbf{T}_T^{T0}}{\partial \Phi_T^{T0}} (\mathbf{p}_{m0/T}^T + \mathbf{d}_{m/m0}^T) \delta \Phi_T^{T0} + \delta \mathbf{O}_{y/y0}^g. \quad (107)$$

Note that since the tower is slaved to the foundation, its reference degrees-of-freedom appear on the right-hand side of (107). The rotational constraints take the form

$$\mathbf{T}_{y0}^g \mathbf{T}_y^{y0} = \mathbf{T}_{T0}^g \mathbf{T}_T^{T0} \mathbf{T}_{m0}^T \mathbf{T}_m^{m0} \mathbf{T}_y^m, \quad \mathbf{T}_y^m = \begin{bmatrix} 0 & 0 & 1 \\ 1 & 0 & 0 \\ 0 & 1 & 0 \end{bmatrix} \begin{bmatrix} c\chi & -s\chi & 0 \\ s\chi & c\chi & 0 \\ 0 & 0 & 1 \end{bmatrix}. \quad (108)$$

At the rear bearing of the driveshaft,

$$\mathbf{T}_{y0}^g \mathbf{T}_y^{y0} \delta \mathbf{d}_{m/m0}^y = -\delta \mathbf{O}_{y/y0}^g - \mathbf{T}_{y0}^g \frac{\partial \mathbf{T}_y^{y0}}{\partial \Phi_y^{y0}} (\mathbf{p}_{m0/y}^y + \mathbf{d}_{m/m0}^y) \delta \Phi_y^{y0} + \delta \mathbf{O}_{d/d0}^g \quad (109)$$

and

$$\mathbf{T}_{d0}^g \mathbf{T}_d^{d0} = \mathbf{T}_{y0}^g \mathbf{T}_y^{y0} \mathbf{T}_{m0}^T \mathbf{T}_m^{m0} \mathbf{T}_d^m, \quad \mathbf{T}_d^m = \begin{bmatrix} 0 & 0 & -1 \\ -1 & 0 & 0 \\ 0 & 1 & 0 \end{bmatrix} \begin{bmatrix} c\Psi & -s\Psi & 0 \\ s\Psi & c\Psi & 0 \\ 0 & 0 & 1 \end{bmatrix}. \quad (110)$$

At the front bearing of the driveshaft, the transverse coordinates are constrained, with the shaft being free to translate in the nacelle's axial direction, as well as rotate. It is simplest to introduce a redundant degree-of-freedom ε_d representing the axial displacement of the shaft slave node with respect to the nacelle master node, expressed in the local coordinate frame of the master node, and write

$$\mathbf{O}_{y0/g}^g + \mathbf{O}_{y/y0}^g + \mathbf{T}_{y0}^g \mathbf{T}_y^{y0} \left(\mathbf{p}_{m0/y}^y + \mathbf{d}_{m/m0}^y + \mathbf{T}_{m0}^T \mathbf{T}_m^{m0} \begin{bmatrix} \varepsilon_d \\ 0 \\ 0 \end{bmatrix} \right) = \quad (111)$$

$$\mathbf{O}_{d0}^g + \mathbf{O}_{d/d0}^g + \mathbf{T}_{d0}^g \mathbf{T}_d^{d0} (\mathbf{p}_{s0}^d + \mathbf{d}_{s/s0}^d),$$

giving the first variation

$$\begin{aligned}
& \mathbf{T}_{y0}^g \mathbf{T}_y^{y0} \delta \mathbf{d}_{m/m0}^y + \mathbf{T}_{y0}^g \mathbf{T}_y^{y0} \left(\mathbf{T}_{m0}^y \frac{\partial \mathbf{T}_m^{m0}}{\partial \boldsymbol{\theta}_m^{m0}} \begin{bmatrix} \varepsilon_d \\ 0 \\ 0 \end{bmatrix} \delta \boldsymbol{\theta}_m^{m0} + \mathbf{T}_{m0}^y \mathbf{T}_m^{m0} \begin{bmatrix} 1 \\ 0 \\ 0 \end{bmatrix} \delta \varepsilon_d \right) \\
& = -\delta \mathbf{O}_{y/y0}^g - \mathbf{T}_{y0}^g \frac{\partial \mathbf{T}_y^{y0}}{\partial \boldsymbol{\Phi}_y^{y0}} \left(\mathbf{p}_{m0/y}^y + \mathbf{d}_{m/m0}^y + \mathbf{T}_{m0}^y \mathbf{T}_m^{m0} \begin{bmatrix} \varepsilon_d \\ 0 \\ 0 \end{bmatrix} \right) \delta \boldsymbol{\Phi}_y^{y0} \\
& + \delta \mathbf{O}_{d/d0}^g + \mathbf{T}_{d0}^g \frac{\partial \mathbf{T}_d^{d0}}{\partial \boldsymbol{\Phi}_d^{d0}} (\mathbf{p}_{s0/d}^d + \mathbf{d}_{s/s0}^d) \delta \boldsymbol{\Phi}_d^{d0} + \mathbf{T}_{d0}^g \mathbf{T}_d^{d0} \delta \mathbf{d}_{s/s0}^d.
\end{aligned} \tag{112}$$

Finally, at each pitch bearing,

$$\mathbf{T}_{d0}^g \mathbf{T}_d^{d0} \delta \mathbf{d}_{m/m0}^d = -\delta \mathbf{O}_{d/d0}^g - \mathbf{T}_{d0}^g \frac{\partial \mathbf{T}_d^{d0}}{\partial \boldsymbol{\Phi}_d^{d0}} (\mathbf{p}_{m0/d}^d + \mathbf{d}_{m/m0}^d) \delta \boldsymbol{\Phi}_d^{d0} + \delta \mathbf{O}_{p/p0}^g \tag{113}$$

and

$$\mathbf{T}_{p0}^g \mathbf{T}_p^{p0} = \mathbf{T}_{d0}^g \mathbf{T}_d^{d0} \mathbf{T}_m^d \mathbf{T}_{m0}^{m0} \mathbf{T}_p^m, \quad \mathbf{T}_p^m = \mathbf{T}_d^m \mathbf{T}_h^d \mathbf{T}_b^h \begin{bmatrix} 1 & 0 & 0 \\ 0 & c\beta & s\beta \\ 0 & -s\beta & c\beta \end{bmatrix}, \quad \mathbf{T}_h^m = \mathbf{I}. \tag{114}$$

The above variational equations can be written as

$$\mathbf{L} \delta \mathbf{q} = \mathbf{0}. \tag{115}$$

These are partitioned as

$$\mathbf{L}_s \delta \mathbf{q}_s + \hat{\mathbf{L}} \delta \hat{\mathbf{q}} = \mathbf{0}, \quad \delta \mathbf{q}_s = -\mathbf{L}_s^{-1} \hat{\mathbf{L}} \delta \hat{\mathbf{q}}, \tag{116}$$

\mathbf{q}_s being the slave and $\hat{\mathbf{q}}$ the retained degrees-of-freedom. Equation (116) applies at any given point in time, provided that $\mathbf{L}_s(\mathbf{q})$ and $\hat{\mathbf{L}}(\mathbf{q})$ are evaluated at the present \mathbf{q} . A matrix

$$\boldsymbol{\Lambda} := \begin{bmatrix} \mathbf{I} \\ -\mathbf{L}_s^{-1} \hat{\mathbf{L}} \end{bmatrix} \tag{117}$$

is defined for subsequent use in constraining the state-space equations.

The time derivative of (98) gives simply

$$\mathbf{L} \frac{d\mathbf{q}}{dt} = \mathbf{0}. \tag{118}$$

Taking another time derivative, the equation for the accelerations is then

$$\frac{dq_k}{dt} \frac{\partial \mathbf{L}}{\partial q_k} \frac{d\mathbf{q}}{dt} + \mathbf{L} \frac{d^2 \mathbf{q}}{dt^2} = \mathbf{0}. \tag{119}$$

Partitioning the latter term,

$$\frac{dq_k}{dt} \frac{\partial \mathbf{L}}{\partial q_k} \frac{d\mathbf{q}}{dt} + \mathbf{L}_s \frac{d^2 \mathbf{q}_s}{dt^2} + \hat{\mathbf{L}} \frac{d^2 \hat{\mathbf{q}}}{dt^2} = \mathbf{0}, \tag{120}$$

which leads to

$$\frac{d^2 \mathbf{q}_s}{dt^2} = -\mathbf{L}_s^{-1} \hat{\mathbf{L}} \frac{d^2 \hat{\mathbf{q}}}{dt^2} - \mathbf{L}_s^{-1} \frac{dq_k}{dt} \frac{\partial \mathbf{L}}{\partial q_k} \frac{d\mathbf{q}}{dt}. \tag{121}$$

The derivatives $\partial \mathbf{L} / \partial q_k$ are obtained in a straightforward manner from (99) through (114). We refrain from writing out these in their entirety.

The first term on the right-hand side of (121) is analogous to (116) for incremental displacements or velocities. It is worth a digression to illustrate the meaning of the second term. For this purpose, consider a simple pendulum, with radius a , mass M , and angle θ . We aim to express the dynamics in the angular range $-\pi/2 \leq \theta \leq \pi/2$ using y as a generalized coordinate. The unconstrained dynamics of the mass are

$$\begin{bmatrix} M & 0 \\ 0 & M \end{bmatrix} \begin{bmatrix} \ddot{x} \\ \ddot{y} \end{bmatrix} = \begin{bmatrix} F_x \\ F_y \end{bmatrix}, \quad (122)$$

with constraint

$$x^2 + y^2 = a^2, \quad (123)$$

giving

$$x \delta x + y \delta y = 0, \quad x \dot{x} + y \dot{y} = 0, \quad \text{and} \quad x \ddot{x} + y \ddot{y} + \dot{x}^2 + \dot{y}^2 = 0. \quad (124)$$

Solving for and eliminating \ddot{x} , the partitioned and reduced equation of motion is

$$\begin{bmatrix} 1 & -x^{-1}y \end{bmatrix} \begin{bmatrix} M & 0 \\ 0 & M \end{bmatrix} \left(\begin{bmatrix} 1 \\ -x^{-1}y \end{bmatrix} \ddot{y} + \begin{bmatrix} 0 \\ -x^{-1}(\dot{x}^2 + \dot{y}^2) \end{bmatrix} \right) = \begin{bmatrix} 1 & -x^{-1}y \end{bmatrix} \begin{bmatrix} F_y \\ F_x \end{bmatrix}, \quad (125)$$

which can be manipulated into

$$M \ddot{y} = \left(\frac{x}{a}\right)^2 F_y - \left(\frac{x}{a}\right) \left(\frac{y}{a}\right) F_x - M y \frac{v^2}{a^2}, \quad (126)$$

or

$$M \ddot{y} = F_y \cos^2 \theta - F_x \cos \theta \sin \theta - M \frac{v^2}{a} \sin \theta. \quad (127)$$

The last term, quadratic in the velocity v , originates from

$$-\mathbf{L}_s^{-1} \frac{dq_k}{dt} \frac{\partial \mathbf{L}}{\partial q_k} \frac{d\mathbf{q}}{dt}$$

in (121). It is seen that this provides the centripetal acceleration, in terms of the generalized coordinate y , that enforces the constraint on the rotary motion, even in the absence of applied forces.

An identical expression (127), as well as the corresponding equation for \dot{x} , can be obtained by a Lagrange multiplier approach. Writing

$$\begin{bmatrix} M & 0 & x \\ 0 & M & y \\ x & y & 0 \end{bmatrix} \begin{bmatrix} \ddot{x} \\ \ddot{y} \\ \lambda \end{bmatrix} = \begin{bmatrix} F_x \\ F_y \\ -(\dot{x}^2 + \dot{y}^2) \end{bmatrix}, \quad (128)$$

and inverting to obtain

$$\begin{bmatrix} \ddot{x} \\ \ddot{y} \\ \lambda \end{bmatrix} = \frac{1}{x^2 + y^2} \begin{bmatrix} y^2/M & -xy/M & x \\ -xy/M & x^2/M & y \\ x & y & -M \end{bmatrix} \begin{bmatrix} F_x \\ F_y \\ -(\dot{x}^2 + \dot{y}^2) \end{bmatrix}, \quad (129)$$

the first two lines are

$$M \ddot{x} = \frac{y^2}{x^2 + y^2} F_x - \frac{xy}{x^2 + y^2} F_y - M \frac{x}{x^2 + y^2} (\dot{x}^2 + \dot{y}^2), \quad (130)$$

and

$$M \ddot{y} = -\frac{xy}{x^2 + y^2} F_x + \frac{x^2}{x^2 + y^2} F_y - M \frac{y}{x^2 + y^2} (\dot{x}^2 + \dot{y}^2), \quad (131)$$

which are seen to be the desired expressions.

2.6 Nonlinear state space

The nonlinear equations of motion (96) are constrained by partitioning the vectors and matrices into retained and slave degrees-of-freedom, and applying the operation

$$\mathbf{\Lambda}^T \tilde{\mathbf{M}} \mathbf{\Lambda} \frac{d^2 \hat{\mathbf{q}}}{dt^2} + (\mathbf{\Lambda}^T \tilde{\mathbf{M}} \mathbf{\Gamma} + \mathbf{\Lambda}^T \tilde{\mathbf{G}} \mathbf{\Lambda}) \frac{d \hat{\mathbf{q}}}{dt} - \mathbf{\Lambda}^T \tilde{\mathbf{H}} + \mathbf{\Lambda}^T \tilde{\mathbf{C}} + \mathbf{\Lambda}^T \tilde{\mathbf{K}} = \mathbf{\Lambda}^T \tilde{\mathbf{Q}} \mathbf{F}^B, \quad (132)$$

where $\mathbf{\Lambda}$ comes from (117), and

$$\mathbf{\Gamma} := \begin{bmatrix} \mathbf{0} \\ -\mathbf{L}_s^{-1} \frac{dq_k}{dt} \frac{\partial \mathbf{L}}{\partial q_k} \mathbf{\Lambda} \end{bmatrix}. \quad (133)$$

The equations can then be put into state-space format, as

$$\begin{bmatrix} \mathbf{I} & \mathbf{0} \\ \mathbf{0} & \mathbf{M}(\mathbf{q}) \end{bmatrix} \frac{d}{dt} \begin{bmatrix} \hat{\mathbf{q}} \\ \dot{\hat{\mathbf{q}}} \end{bmatrix} = \begin{bmatrix} \mathbf{0} & \mathbf{I} \\ \mathbf{0} & -\mathbf{G}(\mathbf{q}, \dot{\mathbf{q}}) \end{bmatrix} \begin{bmatrix} \hat{\mathbf{q}} \\ \dot{\hat{\mathbf{q}}} \end{bmatrix} + \begin{bmatrix} \mathbf{0} \\ \mathbf{H}(\mathbf{q}, \dot{\mathbf{q}}) - \mathbf{C}(\mathbf{q}, \dot{\mathbf{q}}) - \mathbf{K}(\mathbf{q}) - \bar{\mathbf{\Gamma}}(\mathbf{q}, \dot{\mathbf{q}}) \end{bmatrix} + \begin{bmatrix} \mathbf{0} \\ \mathbf{Q}(\mathbf{q}) \mathbf{F} \end{bmatrix}. \quad (134)$$

Here the $\mathbf{\Lambda}$ and $\mathbf{\Gamma}$ operations have been absorbed into each symbol.

Equation (134) can be integrated numerically over time; numerical integration routines require computing the right-hand side at a given $\mathbf{q}(t)$ and $\dot{\mathbf{q}}(t)$. A point of steady-state operation is found by solving (134) for a zero left-hand side. This is discussed further in Section 5.5.

3 Linear structural dynamics

Linearizing (134) is straightforward, but tedious. Start with the *unconstrained* equation (96) in the form

$$\tilde{\mathbf{M}}(\mathbf{q}) \frac{d^2 \mathbf{q}}{dt^2} + \tilde{\mathbf{G}}(\mathbf{q}, \dot{\mathbf{q}}) \frac{d \mathbf{q}}{dt} - \tilde{\mathbf{H}}(\mathbf{q}, \dot{\mathbf{q}}) + \tilde{\mathbf{C}}(\mathbf{q}, \dot{\mathbf{q}}) + \tilde{\mathbf{K}}(\mathbf{q}) = \tilde{\mathbf{Q}}(\mathbf{q}) \mathbf{F}^B. \quad (135)$$

Starting at some operating point, or initial condition, which occurs at some time t_0 indicated by a “0” subscript, a generic function is linearized as

$$\mathbf{f}(\mathbf{q}, \dot{\mathbf{q}}) = \mathbf{f}_0 + \frac{\partial \mathbf{f}}{\partial \mathbf{q}} \Delta \mathbf{q} + \frac{\partial \mathbf{f}}{\partial \dot{\mathbf{q}}} \frac{d \Delta \mathbf{q}}{dt}. \quad (136)$$

Applying this to (135),

$$\begin{aligned} & \tilde{\mathbf{M}}_0 \left. \frac{d^2 \mathbf{q}}{dt^2} \right|_0 + \tilde{\mathbf{G}}_0 \left. \frac{d \mathbf{q}}{dt} \right|_0 - \tilde{\mathbf{H}}_0 + \tilde{\mathbf{C}}_0 + \tilde{\mathbf{K}}_0 \\ & + \left. \frac{\partial \tilde{\mathbf{M}}}{\partial q_i} \right|_0 \left. \frac{d^2 \mathbf{q}}{dt^2} \right|_0 \Delta q_i + \tilde{\mathbf{M}}_0 \frac{d^2 \Delta q_i}{dt^2} \\ & + \left. \frac{\partial \tilde{\mathbf{G}}}{\partial q_i} \right|_0 \left. \frac{d \mathbf{q}}{dt} \right|_0 \Delta q_i + \left. \frac{\partial \tilde{\mathbf{G}}}{\partial \dot{q}_i} \right|_0 \left. \frac{d \mathbf{q}}{dt} \right|_0 \frac{d \Delta q_i}{dt} + \tilde{\mathbf{G}}_0 \frac{d \Delta q_i}{dt} \\ & - \left. \frac{\partial \tilde{\mathbf{H}}}{\partial q_i} \right|_0 \Delta q_i - \left. \frac{\partial \tilde{\mathbf{H}}}{\partial \dot{q}_i} \right|_0 \frac{d \Delta q_i}{dt} + \left. \frac{\partial \tilde{\mathbf{C}}}{\partial q_i} \right|_0 \Delta q_i + \left. \frac{\partial \tilde{\mathbf{C}}}{\partial \dot{q}_i} \right|_0 \frac{d \Delta q_i}{dt} + \left. \frac{\partial \tilde{\mathbf{K}}}{\partial q_i} \right|_0 \Delta q_i \\ & = \tilde{\mathbf{Q}}_0 \mathbf{F}_0^B + \tilde{\mathbf{Q}}_0 \Delta \mathbf{F}^B + \left. \frac{\partial \tilde{\mathbf{Q}}}{\partial q_i} \right|_0 \mathbf{F}_0^B \Delta q_i. \end{aligned} \quad (137)$$

For the initial condition, this gives

$$\tilde{\mathbf{M}}_0 \left. \frac{d^2 \mathbf{q}}{dt^2} \right|_0 + \tilde{\mathbf{G}}_0 \left. \frac{d\mathbf{q}}{dt} \right|_0 - \tilde{\mathbf{H}}_0 + \tilde{\mathbf{C}}_0 + \tilde{\mathbf{K}}_0 = \tilde{\mathbf{Q}}_0 \mathbf{F}_0^B, \quad (138)$$

and for perturbations with respect to the initial state,

$$\begin{aligned} \tilde{\mathbf{M}}_0 \frac{d^2 \Delta q_i}{dt^2} + \left(\left. \frac{\partial \tilde{\mathbf{G}}}{\partial \dot{q}_i} \right|_0 \left. \frac{d\mathbf{q}}{dt} \right|_0 + \tilde{\mathbf{G}}_0 - \left. \frac{\partial \tilde{\mathbf{H}}}{\partial \dot{q}_i} \right|_0 + \left. \frac{\partial \tilde{\mathbf{C}}}{\partial \dot{q}_i} \right|_0 \right) \frac{d\Delta q_i}{dt} \\ + \left(\left. \frac{\partial \tilde{\mathbf{M}}}{\partial q_i} \right|_0 \left. \frac{d^2 \mathbf{q}}{dt^2} \right|_0 + \left. \frac{\partial \tilde{\mathbf{G}}}{\partial q_i} \right|_0 \left. \frac{d\mathbf{q}}{dt} \right|_0 - \left. \frac{\partial \tilde{\mathbf{H}}}{\partial q_i} \right|_0 + \left. \frac{\partial \tilde{\mathbf{C}}}{\partial q_i} \right|_0 + \left. \frac{\partial \tilde{\mathbf{K}}}{\partial q_i} \right|_0 - \left. \frac{\partial \tilde{\mathbf{Q}}}{\partial q_i} \right|_0 \mathbf{F}_0^B \right) \Delta q_i \\ = \tilde{\mathbf{Q}}_0 \Delta \mathbf{F}^B, \end{aligned} \quad (139)$$

or

$$\mathbf{M}_0 \frac{d^2 \Delta \mathbf{q}}{dt^2} + \mathbf{C}_0 \frac{d\Delta \mathbf{q}}{dt} + \mathbf{K}_0 \Delta \mathbf{q} = \mathbf{Q}_0 \Delta \mathbf{F}^B. \quad (140)$$

For many purposes, the operating point is taken to be an equilibrium point; but it does not have to be. If the operating point is not at equilibrium, then it serves as an initial condition, and (140) gives the tangent dynamics – that is, the effective linear dynamics near the initial condition. To put it another way, if the model (134) were linear, then the dynamic characteristics of the linearization (140) would be the same for any initial condition. Most importantly, the eigenvalues, mode shapes, and stability properties would be identical. The tangent dynamics therefore indicate the effective poles and zeros governing the local dynamics of the nonlinear model, as it traverses some trajectory.⁶

3.1 Expressions for partial derivatives

Starting with the mass matrix,

$$\begin{aligned} \frac{\partial \tilde{M}_{ij}}{\partial q_k} &= \frac{\partial \mathbf{u}_e^T}{\partial \dot{q}_j} \mathbf{T}_s^B \mathbf{m}_e^s \mathbf{T}_B^s \frac{\partial^2 \mathbf{u}_e}{\partial \dot{q}_i \partial q_k} + \frac{\partial \mathbf{u}_e^T}{\partial \dot{q}_i} \mathbf{T}_s^B \mathbf{m}_e^s \mathbf{T}_B^s \frac{\partial^2 \mathbf{u}_e}{\partial \dot{q}_j \partial q_k} \\ &+ \frac{\partial \mathbf{u}_e^T}{\partial \dot{q}_i} \left(\frac{\partial \mathbf{T}_s^B}{\partial q_k} \mathbf{m}_e^s \mathbf{T}_B^s + \mathbf{T}_s^B \mathbf{m}_e^s \frac{\partial \mathbf{T}_B^s}{\partial q_k} \right) \frac{\partial \mathbf{u}_e}{\partial \dot{q}_j}. \end{aligned} \quad (141)$$

Then the gyroscopic matrices,

$$\begin{aligned} \frac{\partial \tilde{G}_{ij}}{\partial \dot{q}_k} &= \frac{\partial^2 \mathbf{u}_e^T}{\partial \dot{q}_i \partial q_j} \mathbf{T}_s^B \mathbf{m}_e^s \mathbf{T}_B^s \frac{\partial \mathbf{u}_e}{\partial \dot{q}_k} + \frac{\partial \mathbf{u}_e^T}{\partial \dot{q}_i} \mathbf{T}_s^B \mathbf{m}_e^s \mathbf{T}_B^s \frac{\partial^2 \mathbf{u}_e}{\partial q_j \partial \dot{q}_k} \\ &+ \frac{\partial \mathbf{u}_e^T}{\partial \dot{q}_i} \left(\frac{\partial \mathbf{T}_s^B}{\partial q_j} \mathbf{m}_e^s \mathbf{T}_B^s + \mathbf{T}_s^B \mathbf{m}_e^s \frac{\partial \mathbf{T}_B^s}{\partial q_j} \right) \frac{\partial \mathbf{u}_e}{\partial \dot{q}_k}, \end{aligned} \quad (142)$$

⁶Looking at the tangent dynamics along trajectories, as opposed to around equilibrium points, is suggested by Leith and Leithead (1998, 2000), in particular for designing gain-scheduled controllers. For some purposes a straightforward perturbation in the form of (140) is equivalent to Leith and Leithead’s “velocity-based linearization”, as the relevant eigenvalues and stability properties are the same: the velocity-based linearization adds $N_x + N_y$ rigid-body (zero-eigenvalue) modes, and requires taking the time derivative of the input.

where several terms have been eliminated by applying $\partial^2 \mathbf{u}_e^T / \partial \dot{q}_i \partial \dot{q}_j = \mathbf{0}$, and

$$\begin{aligned}
\frac{\partial \tilde{G}_{ij}}{\partial q_k} &= \frac{\partial^3 \mathbf{u}_e^T}{\partial \dot{q}_i \partial \dot{q}_j \partial q_k} \mathbf{T}_s^B \mathbf{m}_e^s \mathbf{T}_B^s \mathbf{u}_e + \frac{\partial^2 \mathbf{u}_e^T}{\partial \dot{q}_i \partial \dot{q}_j} \left(\frac{\partial \mathbf{T}_s^B}{\partial q_k} \mathbf{m}_e^s \mathbf{T}_B^s + \mathbf{T}_s^B \mathbf{m}_e^s \frac{\partial \mathbf{T}_B^s}{\partial q_k} \right) \mathbf{u}_e \\
&+ \frac{\partial^2 \mathbf{u}_e^T}{\partial \dot{q}_i \partial q_j} \mathbf{T}_s^B \mathbf{m}_e^s \mathbf{T}_B^s \frac{\partial \mathbf{u}_e}{\partial q_k} + \frac{\partial \mathbf{u}_e^T}{\partial \dot{q}_i} \mathbf{T}_s^B \mathbf{m}_e^s \mathbf{T}_B^s \frac{\partial^2 \mathbf{u}_e}{\partial q_j \partial q_k} \\
&+ \frac{\partial^2 \mathbf{u}_e^T}{\partial \dot{q}_i \partial q_k} \mathbf{T}_s^B \mathbf{m}_e^s \mathbf{T}_B^s \frac{\partial \mathbf{u}_e}{\partial q_j} + \frac{\partial \mathbf{u}_e^T}{\partial \dot{q}_i} \left(\frac{\partial \mathbf{T}_s^B}{\partial q_k} \mathbf{m}_e^s \mathbf{T}_B^s + \mathbf{T}_s^B \mathbf{m}_e^s \frac{\partial \mathbf{T}_B^s}{\partial q_k} \right) \frac{\partial \mathbf{u}_e}{\partial q_j} \\
&+ \frac{\partial^2 \mathbf{u}_e^T}{\partial \dot{q}_i \partial q_k} \left(\frac{\partial \mathbf{T}_s^B}{\partial q_j} \mathbf{m}_e^s \mathbf{T}_B^s + \mathbf{T}_s^B \mathbf{m}_e^s \frac{\partial \mathbf{T}_B^s}{\partial q_j} \right) \mathbf{u}_e + \frac{\partial \mathbf{u}_e^T}{\partial \dot{q}_i} \left(\frac{\partial \mathbf{T}_s^B}{\partial q_j} \mathbf{m}_e^s \mathbf{T}_B^s + \mathbf{T}_s^B \mathbf{m}_e^s \frac{\partial \mathbf{T}_B^s}{\partial q_j} \right) \frac{\partial \mathbf{u}_e}{\partial q_k} \\
&+ \frac{\partial \mathbf{u}_e^T}{\partial \dot{q}_i} \left(\frac{\partial^2 \mathbf{T}_s^B}{\partial q_j \partial q_k} \mathbf{m}_e^s \mathbf{T}_B^s + \frac{\partial \mathbf{T}_s^B}{\partial q_j} \mathbf{m}_e^s \frac{\partial \mathbf{T}_B^s}{\partial q_k} + \mathbf{T}_s^B \mathbf{m}_e^s \frac{\partial^2 \mathbf{T}_B^s}{\partial q_j \partial q_k} + \frac{\partial \mathbf{T}_s^B}{\partial q_k} \mathbf{m}_e^s \frac{\partial \mathbf{T}_B^s}{\partial q_j} \right) \mathbf{u}_e.
\end{aligned} \tag{143}$$

It is evident that some of these terms are transposes of others. Only one of the transposed terms need be computed, but they are inserted into the global $\tilde{\mathbf{G}}$ matrix in different places, according to the indices on the $\partial \dot{q}$'s.

The centrifugal vector is linearized as

$$\begin{aligned}
\frac{\partial \tilde{H}_i}{\partial \dot{q}_k} &= \mathbf{u}_e^T \mathbf{T}_s^B \mathbf{m}_e^s \mathbf{T}_B^s \frac{\partial^2 \mathbf{u}_e}{\partial q_i \partial \dot{q}_k} + \frac{\partial \mathbf{u}_e^T}{\partial q_i} \mathbf{T}_s^B \mathbf{m}_e^s \mathbf{T}_B^s \frac{\partial \mathbf{u}_e}{\partial \dot{q}_k} \\
&+ \mathbf{u}_e^T \left(\frac{\partial \mathbf{T}_s^B}{\partial q_i} \mathbf{m}_e^s \mathbf{T}_B^s + \mathbf{T}_s^B \mathbf{m}_e^s \frac{\partial \mathbf{T}_B^s}{\partial q_i} \right) \frac{\partial \mathbf{u}_e}{\partial \dot{q}_k}
\end{aligned} \tag{144}$$

and

$$\begin{aligned}
\frac{\partial \tilde{H}_i}{\partial q_k} &= \frac{\partial^2 \mathbf{u}_e^T}{\partial q_i \partial q_k} \mathbf{T}_s^B \mathbf{m}_e^s \mathbf{T}_B^s \mathbf{u}_e + \frac{\partial \mathbf{u}_e^T}{\partial q_i} \mathbf{T}_s^B \mathbf{m}_e^s \mathbf{T}_B^s \frac{\partial \mathbf{u}_e}{\partial q_k} \\
&+ \frac{\partial \mathbf{u}_e^T}{\partial q_i} \left(\frac{\partial \mathbf{T}_s^B}{\partial q_k} \mathbf{m}_e^s \mathbf{T}_B^s + \mathbf{T}_s^B \mathbf{m}_e^s \frac{\partial \mathbf{T}_B^s}{\partial q_k} \right) \mathbf{u}_e \\
&+ \mathbf{u}_e^T \left(\frac{\partial \mathbf{T}_s^B}{\partial q_i} \mathbf{m}_e^s \mathbf{T}_B^s + \mathbf{T}_s^B \mathbf{m}_e^s \frac{\partial \mathbf{T}_B^s}{\partial q_i} \right) \frac{\partial \mathbf{u}_e}{\partial q_k} \\
&+ \mathbf{u}_e^T \left(\frac{\partial^2 \mathbf{T}_s^B}{\partial q_i \partial q_k} \mathbf{m}_e^s \mathbf{T}_B^s + \frac{\partial \mathbf{T}_s^B}{\partial q_i} \mathbf{m}_e^s \frac{\partial \mathbf{T}_B^s}{\partial q_k} \right) \mathbf{u}_e.
\end{aligned} \tag{145}$$

The damping $\tilde{\mathbf{C}}$ is formulated in terms of modal damping ratios in Section 3.3. The stiffness vector $\tilde{\mathbf{K}}$ is linearized as

$$\frac{\partial \tilde{K}_i}{\partial q_k} = \frac{\partial^2 \boldsymbol{\mu}_e^T}{\partial q_i \partial q_k} \mathbf{k}_e^s \boldsymbol{\mu}_e + \frac{\partial \boldsymbol{\mu}_e^T}{\partial q_i} \mathbf{k}_e^s \frac{\partial \boldsymbol{\mu}_e}{\partial q_k}. \tag{146}$$

Here the required derivatives of $\boldsymbol{\mu}$ are composed of

$$\mathbf{a}^B := \mathbf{P}_2^B + \mathbf{d}_2^B - \mathbf{P}_1^B - \mathbf{d}_1^B, \tag{147}$$

$$\frac{\partial \delta_x}{\partial d_i} = [1 \ 0 \ 0] \left\{ \mathbf{T}_B^s (\pm \mathbf{e}_i) + \frac{\partial \mathbf{T}_B^s}{\partial d_i} \mathbf{a}^B \right\}, \tag{148}$$

$$\frac{\partial \delta_x}{\partial \theta_i} = [1 \ 0 \ 0] \frac{\partial \mathbf{T}_B^s}{\partial \theta_i} \mathbf{a}^B, \tag{149}$$

$$\frac{\partial^2 \delta_x}{\partial d_i \partial d_j} = [1 \ 0 \ 0] \left\{ \frac{\partial \mathbf{T}_B^s}{\partial d_j} (\pm \mathbf{e}_i) + \frac{\partial \mathbf{T}_B^s}{\partial d_i} (\pm \mathbf{e}_j) + \frac{\partial^2 \mathbf{T}_B^s}{\partial d_i \partial d_j} \mathbf{a}^B \right\}, \tag{150}$$

$$\frac{\partial^2 \delta_x}{\partial d_i \partial \theta_j} = [1 \ 0 \ 0] \left\{ \frac{\mathbf{T}_B^s}{\partial \theta_j} (\pm \mathbf{e}_i) + \frac{\partial^2 \mathbf{T}_B^s}{\partial d_i \partial \theta_j} \mathbf{a}^B \right\}, \quad (151)$$

and

$$\frac{\partial^2 \delta_x}{\partial \theta_i \partial \theta_j} = [1 \ 0 \ 0] \frac{\partial^2 \mathbf{T}_B^s}{\partial \theta_i \partial \theta_j} \mathbf{a}^B, \quad (152)$$

where half of δ_x is associated with each node; and

$$\frac{\partial \mathbf{T}_n^s}{\partial d_i} = \frac{\partial \mathbf{T}_B^s}{\partial d_i} \mathbf{T}_{s0}^B \mathbf{T}_n^{n0}, \quad (153)$$

$$\frac{\partial \mathbf{T}_n^s}{\partial \theta_i} = \frac{\partial \mathbf{T}_B^s}{\partial \theta_i} \mathbf{T}_{s0}^B \mathbf{T}_n^{n0} + \mathbf{T}_B^s \mathbf{T}_{s0}^B \frac{\partial \mathbf{T}_n^{n0}}{\partial \theta_i}, \quad (154)$$

$$\frac{\partial^2 \mathbf{T}_n^s}{\partial d_i \partial d_j} = \frac{\partial^2 \mathbf{T}_B^s}{\partial d_i \partial d_j} \mathbf{T}_{s0}^B \mathbf{T}_n^{n0}, \quad (155)$$

$$\frac{\partial^2 \mathbf{T}_n^s}{\partial d_i \partial \theta_j} = \frac{\partial^2 \mathbf{T}_B^s}{\partial d_i \partial \theta_j} \mathbf{T}_{s0}^B \mathbf{T}_n^{n0} + \frac{\partial \mathbf{T}_B^s}{\partial d_i} \mathbf{T}_{s0}^B \frac{\partial \mathbf{T}_n^{n0}}{\partial \theta_j}, \quad (156)$$

and

$$\frac{\partial^2 \mathbf{T}_n^s}{\partial \theta_i \partial \theta_j} = \frac{\partial^2 \mathbf{T}_B^s}{\partial \theta_i \partial \theta_j} \mathbf{T}_{s0}^B \mathbf{T}_n^{n0} + \frac{\partial \mathbf{T}_B^s}{\partial \theta_j} \mathbf{T}_{s0}^B \frac{\partial \mathbf{T}_n^{n0}}{\partial \theta_i} + \frac{\partial \mathbf{T}_B^s}{\partial \theta_i} \mathbf{T}_{s0}^B \frac{\partial \mathbf{T}_n^{n0}}{\partial \theta_j} + \mathbf{T}_B^s \mathbf{T}_{s0}^B \frac{\partial^2 \mathbf{T}_n^{n0}}{\partial \theta_i \partial \theta_j}. \quad (157)$$

The generalized force matrix $\tilde{\mathbf{Q}}$ is related to the velocity \mathbf{u}_e . This velocity depends on both the translation and rotation degrees-of-freedom. It is linear in $\dot{\mathbf{q}}$ and nonlinear, with multiple nonzero derivatives, in \mathbf{q} . The first derivatives were given previously in (78) through (81). Higher-order derivatives are

$$\frac{\partial^2 (\mathbf{Q}_v)_i}{\partial O_j \partial O_k} = \frac{\partial^2 (\mathbf{Q}_v)_i}{\partial O_j \partial \Phi_k} = \frac{\partial^2 (\mathbf{Q}_v)_i}{\partial d_j \partial d_k} = \frac{\partial^2 (\mathbf{Q}_v)_i}{\partial O_j \partial d_k} = \frac{\partial^2 (\mathbf{Q}_v)_i}{\partial O_j \partial \theta_k} = \frac{\partial^2 (\mathbf{Q}_v)_i}{\partial d_j \partial \theta_k} = \mathbf{0}, \quad (158)$$

$$\frac{\partial^2 (\mathbf{Q}_v)_i}{\partial d_j \partial \Phi_k} = \frac{\partial \mathbf{T}_{B0}^B}{\partial \Phi_k} \mathbf{T}_g^{B0} \left(\mathbf{A}_n \tilde{\mathbf{T}}_{B0}^g \frac{\partial \tilde{\mathbf{T}}_B^{B0}}{\partial \Phi_i} \right)_j + \mathbf{T}_{B0}^B \mathbf{T}_g^{B0} \left(\mathbf{A}_n \tilde{\mathbf{T}}_{B0}^g \frac{\partial^2 \tilde{\mathbf{T}}_B^{B0}}{\partial \Phi_i \partial \Phi_k} \right)_j, \quad (159)$$

$$\begin{aligned} \frac{\partial^2 (\mathbf{Q}_v)_i}{\partial \Phi_j \partial \Phi_k} &= \frac{\partial^2 \mathbf{T}_{B0}^B}{\partial \Phi_j \partial \Phi_k} \mathbf{T}_g^{B0} \left(\left(\tilde{\mathbf{A}}_n \tilde{\mathbf{T}}_{B0}^g \tilde{\mathbf{T}}_B^{B0} \right)_i + \mathbf{A}_n \tilde{\mathbf{T}}_{B0}^g \frac{\partial \tilde{\mathbf{T}}_B^{B0}}{\partial \Phi_i} (\mathbf{q} + \mathbf{P}) \right) \\ &+ \frac{\partial \mathbf{T}_{B0}^B}{\partial \Phi_j} \mathbf{T}_g^{B0} \left[\left(\frac{\partial \tilde{\mathbf{A}}_n}{\partial \Phi_k} \tilde{\mathbf{T}}_{B0}^g \tilde{\mathbf{T}}_B^{B0} + \tilde{\mathbf{A}}_n \tilde{\mathbf{T}}_{B0}^g \frac{\partial \tilde{\mathbf{T}}_B^{B0}}{\partial \Phi_k} \right)_i \right. \\ &+ \left. \mathbf{A}_n \tilde{\mathbf{T}}_{B0}^g \frac{\partial^2 \tilde{\mathbf{T}}_B^{B0}}{\partial \Phi_i \partial \Phi_k} (\mathbf{q} + \mathbf{P}) \right] \\ &+ \frac{\partial \mathbf{T}_{B0}^B}{\partial \Phi_k} \mathbf{T}_g^{B0} \left(\frac{\partial \tilde{\mathbf{A}}_n}{\partial \Phi_j} \tilde{\mathbf{T}}_{B0}^g \tilde{\mathbf{T}}_B^{B0} + \tilde{\mathbf{A}}_n \tilde{\mathbf{T}}_{B0}^g \frac{\partial \tilde{\mathbf{T}}_B^{B0}}{\partial \Phi_j} \right)_i \\ &+ \mathbf{T}_{B0}^B \mathbf{T}_g^{B0} \left(\frac{\partial^2 \tilde{\mathbf{A}}_n}{\partial \Phi_j \partial \Phi_k} \tilde{\mathbf{T}}_{B0}^g \tilde{\mathbf{T}}_B^{B0} + \frac{\partial \tilde{\mathbf{A}}_n}{\partial \Phi_j} \tilde{\mathbf{T}}_{B0}^g \frac{\partial \tilde{\mathbf{T}}_B^{B0}}{\partial \Phi_k} \right. \\ &+ \left. \frac{\partial \tilde{\mathbf{A}}_n}{\partial \Phi_k} \tilde{\mathbf{T}}_{B0}^g \frac{\partial \tilde{\mathbf{T}}_B^{B0}}{\partial \Phi_j} + \tilde{\mathbf{A}}_n \tilde{\mathbf{T}}_{B0}^g \frac{\partial^2 \tilde{\mathbf{T}}_B^{B0}}{\partial \Phi_j \partial \Phi_k} \right)_i \\ &+ \frac{\partial \mathbf{T}_{B0}^B}{\partial \Phi_k} \mathbf{T}_g^{B0} \mathbf{A}_n \tilde{\mathbf{T}}_{B0}^g \frac{\partial^2 \tilde{\mathbf{T}}_B^{B0}}{\partial \Phi_i \partial \Phi_j} (\mathbf{q} + \mathbf{P}) \\ &+ \mathbf{T}_{B0}^B \mathbf{T}_g^{B0} \mathbf{A}_n \tilde{\mathbf{T}}_{B0}^g \frac{\partial^3 \tilde{\mathbf{T}}_B^{B0}}{\partial \Phi_i \partial \Phi_j \partial \Phi_k} (\mathbf{q} + \mathbf{P}), \end{aligned} \quad (160)$$

$$\begin{aligned} \frac{\partial^2(\mathbf{Q}_v)_i}{\partial\Phi_j\partial\theta_k} &= \frac{\partial\mathbf{T}_{B0}^B}{\partial\Phi_j}\mathbf{T}_g^{B0} \left(\frac{\partial\tilde{\mathbf{A}}_n}{\partial\theta_k}\tilde{\mathbf{T}}_{B0}^g\tilde{\mathbf{T}}_B^{B0} \right)_i \\ &+ \mathbf{T}_{B0}^B\mathbf{T}_g^{B0} \left(\frac{\partial^2\tilde{\mathbf{A}}_n}{\partial\Phi_j\partial\theta_k}\tilde{\mathbf{T}}_{B0}^g\tilde{\mathbf{T}}_B^{B0} + \frac{\partial\tilde{\mathbf{A}}_n}{\partial\theta_k}\tilde{\mathbf{T}}_{B0}^g\frac{\partial\tilde{\mathbf{T}}_B^{B0}}{\partial\Phi_j} \right)_i, \end{aligned} \quad (161)$$

with $\partial^2(\mathbf{Q}_v)_i/\partial\theta_k\partial\Phi_k$ obtained by a similar equation, and

$$\frac{\partial^2(\mathbf{Q}_v)_i}{\partial\theta_j\partial\theta_k} = \mathbf{T}_{B0}^B\mathbf{T}_g^{B0} \left(\frac{\partial^2\tilde{\mathbf{A}}_n}{\partial\theta_j\partial\theta_k}\tilde{\mathbf{T}}_{B0}^g\tilde{\mathbf{T}}_B^{B0} \right)_i. \quad (162)$$

The above equations require a second derivative of \mathbf{T}_s^B . Continuing from (60) and (61), the second derivatives are

$$\frac{\partial^2\mathbf{T}_s^B}{\partial r_i\partial r_j} = \left[\begin{array}{c} \frac{\partial^2\mathbf{x}_s^B}{\partial r_i\partial r_j}, \\ \left\{ \begin{array}{l} \frac{\partial^2\mathbf{y}_s^B}{(\partial\mathbf{x}_s^B)^2}\frac{\partial\mathbf{x}_s^B}{\partial r_i}\frac{\partial\mathbf{x}_s^B}{\partial r_j} + \frac{\partial\mathbf{y}_s^B}{\partial\mathbf{x}_s^B}\frac{\partial^2\mathbf{x}_s^B}{\partial r_i\partial r_j} + \frac{\partial^2\mathbf{y}_s^B}{\partial\mathbf{x}_s^B\mathbf{z}_s^B}\frac{\partial\mathbf{x}_s^B}{\partial r_i}\frac{\partial\mathbf{x}_s^B}{\partial r_j} \\ + \frac{\partial^2\mathbf{y}_s^B}{\partial(\mathbf{z}_s^B)^2}\frac{\partial\mathbf{z}_s^B}{\partial r_i}\frac{\partial\mathbf{x}_s^B}{\partial r_j} + \frac{\partial^2\mathbf{y}_s^B}{\partial\mathbf{z}_s^B\mathbf{x}_s^B}\frac{\partial\mathbf{x}_s^B}{\partial r_i}\frac{\partial\mathbf{x}_s^B}{\partial r_j} \\ + \frac{\partial\mathbf{y}_s^B}{\partial\mathbf{z}_s^B}\frac{\partial^2\mathbf{z}_s^B}{(\partial\mathbf{x}_s^B)^2}\frac{\partial\mathbf{x}_s^B}{\partial r_i}\frac{\partial\mathbf{x}_s^B}{\partial r_j} + \frac{\partial\mathbf{y}_s^B}{\partial\mathbf{z}_s^B}\frac{\partial\mathbf{z}_s^B}{\partial\mathbf{x}_s^B}\frac{\partial^2\mathbf{x}_s^B}{\partial r_i\partial r_j} \end{array} \right\}, \\ \frac{\partial^2\mathbf{z}_s^B}{(\partial\mathbf{x}_s^B)^2}\frac{\partial\mathbf{x}_s^B}{\partial r_i}\frac{\partial\mathbf{x}_s^B}{\partial r_j} + \frac{\partial\mathbf{z}_s^B}{\partial\mathbf{x}_s^B}\frac{\partial\mathbf{x}_s^B}{\partial r_i\partial r_j} \end{array} \right] \quad (163)$$

with

$$\begin{aligned} &\frac{\partial}{\partial a_j} \frac{\mathbf{e}_i(\mathbf{a}-\mathbf{b})^T(\mathbf{a}-\mathbf{b}) - (\mathbf{a}-\mathbf{b})\mathbf{e}_i^T(\mathbf{a}-\mathbf{b})}{|\mathbf{a}-\mathbf{b}|(\mathbf{a}-\mathbf{b})^T(\mathbf{a}-\mathbf{b})} \\ &= -3 \frac{[\mathbf{e}_i(\mathbf{a}-\mathbf{b})^T(\mathbf{a}-\mathbf{b}) - (\mathbf{a}-\mathbf{b})\mathbf{e}_i^T(\mathbf{a}-\mathbf{b})]\mathbf{e}_j^T(\mathbf{a}-\mathbf{b})}{[(\mathbf{a}-\mathbf{b})^T(\mathbf{a}-\mathbf{b})]^{5/2}} \\ &+ \frac{2\mathbf{e}_i\mathbf{e}_j^T(\mathbf{a}-\mathbf{b}) - \mathbf{e}_j\mathbf{e}_i^T(\mathbf{a}-\mathbf{b}) - (\mathbf{a}-\mathbf{b})\delta_{ij}}{[(\mathbf{a}-\mathbf{b})^T(\mathbf{a}-\mathbf{b})]^{3/2}} \\ &= -\frac{\partial}{\partial b_j}(\dots) \end{aligned} \quad (164)$$

$$\begin{aligned} &\frac{\partial}{\partial a_j} \frac{(\mathbf{e}_i \times \mathbf{b})(\mathbf{a} \times \mathbf{b})^T(\mathbf{a} \times \mathbf{b}) - (\mathbf{a} \times \mathbf{b})(\mathbf{e}_i^T \times \mathbf{b})(\mathbf{a} \times \mathbf{b})}{|\mathbf{a} \times \mathbf{b}|(\mathbf{a} \times \mathbf{b})^T(\mathbf{a} \times \mathbf{b})} \\ &= -3 \frac{[(\mathbf{e}_i \times \mathbf{b})(\mathbf{a} \times \mathbf{b})^T(\mathbf{a} \times \mathbf{b}) - (\mathbf{a} \times \mathbf{b})(\mathbf{e}_i^T \times \mathbf{b})(\mathbf{a} \times \mathbf{b})](\mathbf{e}_j \times \mathbf{b})^T(\mathbf{a} \times \mathbf{b})}{[(\mathbf{a} \times \mathbf{b})^T(\mathbf{a} \times \mathbf{b})]^{5/2}} \\ &+ \frac{2(\mathbf{e}_i \times \mathbf{b})(\mathbf{e}_j \times \mathbf{b})^T(\mathbf{a} \times \mathbf{b}) - (\mathbf{e}_j \times \mathbf{b})(\mathbf{e}_i \times \mathbf{b})^T(\mathbf{a} \times \mathbf{b}) - (\mathbf{a} \times \mathbf{b})(\mathbf{e}_i \times \mathbf{b})^T(\mathbf{e}_j \times \mathbf{b})}{|\mathbf{a} \times \mathbf{b}|(\mathbf{a} \times \mathbf{b})^T(\mathbf{a} \times \mathbf{b})} \end{aligned} \quad (165)$$

and

$$\begin{aligned}
& \frac{\partial}{\partial b_j} \frac{(\mathbf{e}_i \times \mathbf{b})(\mathbf{a} \times \mathbf{b})^T(\mathbf{a} \times \mathbf{b}) - (\mathbf{a} \times \mathbf{b})(\mathbf{e}_i^T \times \mathbf{b})(\mathbf{a} \times \mathbf{b})}{|\mathbf{a} \times \mathbf{b}|(\mathbf{a} \times \mathbf{b})^T(\mathbf{a} \times \mathbf{b})} \\
&= -3 \frac{[(\mathbf{e}_i \times \mathbf{b})(\mathbf{a} \times \mathbf{b})^T(\mathbf{a} \times \mathbf{b}) - (\mathbf{a} \times \mathbf{b})(\mathbf{e}_i^T \times \mathbf{b})(\mathbf{a} \times \mathbf{b})](\mathbf{a} \times \mathbf{e}_j)^T(\mathbf{a} \times \mathbf{b})}{[(\mathbf{a} \times \mathbf{b})^T(\mathbf{a} \times \mathbf{b})]^{5/2}} \\
&+ \frac{(\mathbf{e}_i \times \mathbf{e}_j)(\mathbf{a} \times \mathbf{b})^T(\mathbf{a} \times \mathbf{b}) + 2(\mathbf{e}_i \times \mathbf{b})(\mathbf{a} \times \mathbf{e}_j)^T(\mathbf{a} \times \mathbf{b})}{[(\mathbf{a} \times \mathbf{b})^T(\mathbf{a} \times \mathbf{b})]^{3/2}} \\
&- \frac{(\mathbf{a} \times \mathbf{e}_j)(\mathbf{e}_i \times \mathbf{b})^T(\mathbf{a} \times \mathbf{b}) + (\mathbf{a} \times \mathbf{b})(\mathbf{e}_i \times \mathbf{e}_j)^T(\mathbf{a} \times \mathbf{b}) + (\mathbf{a} \times \mathbf{b})(\mathbf{e}_i \times \mathbf{b})^T(\mathbf{a} \times \mathbf{e}_j)}{[(\mathbf{a} \times \mathbf{b})^T(\mathbf{a} \times \mathbf{b})]^{3/2}}
\end{aligned} \tag{166}$$

Also,

$$\frac{\partial^2 \mathbf{T}_s^B}{\partial \theta_i \partial \theta_j} = \left[\begin{array}{c} \mathbf{0}, \\ \left\{ \frac{\partial^2 \mathbf{y}_s^B}{(\mathbf{z}_s^B)^2} \frac{\partial \mathbf{z}_s^B}{\mathbf{y}_{s'}^B} \frac{\partial \mathbf{y}_{s'}^B}{\partial \theta_i} \frac{\partial \mathbf{z}_s^B}{\mathbf{y}_{s'}^B} \frac{\partial \mathbf{y}_{s'}^B}{\partial \theta_j} \right. \\ \left. + \frac{\partial \mathbf{y}_s^B}{\partial \mathbf{z}_s^B} \frac{\partial^2 \mathbf{z}_s^B}{(\partial \mathbf{y}_{s'}^B)^2} \frac{\partial \mathbf{y}_{s'}^B}{\partial \theta_i} \frac{\partial \mathbf{y}_{s'}^B}{\partial \theta_j} + \frac{\partial \mathbf{y}_s^B}{\partial \mathbf{z}_s^B} \frac{\partial^2 \mathbf{z}_s^B}{\partial \mathbf{y}_{s'}^B} \frac{\partial^2 \mathbf{y}_{s'}^B}{\partial \theta_i \partial \theta_j} \right\}, \\ \frac{\partial^2 \mathbf{z}_s^B}{(\partial \mathbf{y}_{s'}^B)^2} \frac{\partial \mathbf{y}_{s'}^B}{\partial \theta_i} \frac{\partial \mathbf{y}_{s'}^B}{\partial \theta_j} + \frac{\partial^2 \mathbf{z}_s^B}{\partial \mathbf{y}_{s'}^B} \frac{\partial^2 \mathbf{y}_{s'}^B}{\partial \theta_i \partial \theta_j} \end{array} \right], \tag{167}$$

and

$$\frac{\partial^2 \mathbf{T}_s^B}{\partial r_i \partial \theta_j} = \left[\begin{array}{c} \mathbf{0}, \\ \left\{ \frac{\partial^2 \mathbf{y}_s^B}{\mathbf{x}_s^B \mathbf{z}_s^B} \frac{\partial \mathbf{x}_s^B}{\partial r_i} \frac{\partial \mathbf{z}_s^B}{\mathbf{y}_{s'}^B} \frac{\partial \mathbf{y}_{s'}^B}{\partial \theta_j} + \frac{\partial^2 \mathbf{y}_s^B}{(\partial \mathbf{z}_s^B)^2} \frac{\partial \mathbf{z}_s^B}{\partial \mathbf{x}_s^B} \frac{\partial \mathbf{x}_s^B}{\partial r_i} \frac{\partial \mathbf{z}_s^B}{\partial \mathbf{y}_{s'}^B} \frac{\partial \mathbf{y}_{s'}^B}{\partial \theta_j} \right. \\ \left. + \frac{\partial \mathbf{y}_s^B}{\partial \mathbf{z}_s^B} \frac{\partial^2 \mathbf{z}_s^B}{\partial \mathbf{x}_s^B} \frac{\partial \mathbf{y}_{s'}^B}{\partial r_i} \frac{\partial \mathbf{y}_{s'}^B}{\partial \theta_j} \right\}, \\ \frac{\partial^2 \mathbf{z}_s^B}{\partial \mathbf{x}_s^B \partial \mathbf{y}_{s'}^B} \frac{\partial \mathbf{x}_s^B}{\partial r_i} \frac{\partial \mathbf{y}_{s'}^B}{\partial \theta_j} \end{array} \right]. \tag{168}$$

3.2 Linear constraints

Let us write (135) in the shorthand

$$\tilde{\mathbf{M}}(\mathbf{q}) \frac{d^2 \mathbf{q}}{dt^2} = \mathbf{R}(\mathbf{q}, \dot{\mathbf{q}}) + \tilde{\mathbf{Q}}(\mathbf{q}) \mathbf{F}^B, \tag{169}$$

where \mathbf{R} now encompasses the stiffness, damping, gyroscopic, and centrifugal terms. Using the acceleration form of the constraint equations, (121),

$$\tilde{\mathbf{M}} \left(\boldsymbol{\Lambda} \frac{d^2 \hat{\mathbf{q}}}{dt^2} + \boldsymbol{\Gamma} \frac{d \hat{\mathbf{q}}}{dt} \right) = \mathbf{R} + \tilde{\mathbf{Q}} \mathbf{F}^B, \tag{170}$$

where, again, the definitions of $\boldsymbol{\Lambda}$ and $\boldsymbol{\Gamma}$ are

$$\boldsymbol{\Lambda} := \begin{bmatrix} \mathbf{I} \\ -\mathbf{L}_s^{-1} \hat{\mathbf{L}} \end{bmatrix} \quad \text{and} \quad \boldsymbol{\Gamma} := \begin{bmatrix} \mathbf{0} \\ -\mathbf{L}_x^{-1} \frac{dq_k}{dt} \frac{\partial \mathbf{L}}{\partial q_k} \boldsymbol{\Lambda} \end{bmatrix}. \tag{171}$$

Premultiplying by $\boldsymbol{\Lambda}^T$,

$$\boldsymbol{\Lambda}^T \tilde{\mathbf{M}} \left(\boldsymbol{\Lambda} \frac{d^2 \hat{\mathbf{q}}}{dt^2} + \boldsymbol{\Gamma} \frac{d \hat{\mathbf{q}}}{dt} \right) = \boldsymbol{\Lambda}^T (\mathbf{R} + \tilde{\mathbf{Q}} \mathbf{F}^B). \tag{172}$$

Linearizing (172),

$$\begin{aligned}
& \boldsymbol{\Lambda}_0^T \tilde{\mathbf{M}}_0 \boldsymbol{\Lambda}_0 \frac{d^2 \Delta \hat{\mathbf{q}}}{dt^2} \\
& + \boldsymbol{\Lambda}_0^T \tilde{\mathbf{M}}_0 \left(\left. \frac{\partial \boldsymbol{\Lambda}}{\partial q_k} \right|_0 \frac{d^2 \hat{\mathbf{q}}}{dt^2} \Big|_0 + \left. \frac{\partial \boldsymbol{\Gamma}}{\partial q_k} \right|_0 \frac{d \hat{\mathbf{q}}}{dt} \Big|_0 \right) \Delta q_k + \boldsymbol{\Lambda}_0^T \tilde{\mathbf{M}}_0 \left. \frac{\partial \boldsymbol{\Gamma}}{\partial \dot{q}_k} \right|_0 \frac{d \hat{\mathbf{q}}}{dt} \Big|_0 \frac{d \Delta q_k}{dt} \\
& = \left. \frac{\partial \boldsymbol{\Lambda}^T}{\partial q_k} \right|_0 \left(-\tilde{\mathbf{M}}_0 \frac{d^2 \hat{\mathbf{q}}}{dt^2} \Big|_0 + \mathbf{R}_0 + \tilde{\mathbf{Q}}_0 \mathbf{F}_0^B \right) \Delta q_k \\
& + \boldsymbol{\Lambda}_0^T \left[\left. \frac{\partial \mathbf{R}}{\partial \dot{q}_k} \right|_0 \frac{d \Delta q_k}{dt} + \left(-\left. \frac{\partial \tilde{\mathbf{M}}}{\partial q_k} \right|_0 \frac{d^2 \hat{\mathbf{q}}}{dt^2} \Big|_0 + \left. \frac{\partial \mathbf{R}}{\partial q_k} \right|_0 + \left. \frac{\partial \tilde{\mathbf{Q}}}{\partial q_k} \right|_0 \mathbf{F}_0^B \right) \Delta q_k + \tilde{\mathbf{Q}}_0 \Delta \mathbf{F}^B \right].
\end{aligned} \tag{173}$$

Note that the first term on the right-hand side is zero, as the expression in parentheses is (169) at the initial condition. The latter term on the right-hand side contains the known terms from (139), premultiplied by $\boldsymbol{\Lambda}_0^T$. As for the remaining terms,

$$\boldsymbol{\Lambda}_0^T \tilde{\mathbf{M}}_0 \left(\left. \frac{\partial \boldsymbol{\Lambda}}{\partial q_k} \right|_0 \frac{d^2 \hat{\mathbf{q}}}{dt^2} \Big|_0 + \left. \frac{\partial \boldsymbol{\Gamma}}{\partial q_k} \right|_0 \frac{d \hat{\mathbf{q}}}{dt} \Big|_0 \right) \Delta q_k \quad \text{and} \quad \boldsymbol{\Lambda}_0^T \tilde{\mathbf{M}}_0 \left. \frac{\partial \boldsymbol{\Gamma}}{\partial \dot{q}_k} \right|_0 \frac{d \hat{\mathbf{q}}}{dt} \Big|_0 \frac{d \Delta q_k}{dt}$$

appear due to the constraints. Reducing Δq_k and $d \Delta q_k / dt$, the result is

$$\begin{aligned}
& \boldsymbol{\Lambda}_0^T \tilde{\mathbf{M}}_0 \boldsymbol{\Lambda}_0 \frac{d^2 \Delta \hat{\mathbf{q}}}{dt^2} \\
& = \boldsymbol{\Lambda}_0^T \tilde{\mathbf{Q}}_0 \Delta \mathbf{F}^B - \boldsymbol{\Lambda}_0^T \tilde{\mathbf{M}}_0 \boldsymbol{\Gamma}_0 \frac{d \Delta \hat{\mathbf{q}}}{dt} \\
& + \boldsymbol{\Lambda}_0^T \left(-\tilde{\mathbf{M}}_0 \left. \frac{\partial \boldsymbol{\Gamma}}{\partial \dot{q}_k} \right|_0 \frac{d \hat{\mathbf{q}}}{dt} \Big|_0 + \left. \frac{\partial \mathbf{R}}{\partial \dot{q}_k} \right|_0 \right) \boldsymbol{\Lambda}_{kp} \frac{d \Delta \hat{q}_p}{dt} \\
& + \boldsymbol{\Lambda}_0^T \left[\left(-\tilde{\mathbf{M}}_0 \left. \frac{\partial \boldsymbol{\Lambda}}{\partial q_k} \right|_0 \frac{d^2 \hat{\mathbf{q}}}{dt^2} \Big|_0 - \tilde{\mathbf{M}}_0 \left. \frac{\partial \boldsymbol{\Gamma}}{\partial q_k} \right|_0 \frac{d \hat{\mathbf{q}}}{dt} \Big|_0 - \left. \frac{\partial \tilde{\mathbf{M}}}{\partial q_k} \right|_0 \frac{d^2 \hat{\mathbf{q}}}{dt^2} \Big|_0 + \left. \frac{\partial \mathbf{R}}{\partial q_k} \right|_0 + \left. \frac{\partial \tilde{\mathbf{Q}}}{\partial q_k} \right|_0 \mathbf{F}_0^B \right) \boldsymbol{\Lambda}_{kp} \\
& + \left(-\tilde{\mathbf{M}}_0 \left. \frac{\partial \boldsymbol{\Gamma}}{\partial \dot{q}_k} \right|_0 \frac{d \hat{\mathbf{q}}}{dt} \Big|_0 + \left. \frac{\partial \mathbf{R}}{\partial \dot{q}_k} \right|_0 \right) \boldsymbol{\Gamma}_{kp} \Delta \hat{q}_p.
\end{aligned} \tag{174}$$

The derivative of $\boldsymbol{\Lambda}$ is obtained by

$$\begin{bmatrix} \mathbf{I} & \mathbf{0} \\ \mathbf{0} & \mathbf{L}_s \end{bmatrix} \boldsymbol{\Lambda} = \begin{bmatrix} \mathbf{I} & \mathbf{0} \\ \mathbf{0} & \mathbf{L}_s \end{bmatrix} \begin{bmatrix} \mathbf{I} \\ -\mathbf{L}_s^{-1} \hat{\mathbf{L}} \end{bmatrix} \tag{175}$$

such that

$$\begin{bmatrix} \mathbf{0} & \mathbf{0} \\ \mathbf{0} & \partial \mathbf{L}_s / \partial q_k \end{bmatrix} \boldsymbol{\Lambda} + \begin{bmatrix} \mathbf{I} & \mathbf{0} \\ \mathbf{0} & \mathbf{L}_s \end{bmatrix} \frac{\partial \boldsymbol{\Lambda}}{\partial q_k} = \begin{bmatrix} \mathbf{0} \\ -\partial \hat{\mathbf{L}} / \partial q_k \end{bmatrix} \tag{176}$$

and

$$\frac{\partial \boldsymbol{\Lambda}}{\partial q_k} = \begin{bmatrix} \mathbf{I} & \mathbf{0} \\ \mathbf{0} & \mathbf{L}_s \end{bmatrix}^{-1} \left\{ \begin{bmatrix} \mathbf{0} \\ -\partial \hat{\mathbf{L}} / \partial q_k \end{bmatrix} - \begin{bmatrix} \mathbf{0} & \mathbf{0} \\ \mathbf{0} & \partial \mathbf{L}_s / \partial q_k \end{bmatrix} \boldsymbol{\Lambda} \right\}. \tag{177}$$

Similarly,

$$\frac{\partial \boldsymbol{\Gamma}}{\partial q_k} = \begin{bmatrix} \mathbf{I} & \mathbf{0} \\ \mathbf{0} & \mathbf{L}_s \end{bmatrix}^{-1} \left\{ \begin{bmatrix} \mathbf{0} \\ -\frac{dq_j}{dt} \frac{\partial^2 \mathbf{L}}{\partial q_j \partial q_k} \boldsymbol{\Lambda} - \frac{dq_j}{dt} \frac{\partial \mathbf{L}}{\partial q_j} \frac{\partial \boldsymbol{\Lambda}}{\partial q_k} \end{bmatrix} - \begin{bmatrix} \mathbf{0} & \mathbf{0} \\ \mathbf{0} & \partial \mathbf{L}_s / \partial q_k \end{bmatrix} \boldsymbol{\Gamma} \right\} \tag{178}$$

and

$$\frac{\partial \Gamma}{\partial \dot{q}_k} = \begin{bmatrix} \mathbf{0} \\ -\mathbf{L}_s^{-1} \frac{\partial \mathbf{L}}{\partial \dot{q}_k} \boldsymbol{\Lambda} \end{bmatrix}. \quad (179)$$

As $\frac{\partial^2 \mathbf{L}}{\partial q_j \partial q_k}$ is challenging to formulate analytically, it is evaluated numerically using finite differences. It is noted that the contribution of $\partial \Gamma / \partial q_k$ to the dynamics is typically small, so a loss of numerical precision within this particular term is not expected to influence the overall results.

In forming the linear state space, it is desired to recover the full $\Delta \mathbf{q}$, $d\Delta \mathbf{q}/dt$, and $d^2\Delta \mathbf{q}/dt^2$ vectors. The constraint equations (98), (118), and (121) give the relationships

$$\Delta \mathbf{q} = \boldsymbol{\Lambda}_0 \Delta \hat{\mathbf{q}}, \quad (180)$$

$$\frac{d\Delta \mathbf{q}}{dt} = \boldsymbol{\Lambda}_0 \frac{d\Delta \hat{\mathbf{q}}}{dt} + \boldsymbol{\Gamma}_0 \Delta \hat{\mathbf{q}}, \quad (181)$$

and

$$\begin{aligned} \frac{d^2\Delta \mathbf{q}}{dt^2} = & \boldsymbol{\Lambda}_0 \frac{d^2\Delta \hat{\mathbf{q}}}{dt^2} + \boldsymbol{\Gamma}_0 \frac{d\Delta \hat{\mathbf{q}}}{dt} + \left. \frac{\partial \Gamma}{\partial \dot{q}_k} \right|_0 \frac{d\hat{\mathbf{q}}}{dt} \bigg|_0 \frac{d\Delta q_k}{dt} \\ & + \left(\left. \frac{\partial \boldsymbol{\Lambda}}{\partial q_k} \right|_0 \frac{d^2\hat{\mathbf{q}}}{dt^2} \bigg|_0 + \left. \frac{\partial \boldsymbol{\Gamma}}{\partial q_k} \right|_0 \frac{d\hat{\mathbf{q}}}{dt} \bigg|_0 \right) \Delta q_k. \end{aligned} \quad (182)$$

3.3 Modal reduction and damping

For the range of frequencies generally of interest for aeroelastic problems, the number of degrees of freedom in the model can be greatly reduced. Modal reduction is especially convenient, because the resulting diagonalization of the system equations allows for a simple, empirical implementation of damping.

If a set of mode shapes – that is, a matrix whose columns contain the mode shapes – is known, then modal degrees-of-freedom are substituted according to

$$\Delta \hat{\mathbf{q}} = \boldsymbol{\Phi} \Delta \boldsymbol{\eta}, \quad \frac{d\Delta \hat{\mathbf{q}}}{dt} = \boldsymbol{\Phi} \frac{d\Delta \boldsymbol{\eta}}{dt}, \quad \frac{d^2\Delta \hat{\mathbf{q}}}{dt^2} = \boldsymbol{\Phi} \frac{d^2\Delta \boldsymbol{\eta}}{dt^2}. \quad (183)$$

We elect to compute the mode shapes on a body-by-body basis. This is done in order to make the degrees-of-freedom intuitive. The modes of the assembled structure can be quite complicated, and it helps if the individual degrees of freedom represent an easily understood quantity like a “tower fore-aft mode” or “blade flap mode”. The elastic degrees-of-freedom associated with each body – omitting the reference node – are partitioned and isolated, giving an unforced eigenvalue equation

$$(\omega^2 \mathbf{M}_\Lambda + \mathbf{K}_\Lambda) = \mathbf{0} \quad (184)$$

Here the Λ subscript indicates that these quantities are constrained; it is beneficial to compute the mode shapes using the *constrained* mass and stiffness matrices. The degrees-of-freedom associated with the joints include the inertia of all outboard bodies, and this leads to body mode shapes that better match the deformations of the assembled structure.

The constrained equations of motion (174) are reduced according to

$$\boldsymbol{\Phi}^T \mathbf{M}_\Lambda \boldsymbol{\Phi} \frac{d^2\Delta \boldsymbol{\eta}}{dt^2} + \boldsymbol{\Phi}^T \mathbf{C}_\Lambda \boldsymbol{\Phi} \frac{d\Delta \boldsymbol{\eta}}{dt} + \boldsymbol{\Phi}^T \mathbf{K}_\Lambda \boldsymbol{\Phi} \Delta \boldsymbol{\eta} = \boldsymbol{\Phi}^T \Delta \mathbf{F}_\Lambda. \quad (185)$$

Going forward, let us write (185) simply as

$$\mathbf{M} \frac{d^2\Delta \boldsymbol{\eta}}{dt^2} + \mathbf{C} \frac{d\Delta \boldsymbol{\eta}}{dt} + \mathbf{K} \Delta \boldsymbol{\eta} = \Delta \mathbf{F}. \quad (186)$$

Structural damping is applied as a damping ratio associated with each body mode. For a given elastic body mode λ , a damping factor is computed as

$$C_\lambda = 2\zeta\sqrt{M_\lambda K_\lambda}, \quad (187)$$

where M_λ and K_λ are the relevant values from the diagonal of the mass and stiffness matrices. C_λ is then added to the diagonal of C . A value of $\zeta = 0.008$ is recommended.

The equations (186) can be put into linear state-space form,

$$\begin{bmatrix} \mathbf{I} & \mathbf{0} \\ \mathbf{0} & \mathbf{M} \end{bmatrix} \frac{d}{dt} \begin{bmatrix} \Delta\boldsymbol{\eta} \\ \Delta\dot{\boldsymbol{\eta}} \end{bmatrix} = \begin{bmatrix} \mathbf{0} & \mathbf{I} \\ -\mathbf{K} & -\mathbf{C} \end{bmatrix} \begin{bmatrix} \Delta\boldsymbol{\eta} \\ \Delta\dot{\boldsymbol{\eta}} \end{bmatrix} + \begin{bmatrix} \mathbf{0} \\ \Delta\mathbf{F} \end{bmatrix} \quad (188)$$

4 Aerodynamics

The aerodynamic calculations are implemented in nonlinear and linear forms. Together with the structural model, a nonlinear analysis is performed in order to find points along dynamic trajectories, at which the system is then linearized for a deeper study of stability or the stochastic response.

4.1 Blade profile input

The initial, undeformed transform from pitch to section coordinates can be obtained by a rotation about the X^p axis by a potentially large twist angle $-\xi_0$ plus blade torsion $(\boldsymbol{\theta}_0^p)_x$, a rotation about the Y^p axis by the small prebend angle η_0 plus elastic rotation $(\boldsymbol{\theta})_y$, and a rotation about the Z^p axis by a small sweep angle ζ_0 plus elastic rotation $(\boldsymbol{\theta})_z$. This way of formulating the transform is accurate provided that the y and z rotation angles remain small.⁷ The resulting transformation matrix is

$$\mathbf{T}_p^s = \begin{bmatrix} 1 & 0 & 0 \\ 0 & c\theta_1 & s\theta_1 \\ 0 & -s\theta_1 & c\theta_1 \end{bmatrix} \begin{bmatrix} c\theta_2 & 0 & -s\theta_2 \\ 0 & 1 & 0 \\ s\theta_2 & 0 & c\theta_2 \end{bmatrix} \begin{bmatrix} c\theta_3 & s\theta_3 & 0 \\ -s\theta_3 & c\theta_3 & 0 \\ 0 & 0 & 1 \end{bmatrix} \quad (189)$$

where $\theta_1 := (\boldsymbol{\theta}_0^p)_x - \xi_0$, $\theta_2 = \eta_0 + (\boldsymbol{\theta}^p)_y$, and $\theta_3 = \zeta_0 + (\boldsymbol{\theta}^p)_z$.

Equation (189) corresponds to the way in which the blade profile is often described, in terms of twist, bend, and sweep. It is thus used for inputting the undeformed shape of the blade. As seen in Section 2, the state variables for large-deformation analysis are not these twist-bend-sweep angles, but rather an alternate set of parameters by which the transform \mathbf{T}_n^{n0} – that is, from deformed to undeformed nodal section coordinates – is derived. In any event, given a set of state variables, the transforms from section (aerodynamic properties) to body (blade pitch) to rotorplane (momentum balance) to global (wind) coordinate frames can be computed.

The transform from aerodynamic to section coordinates,

$$\mathbf{T}_a^s = \begin{bmatrix} 0 & 0 & 1 \\ -c\xi_s & s\xi_s & 0 \\ s\xi_s & c\xi_s & 0 \end{bmatrix}, \quad (190)$$

is not influenced by blade deformation, since both these coordinate systems follow the airfoil profiles. The transform from pitch to rotorplane coordinates is also unchanged, as the displacements at the nacelle are assumed to be small.

⁷Small means below about 10°. If prebend and sweep are simply tabulated as part of the input data, then the associated rotation angles *must* be small, otherwise additional information must be given regarding the orientation of the airfoil section. The matter is helped by the fact that flapwise deflection under operating loads will tend to cancel the prebend.

4.2 Nonlinear blade element momentum model

The blade element momentum method involves the computation of local airfoil forces based on the flow characteristics at the airfoil profiles along the blades, and momentum balance for the flow passing through the rotor plane.

Computing the airfoil forces involves finding the relative airflow at each element along the blades. To this end, define an airfoil coordinate system as sketched in Fig. 2. The quasi-steady angle-of-attack α_q is defined as the angle from the X^a axis (aligned with the chordline towards the trailing edge) to the local flow vector \mathbf{U}^a , projected onto the airfoil section, such that

$$\tan \alpha_q = \frac{(\mathbf{U}^a)_y}{(\mathbf{U}^a)_x}. \quad (191)$$

A dynamic angle-of-attack, used in the computation of airfoil forces, is obtained from the linear state-space model (Merz 2015, Leishman 2002)

$$\frac{d}{dt} \begin{bmatrix} \alpha \\ a_1 \\ a_2 \end{bmatrix} = \begin{bmatrix} -\tau^{-1} & \tau^{-1}K_1 & \tau^{-1}K_2 \\ 0 & 0 & 1 \\ 0 & A_{32} & A_{33} \end{bmatrix} \begin{bmatrix} \alpha \\ a_1 \\ a_2 \end{bmatrix} + \begin{bmatrix} \tau^{-1}K_3 \\ 0 \\ 1 \end{bmatrix} \alpha_q, \quad (192)$$

which accounts for dynamic stall and circulation lag. Parameters are

$$\begin{aligned} A_{32} &= -b_1 b_2 \left(\frac{2U}{c}\right)^2, & A_{33} &= -(b_1 + b_2) \left(\frac{2U}{c}\right), & K_1 &= (A_1 + A_2) b_1 b_2 \left(\frac{2U}{c}\right)^2, \\ K_2 &= (A_1 b_1 + A_2 b_2) \left(\frac{2U}{c}\right), & K_3 &= 1 - A_1 - A_2, & A_1 &= 0.165, & A_2 &= 0.335, \\ b_1 &= 0.0455, & b_2 &= 0.3, & \tau &= 4.3 \frac{c}{U}. \end{aligned} \quad (193)$$

Here c is the airfoil chord length and

$$U = \sqrt{(\mathbf{U}_{/g}^a)_x^2 + (\mathbf{U}_{/g}^a)_y^2}, \quad (194)$$

the local air velocity, neglecting the spanwise component.

The local flow vector, with respect to the fixed, global coordinate system, expressed in instantaneous airfoil coordinates, is

$$\mathbf{U}_{/g}^a = \mathbf{V}_\infty^a + \mathbf{V}_i^a - \mathbf{w}_{/g}^a. \quad (195)$$

The terms on the right-hand side are respectively the remote incoming wind (including turbulence), induced velocity, and structural motion, including rotor rotation. The structural motion of a given node follows from (76),⁸

$$\begin{bmatrix} \mathbf{w}_{n/g}^a \\ \boldsymbol{\omega}_{n/g}^a \end{bmatrix} = \mathbf{T}_s^a \mathbf{T}_B^s \mathbf{T}_{B0}^B \mathbf{T}_g^{B0} \left(\tilde{\mathbf{A}}_n \tilde{\mathbf{T}}_{B0}^g \mathbf{T}_B^{B0} + \mathbf{A}_n \tilde{\mathbf{T}}_{B0}^g \frac{\partial \tilde{\mathbf{T}}_B^{B0}}{\partial \mathbf{q}} (\mathbf{q} + \mathbf{P}) \right) \frac{d\mathbf{q}}{dt}, \quad (196)$$

or

$$\begin{bmatrix} \mathbf{w}_{n/g}^a \\ \boldsymbol{\omega}_{n/g}^a \end{bmatrix} = \mathbf{T}_s^a \mathbf{T}_B^s \mathbf{Q}_v(\mathbf{q}) \frac{d\mathbf{q}}{dt}. \quad (197)$$

The element velocity is taken as the average of that of the adjacent nodes. With the velocity (197), and dynamic angle-of-attack from (192), the airfoil forces can be computed by

$$F_L = C_L(\alpha, \alpha_q) \frac{1}{2} \rho c L \left[(\mathbf{U}_{/g}^a)_x^2 + (\mathbf{U}_{/g}^a)_y^2 \right], \quad (198)$$

⁸The angular velocity $\boldsymbol{\omega}$, it is assumed, does not influence the aerodynamic forces. We represent the structural motion here as \mathbf{w} , rather than \mathbf{v} , to avoid confusion with the windspeed.

$$F_D = C_D(\alpha_q) \frac{1}{2} \rho c L [(\mathbf{U}_{/g}^a)_x^2 + (\mathbf{U}_{/g}^a)_y^2], \quad (199)$$

where

$$C_L(\alpha, \alpha_q) = C_L(\alpha) \left(1 + \frac{\alpha_q - \alpha}{\alpha - \alpha_z} \right) \quad (200)$$

and

$$\lim_{\alpha \rightarrow \alpha_z} C_L(\alpha, \alpha_q) = \frac{dC_L}{d\alpha} (\alpha_q - \alpha). \quad (201)$$

Here α_z is the zero-lift intercept of a line representing the linear part of the lift coefficient curve.⁹ The relationships (200) and (201) are not valid for deep stall, when the airfoil behaves as a flat plate in a cross-flow. Beyond some maximum angle-of-attack, τ may be scheduled such that $\alpha \rightarrow \alpha_q$ over the relevant frequency band.

The lift and drag are expressed in a coordinate frame associated with the instantaneous angle-of-attack. We can therefore write

$$\mathbf{F}^a = \frac{1}{2} \rho c L [(\mathbf{U}_{/g}^a)_x^2 + (\mathbf{U}_{/g}^a)_y^2] \begin{bmatrix} -s\alpha_q & c\alpha_q & 0 \\ c\alpha_q & s\alpha_q & 0 \\ 0 & 0 & 0 \\ 0 & 0 & 0 \\ 0 & 0 & 0 \\ -c\alpha_q x - s\alpha_q y & -s\alpha_q x + c\alpha_q y & -c \end{bmatrix} \begin{bmatrix} C_L \\ C_D \\ C_M \end{bmatrix} \quad (202)$$

to obtain the forces in airfoil coordinates.¹⁰ Here x and y are the in-plane coordinates of the origin of the section coordinate system with respect to the aerodynamic center where the moment coefficient is defined, typically the quarter-chord point.

Considering an annulus of the rotor associated with a given blade station, momentum balance gives an expression for the *quasi-steady* induced velocity \mathbf{V}_{iq}

$$\mathbf{F}^r = -2\rho A f W \mathbf{V}_{iq}^r, \quad (203)$$

with

$$f = \frac{2}{\pi} \cos^{-1} \left\{ \exp \left[\frac{N_b(r - D/2)}{2r \sin \phi} \right] \right\}, \quad \phi = \tan^{-1} \frac{(\mathbf{U}_{/r}^r)_z}{(\mathbf{U}_{/r}^r)_t}, \quad (204)$$

$$\begin{aligned} W &:= \sqrt{[(\mathbf{V}_{/r}^r)_z + f(\mathbf{V}_{iq}^r)_z]^2 + (\mathbf{V}_{/r}^r)_t^2 + (\mathbf{V}_{/r}^r)_s^2} \\ &= \sqrt{[(\mathbf{V}_{/r}^r)_z + f(\mathbf{V}_{iq}^r)_z]^2 + (\mathbf{V}_{/r}^r)_x^2 + (\mathbf{V}_{/r}^r)_y^2} \end{aligned} \quad (205)$$

and

$$\mathbf{V}_{/r}^r = \mathbf{V}_{\infty/g}^r - \mathbf{w}_{r/g}^r \quad \text{or} \quad \mathbf{V}_{/r}^r = \mathbf{V}_{\infty/g}^r \quad (206)$$

depending on the choice of the rotorplane coordinate system.¹¹ Equation (203) is decomposed into axial and tangential components. The spanwise momentum balance is neglected, as it has no influence on the aerodynamic forces; $(\mathbf{F}^r)_s = 0$. If

$$(\mathbf{V}_i^r)_z < -\frac{(\mathbf{V}_{/r}^r)_z}{f} a_1, \quad (207)$$

⁹For thick inboard airfoil profiles, it may not be obvious what the zero-lift angle-of-attack should be. Indeed, the simplified aerodynamic theory breaks down near the blade root, where 3D rotational effects become significant. For root airfoils the parameters have to be tuned for different operating conditions, based on more advanced theories or CFD analyses.

¹⁰By these formulas we define the ‘‘airfoil’’ coordinate system with its origin identical to that of the section coordinate system, associated with the beam section properties. Alternatively we could have defined the airfoil coordinate system at the aerodynamic center, and then x and y would have appeared in the transform to section coordinates.

¹¹The rotor plane is not well defined; see the subsequent text for a discussion.

then the axial component is given an alternate expression

$$(\mathbf{V}_{iq}^r)_z = -\frac{(\mathbf{V}_{/r}^r)_z}{f} \left[\left(\frac{(\mathbf{F}^r)_z}{(1/2)(C_{T2} - C_{T1})\rho A |\mathbf{V}_{/r}^r|^2} - \frac{C_{T1}}{C_{T2} - C_{T1}} \right) (a_2 - a_1) + a_1 \right], \quad (208)$$

with $a_2 = 1$, $C_{T2} = 1.82$, $a_1 = 1 - 0.5\sqrt{C_{T2}}$, and $C_{T1} = 4a_1(1 - a_1)$.

Wake dynamics are represented by a second-order filter of the form

$$\frac{d}{dt} \begin{bmatrix} \widehat{V}_i \\ V_i \end{bmatrix} = \begin{bmatrix} -\tau_1^{-1} & 0 \\ \tau_2^{-1} & -\tau_2^{-1} \end{bmatrix} \begin{bmatrix} \widehat{V}_i \\ V_i \end{bmatrix} + \begin{bmatrix} 0.4\tau_1^{-1} \\ 0.6\tau_2^{-1} \end{bmatrix} V_{iq}, \quad (209)$$

with time parameters

$$\tau_1 = \frac{1.1}{1 - 0.3a} \left(\frac{D}{2|\mathbf{V}_{/r}^r|} \right), \quad a = \frac{(\mathbf{V}_i^r)_z}{(\mathbf{V}_{/r}^r)_z}, \quad \tau_2 = \left[0.39 - 0.26 \left(\frac{2r}{D} \right)^2 \right] \tau_1. \quad (210)$$

Equation (209) requires the quasi-steady induced velocity from the nonlinear equation (203) as an input. During simulation it is inconvenient to solve (203) for a precise value of \mathbf{V}_{iq} at each timestep. To avoid this, apply the approximation

$$\mathbf{V}_{iq}^r \approx \frac{-\mathbf{F}^r}{2\rho A f \widetilde{W}}, \quad \widetilde{W} := \sqrt{[(\mathbf{V}_{/r}^r)_z + f(\mathbf{V}_i^r)_z]^2 + (\mathbf{V}_{/r}^r)_t^2 + (\mathbf{V}_{/r}^r)_s^2} \quad (211)$$

that is, using the existing state \mathbf{V}_i^r in place of \mathbf{V}_{iq}^r in the expression for W .

In practical simulations it is often assumed that (209) evolves independently for each blade. It is more appropriate, based on the physics of the wake, to implement the equations in multi-blade coordinates; that is, the collective, cosine, and sine components evolve independently according to (209). We can write the dynamics in multi-blade coordinates as

$$\frac{d}{dt} \begin{bmatrix} \widehat{\mathbf{V}}_i^\psi \\ \mathbf{V}_i^\psi \end{bmatrix} = \mathbf{A}_\tau \begin{bmatrix} \widehat{\mathbf{V}}_i^\psi \\ \mathbf{V}_i^\psi \end{bmatrix} + \mathbf{B}_\tau \mathbf{V}_{iq}^\psi. \quad (212)$$

We then apply the nonlinear transformation

$$\begin{bmatrix} \widehat{\mathbf{V}}_i^\psi \\ \mathbf{V}_i^\psi \end{bmatrix} = \mathbf{T}_B^\psi \begin{bmatrix} \widehat{\mathbf{V}}_i^r \\ \mathbf{V}_i^r \end{bmatrix}, \quad \frac{d}{dt} \begin{bmatrix} \widehat{\mathbf{V}}_i^\psi \\ \mathbf{V}_i^\psi \end{bmatrix} = \mathbf{T}_B^\psi \frac{d}{dt} \begin{bmatrix} \widehat{\mathbf{V}}_i^r \\ \mathbf{V}_i^r \end{bmatrix} + \Omega \frac{d\mathbf{T}_B^\psi}{d\Psi} \begin{bmatrix} \widehat{\mathbf{V}}_i^r \\ \mathbf{V}_i^r \end{bmatrix}. \quad (213)$$

For a given component (axial, tangential) associated with each of the three blades, the blade-by-blade values become

$$\frac{d}{dt} \begin{bmatrix} \widehat{\mathbf{V}}_i^r \\ \mathbf{V}_i^r \end{bmatrix} = \mathbf{T}_\psi^B \left(\mathbf{A}_\tau \mathbf{T}_B^\psi - \Omega \frac{d\mathbf{T}_B^\psi}{d\Psi} \right) \begin{bmatrix} \widehat{\mathbf{V}}_i^r \\ \mathbf{V}_i^r \end{bmatrix} + \mathbf{T}_\psi^B \mathbf{B}_\tau \mathbf{T}_B^\psi \mathbf{V}_{iq}, \quad (214)$$

with

$$\mathbf{T}_\psi^B = \begin{bmatrix} 1 & c\Psi & s\Psi \\ 1 & c(\Psi + 2\pi/3) & s(\Psi + 2\pi/3) \\ 1 & c(\Psi + 4\pi/3) & s(\Psi + 4\pi/3) \end{bmatrix} \quad (215)$$

and

$$\mathbf{T}_B^\psi = \frac{1}{3} \begin{bmatrix} 1 & 1 & 1 \\ 2c\Psi & 2c(\Psi + 2\pi/3) & 2c(\Psi + 4\pi/3) \\ 2s\Psi & 2s(\Psi + 2\pi/3) & 2s(\Psi + 4\pi/3) \end{bmatrix}. \quad (216)$$

Contrast (214) with the baseline blade-by-blade version

$$\frac{d}{dt} \begin{bmatrix} \widehat{\mathbf{V}}_i^r \\ \mathbf{V}_i^r \end{bmatrix} = \mathbf{A}_\tau \begin{bmatrix} \widehat{\mathbf{V}}_i^r \\ \mathbf{V}_i^r \end{bmatrix} + \mathbf{B}_\tau \mathbf{V}_{iq}. \quad (217)$$

In yawed flow conditions, the quasi-steady induced velocity is modified according to

$$\tilde{\mathbf{V}}_{iq}^r = \left[1 + \frac{2r}{D} \tan \left\{ \frac{1}{2} \cos^{-1} \left(\frac{(\mathbf{V}_{/r}^r)_z + f(\mathbf{V}_i^r)_z}{\tilde{W}} \right) \right\} \cos(\Psi_b - \Psi_0) \right] \mathbf{V}_{iq}^r, \quad (218)$$

where Ψ_b is the blade azimuth angle, and Ψ_0 is the azimuth angle at which the blade is deepest into the wake. By these definitions, the cosine expression in (218) can be replaced by

$$\cos(\Psi_b - \Psi_0) = \frac{(\mathbf{V}_{/r}^r)_s}{\sqrt{(\mathbf{V}_{/r}^r)_t^2 + (\mathbf{V}_{/r}^r)_s^2}}. \quad (219)$$

The key to linking the airfoil and momentum equations is the transform between the airfoil and rotorplane coordinate systems. This requires the definition of a rotor plane, the fictitious control surface at which the momentum balance is applied. Much of the blade element momentum method and semi-empirical corrections have been developed for a flat circular shape. In fact, the control volume analysis that forms the basis for the momentum balance does not restrict the shape to a flat plane. However, the theory of elliptical wings applied for the analysis of yawed flow assumes a planar geometry. Analysis of dramatically deflected or coned blades requires an explicit representation of the vortical wake, which is beyond the present scope. Limited to the confines of blade element momentum theory, it is reasonable to assume that the rotor plane is a flat disk, and project the airfoil forces onto this plane. In this case, it is appropriate to neglect the radial (spanwise) component of the force.

The appropriate form of the airfoil-to-rotorplane transform depends on whether the rotor plane is assumed to follow nacelle deflection, or remain stationary.¹² Assuming the former, the transform can be written

$$\mathbf{T}_a^r = \mathbf{T}_y^r \mathbf{T}_{y0}^y(\Phi_y^{y0}) \mathbf{T}_g^{y0} \mathbf{T}_{p0}^g \mathbf{T}_p^{p0}(\Phi_p^{p0}) \mathbf{T}_{s0}^p \mathbf{T}_s^{s0}(\theta_s^{s0}) \mathbf{T}_a^s. \quad (220)$$

The sequence

$$\mathbf{T}_{s0}^p \mathbf{T}_s^{s0}(\theta_s^{s0})$$

is familiar as the section-to-body transform from (50) through (53), for each blade, while \mathbf{T}_p^{p0} is the rotational displacement of the blade root, principally pitch, and \mathbf{T}_y^{y0} represents rotation of the nacelle at the yaw bearing, principally the yaw angle. The remaining transforms are fixed relationships that can be determined from the turbine's undeformed geometry.

Equation (214) requires the definition of a rotor speed Ω and rotor azimuth Ψ , such that $\Omega = d\Psi/dt$. We can define these quantities in terms of the orientation of a representative node – the hub center is an obvious candidate – with respect to the rotorplane coordinate system. The transform from hub section coordinates to rotorplane coordinates is

$$\mathbf{T}_s^r = \mathbf{T}_y^r \mathbf{T}_{y0}^y(\Phi_y^{y0}) \mathbf{T}_g^{y0} \mathbf{T}_{d0}^g \mathbf{T}_d^{d0}(\Phi_d^{d0}) \mathbf{T}_{s0}^d \mathbf{T}_s^{s0}(\theta_s^{s0}). \quad (221)$$

At zero azimuth, the hub element section Y^s axis lies opposite the X^r axis. Thus the negative of the second column of the \mathbf{T}_s^r matrix is a vector \mathbf{r}^r , in rotorplane coordinates, pointing towards the rotor azimuth. The azimuth angle for the multi-blade coordinate transform is obtained as

$$\Psi := \tan^{-1} \frac{r_y}{r_x}, \quad (222)$$

where r_x and r_y are the x and y components of \mathbf{r}^r , and the ‘‘aerodynamic’’ rotor speed is defined as

$$\Omega := \frac{d\Psi}{dt} = \frac{\partial \Psi}{\partial r_i^r} \frac{\partial r_i^r}{\partial q_k} \frac{dq_k}{dt}. \quad (223)$$

¹²On a fixed-foundation wind turbine, it is simplest to select a rotorplane coordinate system that follows the yaw angle of the rotor. On a floating wind turbine, which may have very low-frequency platform motions, the rotorplane coordinate system is ill-defined. Does it follow the pitch, surge, and heave motion of the nacelle, or remain stationary? The correct choice depends on the period of platform motion relative to the evolution of the vortex wake, with some uncertainty at intermediate timescales.

4.3 Linearized aerodynamic equations

The linearized equations are developed as a series of modules. Each module consists of a group of equations of one or both of the forms

$$\begin{aligned}\frac{d\mathbf{x}}{dt} &= \mathbf{A}\mathbf{x} + \mathbf{B}_u\mathbf{u} + \mathbf{B}_y\mathbf{y}, \\ \mathbf{y} &= \mathbf{C}\mathbf{x} + \mathbf{D}_u\mathbf{u} + \mathbf{D}_y\mathbf{y}.\end{aligned}\quad (224)$$

Assembling these, together with the structural equations (188), the modules can be linked automatically into an aeroelastic model of the wind turbine by

$$\begin{aligned}\mathbf{y} &= (\mathbf{I} - \mathbf{D}_y)^{-1}\mathbf{C}\mathbf{x} + (\mathbf{I} - \mathbf{D}_y)^{-1}\mathbf{D}_u\mathbf{u} \\ \mathbf{N}\frac{d\mathbf{x}}{dt} &= [\mathbf{A} + \mathbf{B}_y(\mathbf{I} - \mathbf{D}_y)^{-1}\mathbf{C}] \mathbf{x} + [\mathbf{B}_u + \mathbf{B}_y(\mathbf{I} - \mathbf{D}_y)^{-1}\mathbf{D}_u] \mathbf{u}.\end{aligned}\quad (225)$$

4.3.1 Structural velocity in global and airfoil coordinates

The structural velocity in global coordinates is given by (197),

$$\mathbf{w}_{n/g}^g = \left(\mathbf{A}_n \tilde{\mathbf{T}}_{B0}^g \tilde{\mathbf{T}}_B^{B0} + \mathbf{A}_n \tilde{\mathbf{T}}_{B0}^g \frac{\partial \tilde{\mathbf{T}}_B^{B0}}{\partial \mathbf{q}} (\mathbf{q} + \mathbf{P}) \right) \frac{d\mathbf{q}}{dt}.\quad (226)$$

If we call the expression in parentheses \mathbf{Q}_w^g , then linearized at an initial condition, this becomes

$$\Delta \mathbf{w}_{n/g}^g = \mathbf{Q}_w^g \frac{d\Delta \mathbf{q}}{dt} + \left. \frac{\partial \mathbf{Q}_w^g}{\partial q_i} \right|_0 \frac{dq_i}{dt} \Big|_0 \Delta q_i\quad (227)$$

along the same lines as (136). Note that $\mathbf{w}_{n/g}^g$ includes rotation of the rotor.

Transforming (227) to airfoil coordinates,

$$\mathbf{w}_{n/g}^a = \mathbf{T}_s^a \mathbf{T}_B^s \mathbf{T}_{B0}^B \mathbf{T}_g^{B0} \mathbf{w}_{n/g}^g,\quad (228)$$

and

$$\Delta \mathbf{w}_{n/g}^a = \mathbf{T}_s^a \mathbf{T}_B^s \mathbf{T}_{B0}^B \mathbf{T}_g^{B0} \Delta \mathbf{w}_{n/g}^g + \left(\mathbf{T}_s^a \frac{\partial \mathbf{T}_B^s}{\partial q_i} \mathbf{T}_{B0}^B \mathbf{T}_g^{B0} + \mathbf{T}_s^a \mathbf{T}_B^s \frac{\partial \mathbf{T}_{B0}^B}{\partial q_i} \mathbf{T}_g^{B0} \right) \mathbf{w}_{n/g}^g \Big|_0 \Delta q_i.\quad (229)$$

4.3.2 Local flow velocity

The local flow velocity (195) can be written

$$\mathbf{U}_{/g}^a = \mathbf{T}_g^a \mathbf{V}_\infty^g + \mathbf{T}_r^a \mathbf{V}_i^r - \mathbf{w}_{/g}^a,\quad (230)$$

such that

$$\Delta \mathbf{U}_{/g}^a = \mathbf{T}_g^a \Delta \mathbf{V}_\infty^g + \mathbf{T}_r^a \Delta \mathbf{V}_i^r + \left(\frac{\partial \mathbf{T}_g^a}{\partial q_i} \mathbf{V}_\infty^g + \frac{\partial \mathbf{T}_r^a}{\partial q_i} \mathbf{V}_i^r \right) \Delta q_i - \Delta \mathbf{w}_{/g}^a.\quad (231)$$

The transform \mathbf{T}_g^a and its derivatives are shown in (228) and (229), while the derivative of \mathbf{T}_r^a follows in a straightforward manner from (220). A linearization of the magnitude U , (194), is also needed. With the shorthand $u_i := (\mathbf{U}^a)_i$, this is

$$\Delta U = \frac{u_x}{\sqrt{u_x^2 + u_y^2}} \Delta u_x + \frac{u_y}{\sqrt{u_x^2 + u_y^2}} \Delta u_y.\quad (232)$$

4.3.3 Quasi-steady angle-of-attack

The quasi-steady angle-of-attack, from (191), is

$$\alpha_q = \tan^{-1} \frac{(\mathbf{U}^a)_y}{(\mathbf{U}^a)_x}. \quad (233)$$

Linearizing gives

$$\Delta\alpha_q = \frac{u_x^2}{u_x^2 + u_y^2} \left(\frac{1}{u_x} \Delta u_y - \frac{u_y}{u_x^2} \Delta u_x \right) = -\frac{u_y}{u_x^2 + u_y^2} \Delta u_x + \frac{u_x}{u_x^2 + u_y^2} \Delta u_y. \quad (234)$$

4.3.4 Dynamic angle-of-attack

Equation (192) may be linearized as

$$\frac{d\Delta\mathbf{x}}{dt} = \mathbf{A} \Delta\mathbf{x} + \mathbf{B} \Delta\alpha_q + \left(\frac{\partial\mathbf{A}}{\partial U} \mathbf{x} + \frac{\partial\mathbf{B}}{\partial U} \alpha_q \right) \Delta U, \quad (235)$$

with

$$\begin{aligned} \frac{\partial A_{11}}{\partial U} &= -\frac{1}{4.3c}, & \frac{\partial A_{12}}{\partial U} &= \frac{K_1}{4.3c} + 8(A_1 + A_2)b_1b_2 \frac{U}{\tau c^2}, \\ \frac{\partial A_{13}}{\partial U} &= \frac{K_2}{4.3c} + \frac{2(A_1b_1 + A_2b_2)}{\tau c}, & \frac{\partial A_{32}}{\partial U} &= -\frac{8b_1b_2U}{c^2}, \\ \frac{\partial A_{33}}{\partial U} &= -2\frac{b_1 + b_2}{c}, & \text{and } \frac{\partial B_1}{\partial U} &= \frac{K_3}{4.3c}. \end{aligned} \quad (236)$$

4.3.5 Airfoil coefficients

The dynamic lift coefficient is linearized as

$$\Delta C_L = \left[\frac{\partial C_L}{\partial \alpha} \left(1 + \frac{\alpha_q - \alpha}{\alpha - \alpha_z} \right) - \frac{C_L}{\alpha - \alpha_z} - C_L \frac{\alpha_q - \alpha}{(\alpha - \alpha_z)^2} \right] \Delta\alpha + \frac{C_L}{\alpha - \alpha_z} \Delta\alpha_q. \quad (237)$$

The drag and moment coefficients are assumed to follow the quasi-steady angle-of-attack,

$$\Delta C_D = \frac{\partial C_D}{\partial \alpha} \Delta\alpha_q \quad \text{and} \quad \Delta C_M = \frac{\partial C_M}{\partial \alpha} \Delta\alpha_q. \quad (238)$$

4.3.6 Airfoil forces

From (202), write

$$\mathbf{F}^a = \frac{1}{2} \rho c L U^2 \mathbf{T} \mathbf{C}. \quad (239)$$

Linearizing this gives

$$\Delta\mathbf{F}^a = \frac{1}{2} \rho c L \left[2U \mathbf{T} \mathbf{C} \Delta U + U^2 \frac{\partial \mathbf{T}}{\partial \alpha} \mathbf{C} \Delta\alpha_q + U^2 \mathbf{T} \Delta \mathbf{C} \right]. \quad (240)$$

4.3.7 Forces in pitch (blade body reference) coordinates

The aerodynamic forces are needed in pitch (blade body reference) coordinates for application to the structural model. The transform from airfoil to body coordinates is

$$\mathbf{F}^B = \mathbf{T}_s^B \mathbf{T}_a^s \mathbf{F}^a, \quad (241)$$

such that

$$\Delta\mathbf{F}^B = \mathbf{T}_s^B \mathbf{T}_a^s \Delta\mathbf{F}^a + \frac{\partial \mathbf{T}_s^B}{\partial q_i} \mathbf{T}_a^s \mathbf{F}^a \Delta q_i. \quad (242)$$

4.3.8 Local flow velocity at the rotor plane

The expression for the Prandtl factor (204) requires the local flow velocity relative to the rotor plane. We take

$$\mathbf{U}_{/r}^r = \mathbf{V}_i^r + \mathbf{T}_g^r (\mathbf{V}_{\infty/g}^g - \mathbf{w}_{/g}^g) \quad (243)$$

to represent this flow velocity.¹³ This is (230) expressed in rotorplane coordinates, so an alternate expression – more convenient, given the existing quantities – is

$$\mathbf{U}_{/r}^r = \mathbf{T}_a^r \mathbf{U}_{/g}^a. \quad (244)$$

This is linearized as

$$\Delta \mathbf{U}_{/r}^r = \frac{\partial \mathbf{T}_a^r}{\partial q_i} \mathbf{U}_{/g}^a \Delta q_i + \mathbf{T}_a^r \Delta \mathbf{U}_{/g}^a. \quad (245)$$

We define $u_i = (\mathbf{U}_{/r}^r)_i$ for use in the following sections.

4.3.9 Projected blade element on the rotor plane

Define nodal positions from (67)

$$\mathbf{r}_{n/g}^g = \mathbf{A}_n \tilde{\mathbf{T}}_B^g (\mathbf{q} + \mathbf{P}) \quad (246)$$

and element position

$$\mathbf{r}_{e/g}^g = \frac{1}{2} (\mathbf{r}_{n2/g}^g + \mathbf{r}_{n1/g}^g). \quad (247)$$

Define also the position of the hub center node $\mathbf{r}_{h/g}^g$. The vector from hub center to the blade element is then

$$\mathbf{r}_{e/r}^r = \mathbf{T}_g^r (\mathbf{r}_{e/g}^g - \mathbf{r}_{h/g}^g). \quad (248)$$

The projected position on the rotor plane is taken to be

$$\tilde{\mathbf{r}}_{e/r}^r = \begin{bmatrix} (\mathbf{r}_{e/r}^r)_x \\ (\mathbf{r}_{e/r}^r)_y \\ 0 \end{bmatrix}. \quad (249)$$

Defining the projected nodal positions similarly, the spanwise element length is

$$\tilde{L} = |\tilde{\mathbf{r}}_{n2/r}^r - \tilde{\mathbf{r}}_{n1/r}^r|. \quad (250)$$

These equations are linearized as

$$\Delta \mathbf{r}_{n/g}^g = \mathbf{A}_n \tilde{\mathbf{T}}_B^g \Delta \mathbf{q} + \mathbf{A}_n \frac{\partial \tilde{\mathbf{T}}_B^g}{\partial q_i} (\mathbf{q} + \mathbf{P}) \Delta q_i \quad (251)$$

$$\Delta \mathbf{r}_{e/g}^g = \mathbf{T}_g^r (\Delta \mathbf{r}_{e/g}^g - \Delta \mathbf{r}_{h/g}^g) + \frac{\partial \mathbf{T}_g^r}{\partial q_i} (\mathbf{r}_{e/g}^g - \mathbf{r}_{h/g}^g) \Delta q_i \quad (252)$$

and

$$\Delta \tilde{L} = \frac{d_i}{|\mathbf{d}|} \Delta d_i, \quad \mathbf{d} := \tilde{\mathbf{r}}_{n2/r}^r - \tilde{\mathbf{r}}_{n1/r}^r. \quad (253)$$

¹³Again, there is some room for interpretation depending on assumptions about the wake dynamics.

4.3.10 Prandtl factor

It is best to break the linearization of the Prandtl factor into steps. First, write (204) as

$$f = \frac{2}{\pi} \cos^{-1} \{ \exp z \}, \quad (254)$$

and obtain

$$\Delta f = - \left(\frac{2}{\pi} \right) \frac{\exp z}{\sqrt{1 - \exp 2z}} \Delta z. \quad (255)$$

Then, we evaluate

$$z = \frac{k}{\sin \phi}, \quad k = \frac{N_b (r - D/2)}{2r} \quad (256)$$

and

$$\begin{aligned} \Delta z = & - \frac{k}{\sin \phi \tan \phi} \left(\frac{\partial \phi}{\partial u_z} \Delta u_z + \frac{\partial \phi}{\partial u_t} \Delta u_t \right) \\ & + \frac{1}{\sin \phi} \left[- \frac{N_b}{4r} \Delta D + \frac{N_b}{2r} \left(1 - \frac{r - D/2}{r} \right) \Delta r \right], \end{aligned} \quad (257)$$

with

$$\frac{\partial \phi}{\partial z} = \frac{u_t}{u_z^2 + u_t^2} \quad \text{and} \quad \frac{\partial \phi}{\partial u_t} = - \frac{u_z}{u_z^2 + u_t^2}. \quad (258)$$

4.3.11 Rotorplane flow velocity

The flow velocity at the rotorplane can be obtained by cancelling the $r\Omega$ rotational speed and induced velocity from the incoming wind $\mathbf{U}_{/r}^r$. That is,

$$\mathbf{V}_{/r}^r = \mathbf{U}_{/r}^r - \mathbf{V}_i^r + \begin{bmatrix} 0 \\ |\tilde{\mathbf{r}}_{e/r}^r| \Omega \\ 0 \end{bmatrix} \quad (259)$$

Linearization gives

$$\Delta \mathbf{V}_{/r}^r = \begin{bmatrix} \Delta u_t - \Delta v_{it} + \frac{r_x \Omega}{\sqrt{r_x^2 + r_y^2}} \Delta r_x + \frac{r_y \Omega}{\sqrt{r_x^2 + r_y^2}} \Delta r_y + |\tilde{\mathbf{r}}_{e/r}^r| \Delta \Omega \\ \Delta u_z - \Delta v_{iz} \\ \Delta u_s \end{bmatrix}. \quad (260)$$

Define the shorthand $v_i = (\mathbf{V}_{/r}^r)_i$ for use in the following sections.

4.3.12 Projected forces on the rotor plane

The aerodynamic forces are projected onto the rotor plane by transforming to rotorplane coordinates,

$$\mathbf{F}^r = \mathbf{T}_a^r \mathbf{F}^a, \quad (261)$$

or

$$\Delta \mathbf{F}^r = \mathbf{T}_a^r \Delta \mathbf{F}^a + \frac{\partial \mathbf{T}_a^r}{\partial q_i} \mathbf{F}^a \Delta q_i. \quad (262)$$

Only the axial and tangential components are considered; the spanwise component is neglected.

4.3.13 Quasi-steady induced velocity

The quasi-steady induced velocity is linearized as

$$\Delta \mathbf{V}_{iq} = \frac{-\Delta \mathbf{F}^r}{2\rho A f \tilde{W}} + \frac{4\pi\rho \mathbf{F}^r}{N_b(2\rho A f \tilde{W})^2} \left(Lf\tilde{W} \Delta r + rf\tilde{W} \Delta L + rL\tilde{W} \Delta f + rLf \Delta \tilde{W} \right), \quad (263)$$

with

$$\Delta \tilde{W} = \frac{(v_z + fv_{i,z})(\Delta v_z + v_{i,z}\Delta f + f \Delta v_{i,z}) + v_t \Delta v_t + v_s \Delta v_s}{\sqrt{(v_z + fv_{i,z})^2 + v_t^2 + v_s^2}}. \quad (264)$$

Recall that $v_{i,z} = (\mathbf{V}_i^r)_z$ is a state. Alternatively, at high values of induction,

$$(\mathbf{V}_{iq}^r)_z = -\frac{(\mathbf{V}_{i,q}^r)_z}{f} C, \quad C := \left(\frac{(\mathbf{F}^r)_z}{(1/2)(C_{T2} - C_{T1})\rho AV^2} - \frac{C_{T1}}{C_{T2} - C_{T1}} \right) (a_2 - a_1) + a_1, \quad (265)$$

such that

$$\Delta(\mathbf{V}_{iq}^r)_z = -\frac{C}{f} \Delta v_z + \frac{Cv_z}{f^2} \Delta f - \frac{v_z}{f} \Delta C, \quad (266)$$

$$\begin{aligned} \Delta C &= \left(\frac{a_2 - a_1}{(1/2)(C_{T2} - C_{T1})\rho AV^2} \right) \Delta(\mathbf{F}^r)_z \\ &- \left(\frac{(\mathbf{F}^r)_z(a_2 - a_1)}{[(1/2)(C_{T2} - C_{T1})\rho AV^2]^2} \right) (C_{T2} - C_{T1})\rho \frac{\pi}{N_b} \\ &\times [LV^2 \Delta r + rV^2 \Delta L + 2rL(v_z \Delta v_z + v_t \Delta v_t + v_s \Delta v_s)]. \end{aligned} \quad (267)$$

The induced velocity in yaw is

$$\tilde{\mathbf{V}}_{iq}^r = \left[1 + \frac{2r}{D} \tan \left\{ \frac{1}{2} \cos^{-1} \left(\frac{v_z + fv_{i,z}}{\tilde{W}} \right) \right\} \frac{v_s}{\sqrt{v_t^2 + v_s^2}} \right] \mathbf{V}_{iq}^r, \quad (268)$$

again using v as a shorthand for $\mathbf{V}_{i,q}^r$. This is linearized as

$$\begin{aligned} \Delta \tilde{\mathbf{V}}_{iq}^r &= \kappa \Delta \mathbf{V}_{iq}^r \\ &+ \mathbf{V}_{iq}^r \left(\frac{\partial \kappa}{\partial v_z} \Delta v_z + \frac{\partial \kappa}{\partial v_t} \Delta v_t + \frac{\partial \kappa}{\partial v_s} \Delta v_s + \frac{\partial \kappa}{\partial v_{i,z}} \Delta v_{i,z} + \frac{\partial \kappa}{\partial \tilde{W}} \Delta \tilde{W} + \frac{\partial \kappa}{\partial r} \Delta r + \frac{\partial \kappa}{\partial D} \Delta D \right). \end{aligned} \quad (269)$$

Define

$$z := \frac{v_z + fv_{i,z}}{\tilde{W}}. \quad (270)$$

The partial derivatives of κ are

$$\frac{\partial \kappa}{\partial v_z} = -\frac{2r}{D} \left(\frac{v_s}{\sqrt{v_t^2 + v_s^2}} \right) \frac{1}{\tilde{W}(z+1)\sqrt{1-z^2}} \quad (271)$$

$$\frac{\partial \kappa}{\partial v_t} = -\frac{2r}{D} \tan \left\{ \frac{1}{2} \cos^{-1} \left(\frac{v_z + fv_{i,z}}{\tilde{W}} \right) \right\} \frac{v_s v_t}{(v_t^2 + v_s^2)^{3/2}} \quad (272)$$

$$\frac{\partial \kappa}{\partial v_s} = \frac{2r}{D} \tan \left\{ \frac{1}{2} \cos^{-1} \left(\frac{v_z + fv_{i,z}}{\tilde{W}} \right) \right\} \frac{v_t^2}{(v_t^2 + v_s^2)^{3/2}} \quad (273)$$

$$\frac{\partial \kappa}{\partial v_{i,z}} = f \frac{\partial \kappa}{\partial v_z} \quad (274)$$

$$\frac{\partial \kappa}{\partial f} = v_{i,z} \frac{\partial \kappa}{\partial v_z} \quad (275)$$

$$\frac{\partial \kappa}{\partial \tilde{W}} = \frac{2r}{D} \left(\frac{v_s}{\sqrt{v_t^2 + v_s^2}} \right) \frac{1}{(z+1)\sqrt{1-z^2}} \frac{v_z + f v_{i,z}}{\tilde{W}^2} \quad (276)$$

$$\frac{\partial \kappa}{\partial r} = \frac{2}{D} \tan \left\{ \frac{1}{2} \cos^{-1} \left(\frac{v_z + f v_{i,z}}{\tilde{W}} \right) \right\} \frac{v_s}{\sqrt{v_t^2 + v_s^2}} \quad (277)$$

$$\frac{\partial \kappa}{\partial D} = -\frac{2r}{D^2} \tan \left\{ \frac{1}{2} \cos^{-1} \left(\frac{v_z + f v_{i,z}}{\tilde{W}} \right) \right\} \frac{v_s}{\sqrt{v_t^2 + v_s^2}}. \quad (278)$$

4.3.14 Dynamic induced velocity

The dynamic induced velocity, where the filter functions are defined in multi-blade coordinates, takes the form

$$\frac{d}{dt} \begin{bmatrix} \hat{\mathbf{V}}_i^r \\ \mathbf{V}_i^r \end{bmatrix} = \mathbf{A}_\tau^\psi \begin{bmatrix} \hat{\mathbf{V}}_i^r \\ \mathbf{V}_i^r \end{bmatrix} + \mathbf{B}_\tau^\psi \mathbf{V}_{iq}, \quad (279)$$

$$\mathbf{A}_\tau^\psi = \mathbf{T}_\psi^B \left(\mathbf{A}_\tau \mathbf{T}_B^\psi - \Omega \frac{d\mathbf{T}_B^\psi}{d\Psi} \right), \quad \mathbf{B}_\tau^\psi = \mathbf{T}_\psi^B \mathbf{B}_\tau \mathbf{T}_B^\psi$$

when expressed in rotating blade element coordinates. The matrices \mathbf{A}_τ and \mathbf{B}_τ are functions of the annulus average (multi-blade collective) timescale variables $\bar{\tau}_1$ and $\bar{\tau}_2$, which are in turn functions of the projected element radius r , projected diameter D , incoming wind v_z , induced velocity $v_{i,z}$, and windspeed V experienced by each element in the annulus.

Linearizing (279),

$$\begin{aligned} \frac{d}{dt} \begin{bmatrix} \Delta \hat{\mathbf{V}}_i^r \\ \Delta \mathbf{V}_i^r \end{bmatrix} &= \mathbf{A}_\tau^\psi \begin{bmatrix} \Delta \hat{\mathbf{V}}_i^r \\ \Delta \mathbf{V}_i^r \end{bmatrix} + \mathbf{B}_\tau^\psi \Delta \mathbf{V}_{iq} \\ &+ \left(\frac{\partial \mathbf{A}_\tau^\psi}{\partial \bar{\tau}_1} \Delta \bar{\tau}_1 + \frac{\partial \mathbf{A}_\tau^\psi}{\partial \bar{\tau}_2} \Delta \bar{\tau}_2 + \frac{\partial \mathbf{A}_\tau^\psi}{\partial \Omega} \Delta \Omega + \frac{\partial \mathbf{A}_\tau^\psi}{\partial \Psi} \Delta \Psi \right) \begin{bmatrix} \hat{\mathbf{V}}_i^r \\ \mathbf{V}_i^r \end{bmatrix} \\ &+ \left(\frac{\partial \mathbf{B}_\tau^\psi}{\partial \bar{\tau}_1} \Delta \bar{\tau}_1 + \frac{\partial \mathbf{B}_\tau^\psi}{\partial \bar{\tau}_2} \Delta \bar{\tau}_2 + \frac{\partial \mathbf{B}_\tau^\psi}{\partial \Psi} \Delta \Psi \right) \mathbf{V}_{iq}. \end{aligned} \quad (280)$$

Expanding each of the perturbed variables,

$$\Delta \bar{\tau}_1 = \frac{1}{3} \sum_{b=1}^3 \left(\frac{\partial \tau_{1,b}}{\partial V_b} \Delta V_b + \frac{\partial \tau_{1,b}}{\partial v_{z,b}} \Delta v_{z,b} + \frac{\partial \tau_{1,b}}{\partial v_{i,z,b}} \Delta v_{i,z,b} + \frac{\partial \tau_{1,b}}{\partial D_b} \Delta D_b \right) \quad (281)$$

$$\Delta \bar{\tau}_2 = \frac{1}{3} \sum_{b=1}^3 \left\{ \left[0.39 - 0.26 \left(\frac{2r_b}{D_b} \right)^2 \right] \Delta \tau_{1,b} - 0.26 \frac{8r_b}{D_b^2} \tau_{1,b} \Delta r_b + 0.26 \frac{8r_b^2}{D_b^3} \tau_{1,b} \Delta D_b \right\}. \quad (282)$$

Partial derivatives of τ_1 are

$$\frac{\partial \tau_1}{\partial V} = -\frac{1.1}{1-0.3a} \left(\frac{D}{2} \right) \frac{1}{V^2} \quad (283)$$

$$\frac{\partial \tau_1}{\partial v_z} = \frac{0.33}{(1-0.3a)^2} \left(\frac{D}{2V} \right) \frac{v_{i,z}}{v_z^2} \quad (284)$$

$$\frac{\partial \tau_1}{\partial v_{i,z}} = -\frac{0.33}{(1-0.3a)^2} \left(\frac{D}{2V} \right) \frac{1}{v_z} \quad (285)$$

$$\frac{\partial \tau_1}{\partial D} = \frac{1.1}{1-0.3a} \left(\frac{1}{2V} \right) \quad (286)$$

and the perturbation to the velocity magnitude is composed of

$$\Delta V = \frac{v_z}{V} \Delta v_z + \frac{v_t}{V} \Delta v_t + \frac{v_s}{V} \Delta v_s. \quad (287)$$

The rotor azimuth is linearized as

$$\Delta \Psi = \left. \frac{\partial \Psi}{\partial r_i} \frac{\partial r_i}{\partial q_k} \right|_0 \Delta q_k, \quad (288)$$

while the effective rotor speed perturbation $\Delta \Omega$ is obtained from

$$\begin{aligned} \Delta \Omega = & \left. \frac{\partial \Psi}{\partial r_i} \frac{\partial r_i}{\partial q_k} \right|_0 \frac{d \Delta q_k}{dt} \\ & + \left(\left. \frac{\partial^2 \Psi}{\partial r_i \partial r_j} \frac{\partial r_i}{\partial q_k} \right|_0 \left. \frac{\partial r_j}{\partial q_p} \right|_0 + \left. \frac{\partial \Psi}{\partial r_i} \frac{\partial^2 r_i}{\partial q_k \partial q_p} \right|_0 \right) \left. \frac{d q_k}{dt} \right|_0 \Delta q_p, \end{aligned} \quad (289)$$

where the r_i are components of \mathbf{r}^r , that is, in rotorplane coordinates, and

$$\begin{aligned} \frac{\partial \psi}{\partial r_x} & := -\frac{r_y}{r_x^2 + r_y^2}, & \frac{\partial \psi}{\partial r_y} & := \frac{r_x}{r_x^2 + r_y^2}, & \frac{\partial^2 \psi}{\partial r_x \partial r_x} & = \frac{2r_x r_y}{(r_x^2 + r_y^2)^2}, \\ \frac{\partial^2 \psi}{\partial r_y \partial r_y} & = -\frac{2r_x r_y}{(r_x^2 + r_y^2)^2}, & \frac{\partial^2 \psi}{\partial r_x \partial r_y} & = \frac{\partial^2 \psi}{\partial r_y \partial r_x} = \frac{r_y^2 - r_x^2}{(r_x^2 + r_y^2)^2}. \end{aligned} \quad (290)$$

The derivatives of \mathbf{r}^r are directly extracted from the derivatives of the transformation (221), using (39) through (48).

4.4 Unified aeroelastic equations

The combined aeroelastic state-space equations are obtained by linking the aerodynamic forces (241) with the nodal force inputs on the blade structures, and feeding the structural motions back to the aerodynamics via (226). The result is a unified state space, in the form

$$\begin{bmatrix} \mathbf{N} & \mathbf{0} \\ \mathbf{0} & \mathbf{I} \end{bmatrix} \frac{d}{dt} \begin{bmatrix} \mathbf{x}_s \\ \mathbf{x}_a \end{bmatrix} = \begin{bmatrix} \mathbf{f}_s(\mathbf{x}_s, \mathbf{x}_a, \mathbf{u}) \\ \mathbf{f}_a(\mathbf{x}_s, \mathbf{x}_a, \mathbf{u}) \end{bmatrix}, \quad \begin{bmatrix} \mathbf{N} & \mathbf{0} \\ \mathbf{0} & \mathbf{I} \end{bmatrix} \frac{d}{dt} \begin{bmatrix} \Delta \mathbf{x}_s \\ \Delta \mathbf{x}_a \end{bmatrix} = \mathbf{A} \begin{bmatrix} \Delta \mathbf{x}_s \\ \Delta \mathbf{x}_a \end{bmatrix} + \mathbf{B} \mathbf{u}. \quad (291)$$

The structural states are those from (188). The aerodynamic states include the airfoil states from (235), and dynamic wake states from (279).

5 Verification of the equations

Here we document some elementary verification exercises, to demonstrate that important parts of the structural and aerodynamic equations are correctly implemented. A full validation of an operating wind turbine is outside the scope of this theory manual, as it requires additional modules: generator, pitch actuators, and control systems.

5.1 Static structural deformation

Referring to (96), we seek here to solve the nonlinear static structural problem

$$\tilde{\mathbf{K}}(\mathbf{q}) = \tilde{\mathbf{Q}}(\mathbf{q}) \mathbf{F}^B \quad (292)$$

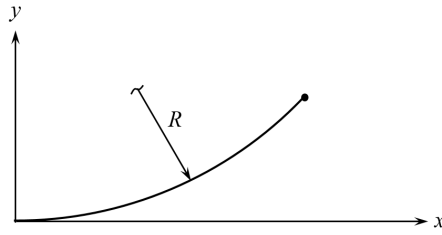


Figure 4: Geometry of the 45° cantilevered bend. The load is applied in the out-of-the-page direction.

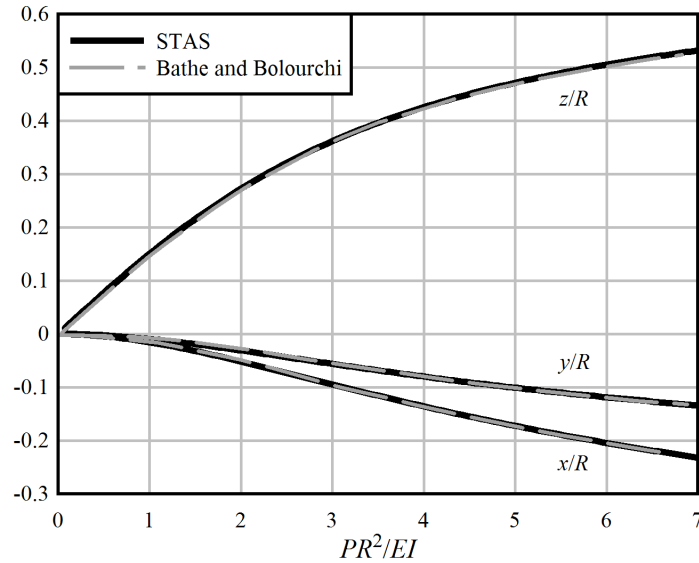


Figure 5: The tip deflection of the 45° cantilevered bend under an out-of-plane load.

for a selected test case. A solution can be obtained by expanding the left-hand side to first order in $\delta\mathbf{q}$ (the tangent stiffness method; Bathe and Bolourchi 1979, Cook et al. 1989)

$$\delta\mathbf{q} = \left(\frac{\partial \tilde{\mathbf{K}}}{\partial \mathbf{q}} \right)^{-1} \left(\tilde{\mathbf{Q}}\bar{\mathbf{F}}^B - \tilde{\mathbf{K}} \right), \quad (293)$$

and iterating the resulting equation numerically to convergence. Note that (293) exercises both the nonlinear expression for the stiffness $\tilde{\mathbf{K}}$, and its linearization $\partial\tilde{\mathbf{K}}/\partial\mathbf{q}$.

Bathe and Bolourchi provide a reference problem consisting of a 45° cantilevered bend, with a square cross-section, subject to an out-of-plane load. The initial geometry is sketched in Fig. 4; the beam is fixed at the origin, and a load applied at the tip in the z direction. The beam is represented by ten evenly-spaced elements along its length. Figure 5 shows a plot of the tip deflection as a function of the load; note that the deformations are large. STAS reproduces the reference results. This indicates that the corotational beam elements, in particular the elastic deformation and section coordinate system of (50) through (61), are implemented correctly.

5.2 Natural frequencies and stress stiffening

Centrifugal stiffening – a subset of the stress stiffening phenomenon (for instance, Cook *et al.* 1989) where the axial loads are caused by centrifugal forces – has an important influence on the resonant frequencies of the rotating blades. To validate the structural equations in regards to the stress stiffening

Table 1: Properties of the hanging cantilever beam. The elastic modulus is calibrated in the manner described by Schäfer, so as to reproduce the observed speed of wave propagation in the beam.

Density	7850 kg/m ³
Elastic modulus	1.722×10^{11} N/m ²
Length	2.9 m
Width	0.1 m
Thickness	0.001 m

Table 2: A comparison of theoretical and experimental results for the natural frequencies of a thin, hanging cantilever beam, compared with numerical results from the STAS program.

	Schäfer			STAS	
	Theoretical No g	Theoretical With g	Experimental With g	20 uniform elements No g	20 uniform elements With g
1	0.09	0.37	0.37	0.090	0.372
2	0.56	1.02	1.02	0.564	1.019
3	1.58	2.14	2.14	1.579	2.129
4	3.09	3.73	3.72	3.093	3.710
5	5.12	5.79	5.80	5.114	5.766
6	7.64	8.35	8.39	7.641	8.309
(*)				8.995	9.003
7	10.67	11.41	11.41	10.676	11.348
8	14.21	14.96	15.1	14.221	14.889
9	18.25	19.01	19.2	18.281	18.938
10	22.80	23.57	23.9	22.860	23.503

(*) First edgewise mode, not included in Schäfer's calculations or measurements.

phenomenon, we look at an experiment conducted by Schäfer (1985), where the natural frequencies of a thin steel plate were measured. The plate, whose material properties and dimensions are summarized in Table 1, was hung vertically, under the influence of gravity. Results are shown in Table 2. This indicates that the STAS model correctly predicts the influence of stress stiffening, as well as the elementary mass-stiffness dynamics of beam structures.

5.3 A rotating cantilever beam

Yoo and Shin (1998) provide theoretical results for the natural frequencies and mode shapes of a rotating cantilever beam, as sketched in Fig. 6. The cantilever beam is attached to a rigid base of radius r , spinning at a prescribed rate Ω . The motion and response of the beam in the out-of-plane (1) and in-plane (2) directions can be described in terms of the time parameters

$$T_1 = \sqrt{\frac{\rho AL^4}{EI_1}} \quad \text{and} \quad T_2 = \sqrt{\frac{\rho AL^4}{EI_2}}, \quad (294)$$

such that the nondimensional rotational speed and natural frequencies are

$$\Omega^* = \Omega T \quad \text{and} \quad \omega_n^* = \omega_n T. \quad (295)$$

The normalized geometry is described by

$$r^* = \frac{r}{L} \quad \text{and} \quad x^* = \frac{x}{L}. \quad (296)$$

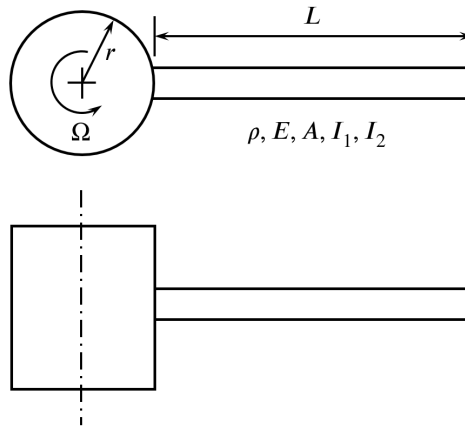


Figure 6: A rotating, flexible cantilever beam, mounted on a rigid base of radius r .

Table 3: Natural frequencies of a rotating cantilever beam.

r^*	Ω^*	STAS (Linear)				Yoo and Shin			
		1st OOP	2nd OOP	1st IP	2nd IP	1st OOP	2nd OOP	1st IP	2nd IP
0	0	3.156	22.036	3.516	22.036	3.516	22.035	3.516	22.035
	1	3.681	22.177	3.542	22.155	3.682	22.181		
	2	4.134	22.593	3.615	22.509	4.137	22.615	3.62	22.5
	3	4.790	23.267	3.729	23.087	4.797	23.320		
	4	5.573	24.186	3.871	23.872	5.585	24.273		
	5	6.433	25.313	4.031	24.845	6.450	25.466		
	6	7.338	26.625	4.201	25.985	7.360	26.809		
	7	8.271	28.092	4.372	27.270	8.300	28.334		
	8	9.221	29.691	4.541	28.679	9.257	29.995		
	9	10.182	31.396	4.703	30.193	10.266	31.771		
10	11.150	33.188	4.858	31.797	11.202	33.640	4.97	32.1	
1	2	4.830	23.297	4.393	23.240	4.83		4.40	23.3
	10	16.449	42.625	12.854	41.090	16.6		13.1	43.2
5	2	6.929	25.948	6.631	25.595	6.94		6.64	26.1
	10	28.545	69.478	26.293	68.242	29.5		27.3	71.4

A cantilever beam model of this type was constructed in STAS, employing the same functions and equations of motion that are used by the program when it builds a wind turbine rotor. A linear, frequency-domain solution was obtained by first solving the nonlinear equations iteratively for the steady-state displacement, then generating a linear model about this equilibrium point.

Results are shown in Table 3, for a STAS model with eight equally-spaced finite elements. The comparison is truncated at $\Omega^* = 10$; STAS includes a torsional degree-of-freedom neglected by Yoo and Shin, and this couples with the bending modes in a way which invalidates the comparison at higher values of Ω^* . (The torsional mode already interferes significantly at $r^* = 5$, $\Omega^* = 10$.) Regardless, a representative value for a wind turbine at rated speed is $\Omega^* \approx 3$, and it is clear that STAS correctly predicts the centrifugal stiffening effect in this range.

5.4 A parked wind turbine

The structural model, and most crucially the constraint equations joining the bodies (foundation, tower, nacelle, driveshaft, blades), were tested by computing the modes and natural frequencies for a

Table 4: Natural frequencies of a parked NREL 5 MW wind turbine. Blade 1 is oriented straight up, in line with the tower.

Mode	Frequency (Hz)				
	FAST	Adams	Ashes	STAS ^(a)	STAS ^(b)
Tower side-to-side	0.312	0.316	0.320	0.316	0.316
Tower fore-aft	0.324	0.320	0.322	0.320	0.321
Drivetrain torsion	0.621	0.609	0.915 ^(c)	0.560	0.561
Blade asymmetric flapwise yaw	0.666	0.630	0.628	0.628	0.679
Blade asymmetric flapwise pitch	0.668	0.669	0.657	0.652	0.669
Blade collective flap	0.699	0.702	0.691	0.751	0.752
Blade asymmetric edgewise pitch	1.079	1.074	1.076	1.100	1.106
Blade asymmetric edgewise yaw	1.090	1.088	1.092	1.118	1.123
Second blade asym. flap. yaw	1.934	1.651	1.711	1.696	1.860
Second blade asym. flap. pitch	1.922	1.856	1.821	1.742	1.797
Second blade collective flap	2.021	1.960	1.967	2.135	2.138
Second tower fore-aft	2.900	2.859	2.905	2.920	2.921
Second tower side-to-side	2.936	2.941	2.834	3.014	3.031

Notes: (a) Full finite element model. (b) Structures represented by body modes: 10 each for the foundation and tower, 2 each for the nacelle and driveshaft, and 16 for each blade. (c) Ashes locks *both* shaft bearings in torsion when performing an eigenvalue analysis, while in the STAS model only the rear bearing was locked.

parked wind turbine. The NREL 5 MW turbine described by Jonkman *et al.* (2009) was used for the comparison.

Table 4 compares natural frequencies obtained from several wind turbine analysis programs. The results from the FAST wind turbine analysis program, and the general-purpose multi-body code Adams, are those reported by Jonkman *et al.* These are compared against results obtained with two STAS models, one with a full finite-element representation of the structures (1134 DOFs), and another where modal reduction has been applied separately to each body (144 DOFs). The model of the nacelle in STAS is based on a direct-drive turbine, and it does not precisely match the geared drivetrain of the baseline NREL 5 MW turbine. As a sanity check, an additional model was constructed in Ashes (Thomassen *et al.* 2012), a dedicated wind turbine aeroelastic analysis code. The Ashes model was constructed to as to match the STAS nacelle geometry. The natural frequencies, and characteristics of each mode, are seen to coincide, within reason. This provides evidence that the constraint equations, assembled mass and stiffness matrices, and body mode reduction are implemented properly in STAS.

5.5 Newton’s method solution of an operating wind turbine

Consider the NREL 5 MW wind turbine (Jonkman *et al.* 2009), operating in a steady wind of 11 m/s. We wish to obtain the equilibrium, or steady-state, operating point. This involves solving the nonlinear aeroelastic equations (291) for $d\mathbf{x}/dt = \mathbf{0}$. This can be achieved using a globally-convergent Newton-Raphson method (Press *et al.* 2007). This is based on a modified Newton-Raphson iteration

$$\Delta\mathbf{x} = -\alpha \left(\frac{\partial \mathbf{f}}{\partial \mathbf{x}} \right)^{-1} \mathbf{f}(\mathbf{x}, \bar{\mathbf{u}}), \quad (297)$$

where the factor α is used to scale the step $\Delta\mathbf{x}$ such that the residual $R := \mathbf{f}^T \mathbf{f}$, which should be zero at convergence, is made to decrease at each iteration.

Initial guesses for the states are zero structural deformation, and an axial induction factor of $a = 1/3$ at each blade element. The convergence history is then as shown in Fig. 7. The model has been set up such that a unit of mass is defined as a Mkg (1×10^6 kg), so the residual forces are in MN; that is to say, the initial residual of around 100 (MN)^2 is quite large. Precise convergence is

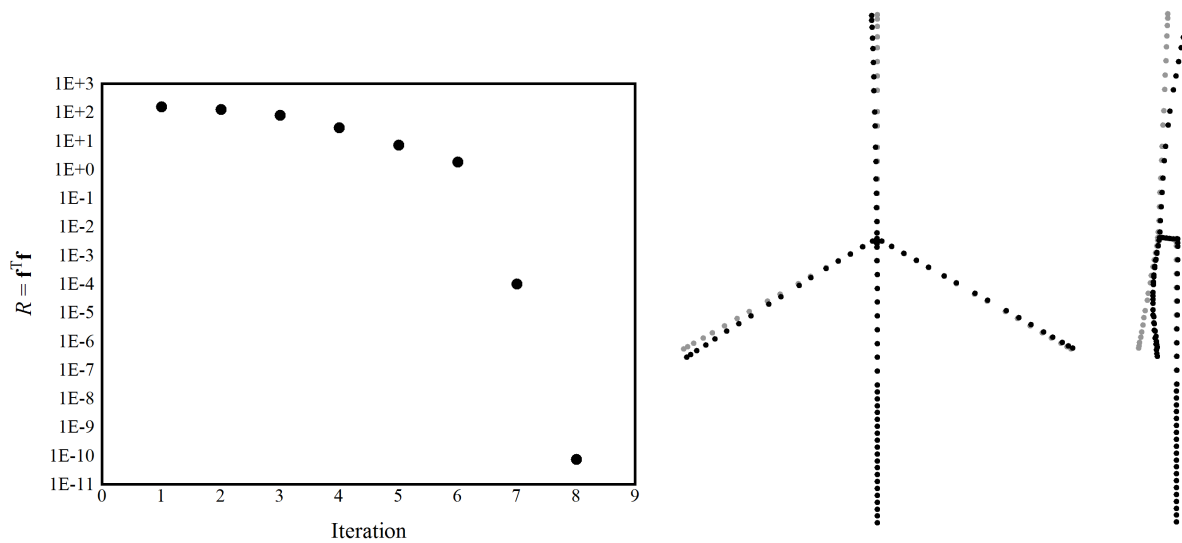


Figure 7: Convergence of the Newton-Raphson method, solving for the equilibrium aeroelastic state of an operating wind turbine. At right, the deflected shape of the wind turbine is shown, with displacements doubled for clarity.

obtained in eight iterations. The “knee” in the curve at iteration 6 occurs when $\alpha = 1$ provides a valid, quadratically-converging solution.

5.6 Equilibrium aerodynamics

DTU (Bak *et al.* 2013) have published rigid-blade rotor loads, obtained with blade element momentum (BEM) and computational fluid dynamics (CFD) methods, for their 10 MW reference wind turbine. Table 5 compares rotor thrust and aerodynamic power over a range of windspeeds. The results match well through the rated windspeed. Above the rated windspeed, the blade pitch angles were prescribed based on values listed by Bak *et al.* At high windspeeds, blade forces are sensitive to the blade pitch, and we see that STAS produces a slightly different trend in thrust and power for the given pitch angles. The repeated entry at 25 m/s illustrates that a minute (0.2°) perturbation to the pitch angle brings the thrust and power into line with the DTU results. The discrepancy is therefore small, and does not suggest that there is any error in the STAS implementation. In a practical sense, the pitch controller would provide this fine adjustment to the pitch angle.

6 Summary and conclusions

An aeroelastic model has been developed for incorporation into the open-source wind power plant analysis code STAS WPP. The model is programmed in plain MATLAB/Octave script, and can be used as a stand-alone module. Structural components are represented by finite beam elements, which can undergo large displacements and rotations. Aerodynamic loads are computed using the blade element momentum method. A distinguishing feature of the STAS Aeroelastic module is the ability to generate linear and nonlinear state-space models that are numerically smooth and agree to high numerical precision. This is instrumental in solving the nonlinear state equations for equilibrium using Newton-Raphson iterations, as well as other optimization and optimal control problems. Important parts of the implemented equations have been verified against theoretical calculations and the output of other aeroelastic models.

Table 5: A comparison of the steady-state aerodynamic thrust and power over a typical turbine operating schedule. “BEM”, “CFD1”, and “CFD2” are results from Bak *et al.*

V_∞	β	Ω	F_T (MN)				P_a (MW)			
			STAS	BEM	CFD1	CFD2	STAS	BEM	CFD1	CFD2
4	2.751	0.628	0.218	0.226			0.292	0.280		
5	1.966	0.628	0.345	0.352	0.356	0.358	0.822	0.799	0.809	0.825
6	0.896	0.628	0.491	0.498	0.506	0.509	1.564	1.533	1.558	1.577
7	0	0.628	0.639	0.643			2.572	2.506		
8	0	0.673	0.796	0.797	0.817	0.823	3.853	3.731	3.848	3.888
9	0	0.757	1.007	1.009	1.037	1.043	5.486	5.312	5.497	5.543
10	0	0.841	1.244	1.246	1.283	1.288	7.525	7.287	7.561	7.611
11	0	0.925	1.505	1.507	1.555	1.560	10.015	9.698	10.089	10.141
12	4.502	1.005	1.268	1.270	1.325	1.329	10.853	10.639	11.170	11.229
13	7.266	1.005	1.069	1.082			10.630	10.649		
14	9.292	1.005	0.949	0.968			10.462	10.639		
15	10.958	1.005	0.869	0.891			10.406	10.684		
16	12.499	1.005	0.800	0.825	0.854	0.858	10.272	10.642	10.876	10.961
17	13.896	1.005	0.748	0.774			10.189	10.640		
18	15.200	1.005	0.705	0.733			10.124	10.640		
19	16.432	1.005	0.670	0.698			10.079	10.653		
20	17.618	1.005	0.640	0.668	0.688	0.693	10.018	10.646	10.679	10.798
21	18.758	1.005	0.614	0.642			9.964	10.644		
22	19.860	1.005	0.591	0.620			9.913	10.641		
23	20.927	1.005	0.571	0.600			9.868	10.640		
24	21.963	1.005	0.554	0.583			9.828	10.644		
25	22.975	1.005	0.539	0.567	0.577	0.582	9.775	10.636	10.193	10.320
25	22.763	1.005	0.575				10.642			

References

- [1] Bak C, *et al.* (2013). *Description of the DTU 10 MW Reference Wind Turbine*. DTU Wind Energy Report-I-0092, Technical University of Denmark, Roskilde.
- [2] Bathe K-J, Bolourchi S (1979). Large displacement analysis of three-dimensional beam structures. *International Journal for Numerical Methods in Engineering* 14: 961-986.
- [3] Cook RD, *et al.* (1989). *Concepts and Applications of Finite Element Analysis*. Third Edition, Wiley.
- [4] Felippa CA, Haugen B (2005). A unified formulation of small-strain corotational finite elements: I. Theory. *Computer Methods in Applied Mechanics and Engineering* 194: 2285-2335.
- [5] Gallego G, Yezzi A (2015). A compact formula for the derivative of a 3-D rotation in exponential coordinates. *Journal of Mathematical Imaging and Vision* 51: 378-384.
- [6] Grassia FS (1998). Practical parameterization of rotations using the exponential map. *Journal of Graphics Tools* 3: 29-48.
- [7] Hansen MH (2004). Aeroelastic stability analysis of wind turbines using an eigenvalue approach. *Wind Energy* 7: 133-143.
- [8] Jonkman JM, *et al.* (2009). *Definition of a 5-MW Reference Wind Turbine for Offshore System Development*. Report NREL/TP-500-38060, National Renewable Energy Laboratory, Golden, CO, USA.
- [9] Leith DJ, Leithead WE (1998). Gain-scheduled and nonlinear systems: Dynamic analysis by velocity-based linearization families. *International Journal of Control* 70: 289-317.
- [10] Leith DJ, Leithead WE (2000). Survey of gain-scheduling analysis and design. *International Journal of Control* 73: 1001-1025.
- [11] Leishman JG (2002). Challenges in modelling the unsteady aerodynamics of wind turbines. *Wind Energy* 5: 85-132.
- [12] Merz KO (2015). *A linear state-space model of an offshore wind turbine, implemented in the STAS wind power plant analysis program*. Report TR A7474, SINTEF Energy Research, Trondheim, Norway.
- [13] Merz KO (2016). Enhanced finite beam elements for wind turbine blades. Memo AN 16.12.18, SINTEF Energy Research.
- [14] Press WH, *et al.* (2007). *Numerical Recipes – The Art of Scientific Computing*. Cambridge University Press.
- [15] Schäfer B (1985). Free vibrations of a gravity-loaded clamped-free beam. *Ingenieur-Archiv* 55: 66-80.
- [16] Shabana AA (2013). *Dynamics of Multibody Systems*. Fourth Edition, Cambridge University Press.
- [17] Thomassen PE, *et al.* (2012). A novel tool for FEM analysis of offshore wind turbines with innovative visualization techniques. Paper ISOPE-I-12-080, presented at the Twenty-second International Offshore and Polar Engineering Conference, 17-22 June, Rhodes, Greece.

- [18] van Engelen T, Braam H (2004). *TURBU Offshore, Computer Program for Frequency Domain Analysis of Horizontal Axis Offshore Wind Turbines*. Report ECN-C--04-079, Energy Research Centre of the Netherlands, Petten.
- [19] Yoo HH, Shin SH (1998). Vibration analysis of rotating cantilever beams. *Journal of Sound and Vibration* 212: 807-828.



Technology for a better society
www.sintef.no